University of Twente

Faculty of Electrical Engineering,
Mathematics & Computer Science

Design of a fully integrated RF transceiver using noise modulation

Dlovan Hoshiar Mahrof

MSc. Thesis

April 2008

Supervisors:
Prof. Dr. Ir. B. Nauta
Prof. Dr. Ir. J.C. Haartsen
Dr. Ing. E.A.M. Klumperink

Report number: 067.3261
Chair of Integrated Circuit Design
Faculty of Electrical Engineering,
Mathematics & Computer Science
University of Twente
P. O. Box 217
7500 AE Enschede
The Netherlands

Abstract

The aim of this project is to build the radio for sensor networks in low throughput applications. Robust communication and low power consumption are the main challenges in building such networks. Wideband modulation provides this robustness by spreading the spectrum of an information signal over a wide frequency spectrum using a broadband reference signal. Broadband spreading is hampered by long acquisition times, because synchronization takes place under very low SNR conditions. By sending the reference signal with the information signal, this problem is resolved. Since the reference signal does not have to be regenerated at the receiver, pure noise can be used. Noise Modulation techniques do not require coordination between the transmitter and the receiver. At the receiver just a correlation is needed between the received information signal and the received reference signal to reconstruct the information data. This attractive property of the Noise Modulation concept may allow building really low power receivers with a current consumption of less than 100 μA, compatible with energy harvesting (no batteries). In this thesis, a brief description of the Noise Modulation in both the frequency as well as in the time domain is presented. Especially the time analysis appears useful to make various design choices on the system level like the choice of frequencies, type of multiplier and type of baseband filtering. After that the focus is moved to the low power receiver in CMOS, with focus on the design of the correlater. Since the noise contribution of this correlater is very large, because it depends on the square value of its input signal, the receiver will consume high current if a long distance radio-link is needed. Therefore we had to review important parameters in our system, namely the transmitted power, the radio range, the overdrive voltage of the correlater transistors and the current consumption of the Front End, to make some rough decisions in order to meet the goal of designing a low power receiver.

Preface

In accordance with the degree of Master of Science in Electrical Engineering, I present this thesis entitled “Design of a fully integrated RF transceiver using noise modulation”.

I wish to take this opportunity to thank my advisors Mr. Bram Nauta, Mr. Eric Klumperink and Mr. Jaap Haartsen in giving me this chance to learn from their experiences throughout this project.
I would like also to express appreciation to the entire IC Design group in University of Twente for their support and nice time.
Also I am very grateful to UAF (De Stichting voor Vluchteling-Studenten UAF) for their intensive support and guiding throughout my study and my life.

To the heart who always loves without limit, my dear mother Zakia Al Hawezi.
To the candle who burns to give the light for his children, my father Dr. Hoshiar Mahrof.

Contents

Chapter 1 Introduction

Recently, a lot of applications require the using of Ad hoc sensor networks, to measure the physical properties of the environment (e.g. temperature, air pressure, humidity ...). In those networks, there are two important challenges regarding the implementation of their transceivers, namely robust communication and low power consumption. The concept of Noise Modulation is explained and motivated to be a potential solution. Building a whole transceiver based on this concept is a big task because it requires deep investigations into a lot of interesting aspects, on the system as well as on the circuit level. Therefore, the focus of this thesis will be presented in the objective section. Finally, the chapter ends with the organization of the thesis.

1.1 Background

Wireless distributed sensor networks consist of a collection of communicating nodes, where each node incorporates:

- One or more sensors
- Processing capability in order to process sensor data and to accomplish local control
- A radio to communicate information to/from neighboring nodes and eventually to external users.

In the recent years, different communication concepts have been developed in sensor ad hoc networks through intensive research. This research has highlighted the relevance of the following specifications:

Cost: Each sensor embraces different complex functions. Those functions must be in coherence with each other so that the total system works properly. Implementing those complex sensors in very large numbers increases the cost. Fortunately, emerging CMOS and MEMS technologies reduce the cost per sensor to adequate prices.

Power consumption: In ad hoc networks, each node has its own digital signal processing capability. Consequently, there are two main contributions to the power per node, digital part (DSP) and the analogue part (Radio).

Theoretically, the attenuation increases at least quadratically with the distance between the transmitter and receiver –node. Therefore, using two hops of length L as shown in Figure 1 is better from the power consumption view of point, than using a single hop with length L. Therefore, the transmitted power can be reduced by using a multi-hop communication scheme.

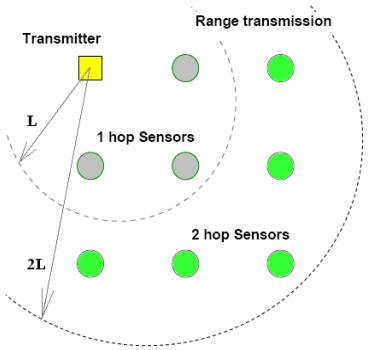

Figure 1: Multiple hope network

Performance: The nodes are distributed in a harsh environment, where there are a lot of interfering signals. In such an environment, Spectral Spreading transmission systems can provide more robust communication than the conventional narrow band systems. By spreading the spectrum of an information signal over a much wider band than the information rate, the system provides attractive capabilities, namely, anti-jam capability, interference (multipath path and other interference signals) rejection and a low probability of intercept (LPI) capability. Moreover, spreading allows for multiple user random access communication with selective addressing (e.g. via different code, CDMA). Processing Gain (PG) measures how much spreading has been achieved and is equal to $PG = B_{ss}/B$, where B_{ss} is the spread spectrum transmitted signal and B is the bandwidth of the information signal. There are different ways to spread the information signal for example: Direct Sequence (DS), frequency hoping, Time hoping and Hybrid systems (Rappaport [6]).

In recent research, a lot of attention has been spent to reduce the power consumption in the Spectral Spreading systems (special in DS systems), while retaining an adequate performance. To explain why the power consumption is critical in wireless sensor networks, the following example is presented.
A typical battery that is usually used in distributed nodes, for instance Lithium Thiony1 Chloride battery, has a capacity of 2000 mAh and a nominal voltage of 1.2 V. By assuming that the battery lasts between 2 to 4 years per sensor, Table 1 shows the maximum allowable current and power consumption.

Number of years	Number of hours	Current consumption [μA]	Power consumption [μW]
2	17 520	114	136.8
4	35 040	57	68.4

Table 1: Power and current budget of a typical battery

However, in many application battery replacement is highly undesired and the use of an energy harvesting techniques (e.g. solar cells). For compact systems with an area $<1cm^2$, typical energy harvesting devices produce a power in the range of 1-100 μW (IEEE [7]).

This research aims at the design of a low power transceiver for a power consumption level compatible with energy harvesting or batteries with very long lifetime. The focus is on ad hoc sensor networks in low throughput applications. In those applications, the measured data, like temperature, moisture and gas, does not change fast. Accordingly, the transmitter of the reporting node needs to be ON just for low "duty cycle", while the receiver of the listening node requires being ON most of the time.

1.2 Problem definition

From one side, the conventional Multiple Access (MA) techniques like FDMA, TDMA and CDMA are not attractive because they require a lot of coordination between the transmitters and the receivers; those techniques are based on an absolute frequency, time and code sequence which must be known in the receiver.
From the other side, it is highly desired to exploit spectral spreading and increase the processing gain to increase the communication robustness, but this will be at the cost of

reducing the received SNR. Reducing the SNR makes it difficult to synchronize the reference signal (i.e. the reference code in the DS technique) in the receiver with respect to that in the transmitter. As a consequence, the transmitted power has to be increased. The conventional Spread spectrum systems are not adequate in relation to this issue. Therefore, additional power must be consumed in the synchronization operation to be able to implement MA and to achieve higher processing gain.

1.3 Proposal solution

A particular WB transmission technique, called the Frequency Offset Division Multiple Access (FODMA) has been studied in the Telecommunication Engineering Group at the University of Twente, Shang [1], Balkema[2] and IEEE paper[3]. In FODMA or Noise Modulation as depicted in Figure 2, the reference signal (X_{ref}) is a broadband noise which is transmitted together with the modulated information data.

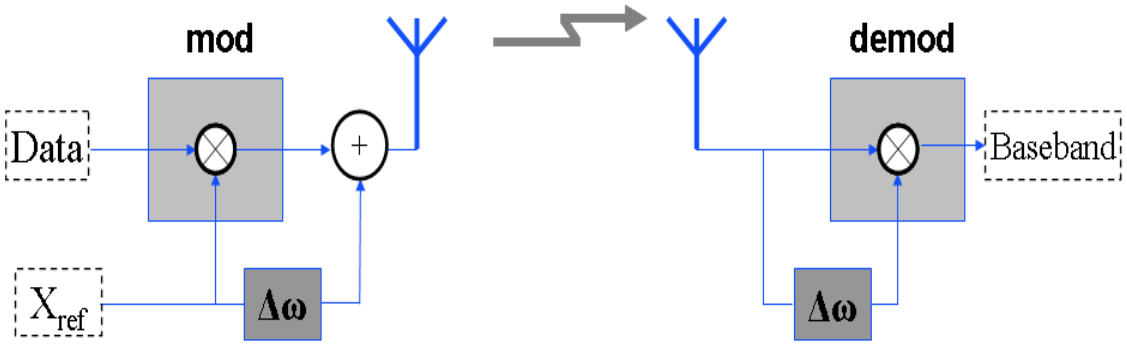

Figure 2: Noise Modulation schema

The clean reference signal is separated from the modulated information data by offset frequency Δω, so that the cross-correlation between those two signals is equal to zero (in other words: the two signals will not disturb each other). At the receiver, the modulated data and the reference signal are simply correlated to reconstruct the information data without the need to regenerate and synchronous the carrier.

The channel definitions in FODMA are not based on *absolute* parameters but *relative* parameters, namely frequency offset. Therefore, this technique does not require much code coordination between the transmitter and the receiver. Hence the processing gain can be increased further with this technique than the conventional WB techniques, while retaining the same level of power consumption.

1.4 Objective

In this Master project, the focus concerns two major points:

1. Investigating the feasibility of an implementation of this transceiver in CMOS.
2. Specifying and designing the critical building blocks with a special emphasis to low power consumption in the receiver.

1.5 Report survey

After a brief introduction was given in this chapter, chapter 2 begins with describing the Noise Modulation system in frequency domain. Then a time analysis of the signal processing is presented. Based on this time analysis the influence of a non integer ratio between $\Delta\omega$ and the bite rate the information data has been investigated. The chapter ends with study the effect of the phase synchronization between the local oscillator in the receiver and the local oscillator at the transmitter. Chapter 3 investigates different subjects in relation to optimize the design of the transceiver's blocks on the system level. Chapter 4 concerns designing low power receivers.

Chapter 2 Noise Modulation system

The aim of this chapter is to provide an understanding about the Noise Modulation system. After a short introduction about the concept of Noise Modulation, the chapter begins with the system description, where two types of communication systems are explained, namely the baseband Noise Modulation transceiver and the Passband Noise Modulation transceiver. After that a time analysis about the system operation is presented. This analysis provides a new way to understand the signal processing, the channel noise contribution and the effect of using a non integer ratio between the offset frequency $\Delta\omega$ and the bit rate, on the bit error rate (BER). Finally, the phase synchronization of the local oscillator in the transmitter to that employed by the receiver has been analyzed to show its influence on the communication performance.

2.1 Noise modulation concept

Shannon's Channel Capacity theory indicates that the signal energy for communications in the AWGN channel should be allocated equally over all frequencies in the band. The signal that is able to achieve that is a sample function of white noise. In the Noise Modulation system, the reference signal is a broad band noise that approximate the Shannon signal. By spreading the spectrum of an information signal with this reference signal, the modulated information will also become a broadband signal. Therefore, both the reference and the modulated signal approximate the Shannon signal so that by using the Noise Modulation concept, a higher capacity can be obtained in comparison to the other spread spectrum techniques.

2.2 System description

Whereas, the theoretical analysis of the Noise modulation system is a complex process, the system can still be analyzed with an intuitive way of understanding. Our intuitive understanding is checked by the interpretation of some simple equations which has been derived. The work of Shang [1] is also used to provide quantitative understanding about the system performance.

2.1.2 Baseband Noise Modulation transceiver

Figure 3 shows the baseband transceiver model. In this model, the transmitted signal is located in the baseband. The information data *m(t)* has the form of polar NRZ[1].

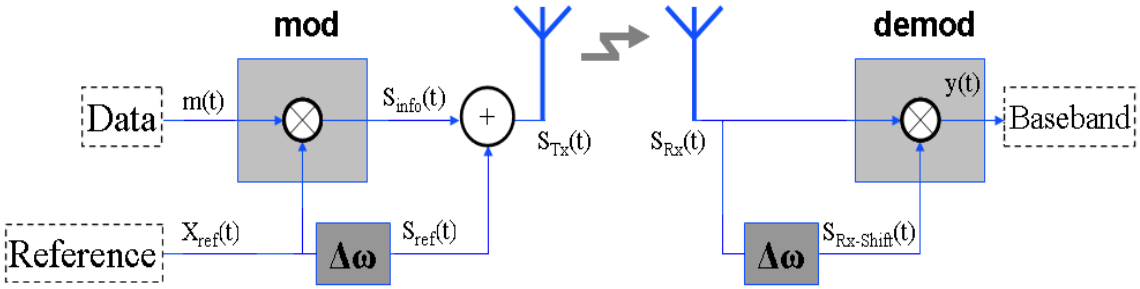

Figure 3: Baseband Noise Modulation transceiver

The wideband noise reference signal $X_{ref}(t)$ is generated by the transmitter and has a Gaussian probability density function, with a mean value equal to zero. The power spectral density of the reference signal is:

$$X_{ref}(f) = \begin{cases} l & -B_X < f < B_X \\ 0 & otherwise \end{cases} \qquad \textbf{Equation 2-1}$$

,with a mean power equal to $2B_X l$. The modulation block spreads the power of the information data over the reference signal to construct the $S_{info}(t)$ signal. The basic principle of the Spreading and De-Spreading operation is explained in Figure 4. When the modulated data and the reference signal are transmitted over a channel as shown in Figure 4, the original information signal can be reconstructed by the following calculation (Balkema [2]):

$$y(t) = \left(m(t) \times X_{ref}(t)\right) \times X_{ref}(t) = m(t) \times X_{ref}^2(t) \qquad \textbf{Equation 2-2}$$

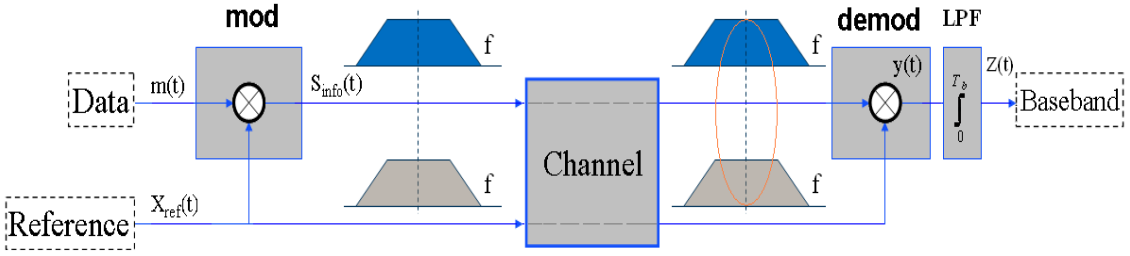

Figure 4: Basic principle behind spreading and de-spreading

By writing $X_{ref}(t)$ as it Fourier series representation, one can see that the signal consists of a series of cosine waves each with random phase shifts. By taking $X_{ref}(t) = cos(\omega t)$ gives:

$$y(t) = m(t) \times \cos^2(\omega t) = m(t) \times \frac{1}{2}\left(1 + \cos(2\omega t)\right) \qquad \textbf{Equation 2-3}$$

When y(t) is low pass filtered only the desired information data remains.

As mentioned in the previous chapter, in order to send both the modulated data $S_{info}(t)$ with the reference signal $X_{ref}(t)$ together without interfering each other, those signals have

[1] polar NRZ : polar Non Return to Zero, symbol 1 and 0 are represented by +1 and -1, respectively.

to be separated by offset frequency $\Delta\omega$ at the transmitter. At the receiver[2] the same shift operation is done to retain the information data as shown in Figure 5. The Figure also shows that this frequency shift in the transceiver is implemented by using an oscillator to generate the offset frequency signal $X_{\Delta\omega}$ and a multiplier.

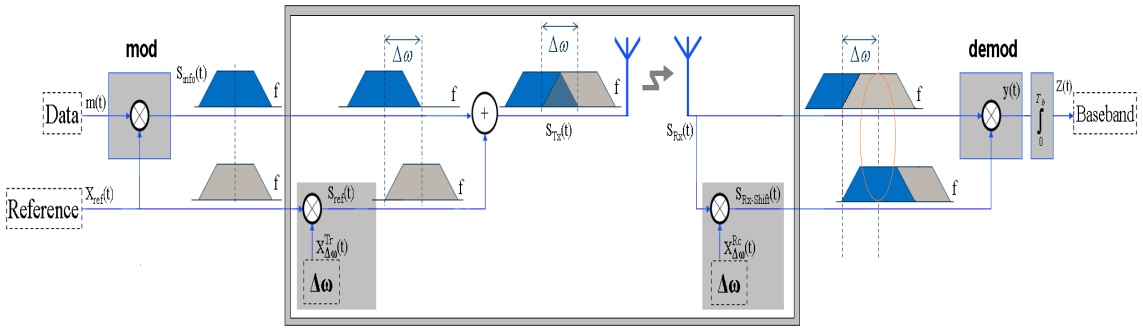

Figure 5: Implementing the offset frequency in the Noise Modulation transceiver

At the transmitter, the $S_{info}(t)$ and the $S_{ref}(t)$ will not interfere with each other, because their cross-correlation is equal to zero:

$$\text{A assuming}: \quad X_{\Delta\omega}(t)=\cos(\omega_{\Delta\omega}t) \quad \text{then}:$$

$$\begin{aligned} R_{\text{Sref Sinfo}}(t,t+\tau) &= E\left[S_{\text{ref}}(t)\times S_{\text{info}}(t+\tau)\right]=E\left[X_{\text{ref}}(t)\times X_{\Delta\omega}^{\text{Tr}}(t)\times m\times X_{\text{ref}}(t+\tau)\right] \\ &= E\left[X_{\text{ref}}(t)\times \sin(\Delta\omega\, t+\phi)\times m\times X_{\text{ref}}(t+\tau)\right] \\ &= m\times E\left[X_{\text{ref}}(t)\times X_{\text{ref}}(t+\tau)\right]\times \underbrace{E\left[\sin(\Delta\omega\, t+\phi)\right]}_{=0} \\ &= 0 \end{aligned}$$

Equation 2-4

Another function for the offset frequency at the transceiver is to implement the Multiple Access by utilizing different frequency. The bandwidth of the reference signal B_X is much larger than the offset frequency and the offset frequency is much larger than the bandwidth of the information data B, hence $B_X >> \Delta\omega >> B$ (later this point will be explained). The frequency spectrum which has been drawn in Figure 5, is just to show the concept of using the offset frequency. In order to have an advanced picture about the frequency spectrum, the power spectral density expression of $S_{TX}(t)$ must be derived and carefully analyzed. The spectral density is derived from the autocorrelation function. The autocorrelation of $S_{Tx}(t)$ has been derived in Appendix 1 for Figure 6 (the role of block C will be explained later) :

$$R_{S_{Tx}S_{Tx}}(\tau)=C^2R_{X_{ref}X_{ref}}(\tau)+\frac{1}{2}R_{X_{ref}X_{ref}}(\tau)\cos(\Delta\omega\,\tau) \qquad \textbf{Equation 2-5}$$

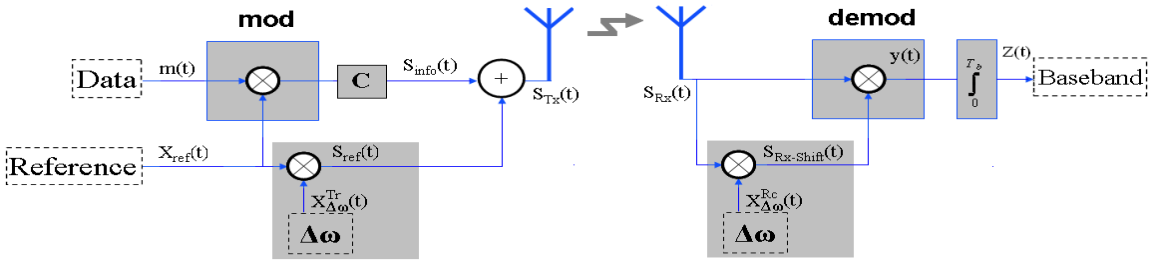

Figure 6: Noise Modulation transceiver

[2] After the antenna, there exist a filter with a bandwidth that is just wide enough to accommodate the bandwidth of the transmitted signal.

Now one can find easily the power spectral density of the $S_{Tx}(t)$:

$$S_{S_{Tx}S_{Tx}}(f) = \int_{-\infty}^{\infty} R_{S_{Tx}S_{Tx}}(\tau) \times e^{(-j\omega\tau)} d\tau$$ **Equation 2-6**

$$S_{S_{Tx}S_{Tx}}(f) = C^2 S_{X_{ref}X_{ref}}(f) + \frac{1}{4} S_{X_{ref}X_{ref}}(f + f_{\Delta\omega}^{Tr}) + \frac{1}{4} S_{X_{ref}X_{ref}}(f - f_{\Delta\omega}^{Tr})$$ **Equation 2-7**

Let's assume that $C = \frac{1}{\sqrt{2}}$

$$S_{S_{Tx}S_{Tx}}(f) = \underbrace{\frac{1}{2} S_{X_{ref}X_{ref}}(f)}_{\text{Power spectral of } S_{info}(t)} + \underbrace{\frac{1}{4} S_{X_{ref}X_{ref}}(f + f_{\Delta\omega}^{Tr}) + \frac{1}{4} S_{X_{ref}X_{ref}}(f - f_{\Delta\omega}^{Tr})}_{\text{Power spectral of } S_{ref}(t)}$$ **Equation 2-8**

The expression of Equation 2-8 shows that the spectral density of the transmitted signal consists of three broadband signals as shown in Figure 7 (the purpose of drawing those three signals in a stacked blocks above each other is to have a clear view, whereas in the real picture they are overlapping on each other with $\Delta\omega << B_X$). Thus, the energy of $X_{ref}(t)$ is divided equally between $S_{info}(t)$ and $S_{ref}(t)$.

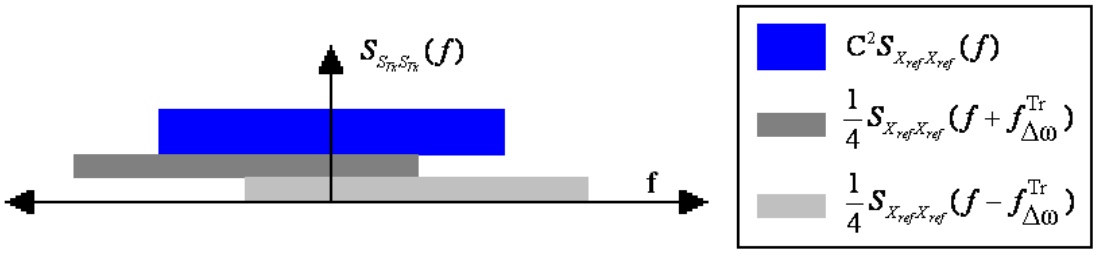

Figure 7: Power spectral density of the transmitted signal $S_{Tx}(t)$

The last point at the transmitter is to calculate the transmitted bit energy[3]:

$$E_b = T_b \int_{-\infty}^{\infty} S_{S_{Tx}S_{Tx}}(f) df \qquad \text{Where } T_b \text{ is the bit time}$$

$$= T_b \left(\int_{-\infty}^{\infty} C^2 S_{X_{ref}X_{ref}}(f) df + \int_{-\infty}^{\infty} \frac{1}{4} S_{X_{ref}X_{ref}}(f + f_{\Delta\omega}^{Tr}) df + \int_{-\infty}^{\infty} \frac{1}{4} S_{X_{ref}X_{ref}}(f - f_{\Delta\omega}^{Tr}) df \right)$$

$$= T_b \left(C^2 2B_X l + \frac{1}{2} B_X l + \frac{1}{2} B_X l \right)$$

$$= T_b \left(C^2 2 + 1 \right) B_X l$$ **Equation 2-9**

$$\xrightarrow{\text{For } C = \frac{1}{\sqrt{2}}} E_b = 2T_b B_X l$$ **Equation 2-10**

[3] This derivation is analogue to what Shang did

For an ideal channel, the received signal $S_{Rx}(t)$ is equal to the transmitted signal $S_{Tx}(t)$ with a spectrum shown in Figure 7. The received signal $S_{Rx}(t)$ will be shifted by a frequency $f_{\Delta\omega}^{Rc}$, which is equal to $f_{\Delta\omega}^{Tr}$ under the condition of ideal phase synchronization between the transmitter and the receiver. This shifting operation produces $S_{Rx\text{-}Shift}(t)$. Then a linear multiplier correlates between $S_{Rx}(t)$ and $S_{Rx\text{-}Shift}(t)$ to produce two baseband peaks, one peak exists around zero [Hz] and the other peak exists around $2\Delta\omega$ [Hz]. Both peaks contain the same information data (i.e. two copies of the same information data). To explain why the de-spreading operation produces those two peaks, let's go throughout the spectrum at the receiver:

The power spectral density of the signal $S_{Rx\text{-}Shift}(t)$ is expressed as follows:

$$S_{S_{Rx-Shift}S_{Rx-Shift}}(f) = S_{S_{Rx}S_{Rx}}(f + f_{\Delta\omega}^{Rc}) + S_{S_{Rx}S_{Rx}}(f - f_{\Delta\omega}^{Rc})$$
$$= S^{\text{First part}}_{S_{Rx-Shift}S_{Rx-Shift}}(f) + S^{\text{Second part}}_{S_{Rx-Shift}S_{Rx-Shift}}(f) \qquad \textbf{Equation 2-11}$$

This power spectrum is drawn in Figure 8:

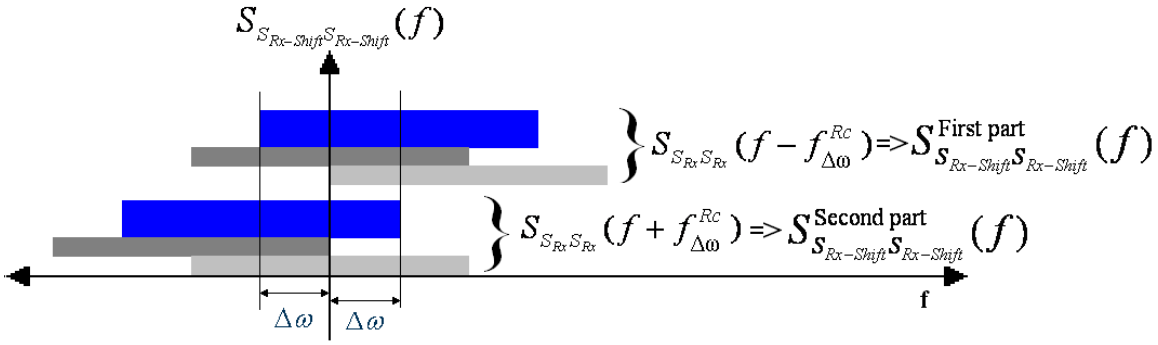

Figure 8: Power spectral density of the signal $S_{Rx\text{-}Shift}(t)$

A linear multiplier between $S_{Rx}(t)$ and $S_{Rx\text{-}Shift}(t)$ in time domain translates to a convolution operation in frequency domain:

$$Y(f) = \int_{-\infty}^{\infty} S_{S_{Rx-Shift}S_{Rx-Shift}}(v) \times S_{S_{Rx}S_{Rx}}(f - v)dv$$
$$= \int_{-\infty}^{\infty} \left(S^{\text{Firstpart}}_{S_{Rx-Shift}S_{Rx-Shift}}(v) + S^{\text{Secondpart}}_{S_{Rx-Shift}S_{Rx-Shift}}(v) \right) \times S_{S_{Rx}S_{Rx}}(f - v)dv$$
$$= \int_{-\infty}^{\infty} S^{\text{Firstpart}}_{S_{Rx-Shift}S_{Rx-Shift}}(v) \times S_{S_{Rx}S_{Rx}}(f - v)dv \qquad \textbf{Equation 2-12}$$
$$+ \int_{-\infty}^{\infty} S^{\text{Secondpart}}_{S_{Rx-Shift}S_{Rx-Shift}}(v) \times S_{S_{Rx}S_{Rx}}(f - v)dv$$

The convolution operation of Equation 2-12 is graphically explained in Figure 9:

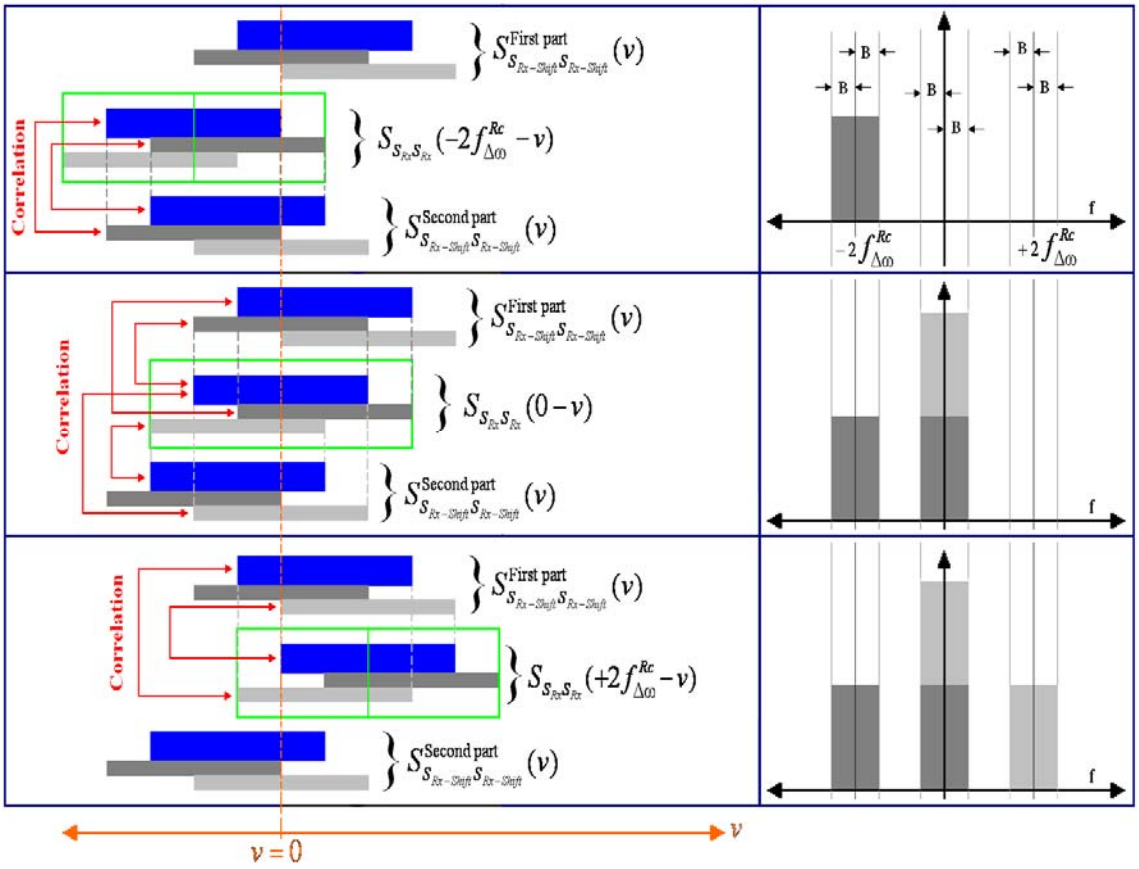

Figure 9: De-spreading operation at the receiver

Thus, the results of the de-spreading process are two peaks. Figure 9 also shows that the offset frequency $\Delta\omega$ must be larger than the bandwidth of the information data B, so that the two peaks does not interfere each other.

The energy of the peak, which is around the 0 [Hz] is two times the energy of the second peak. By using a low pass filter as shown in Figure 10, the information data will be reconstructed.

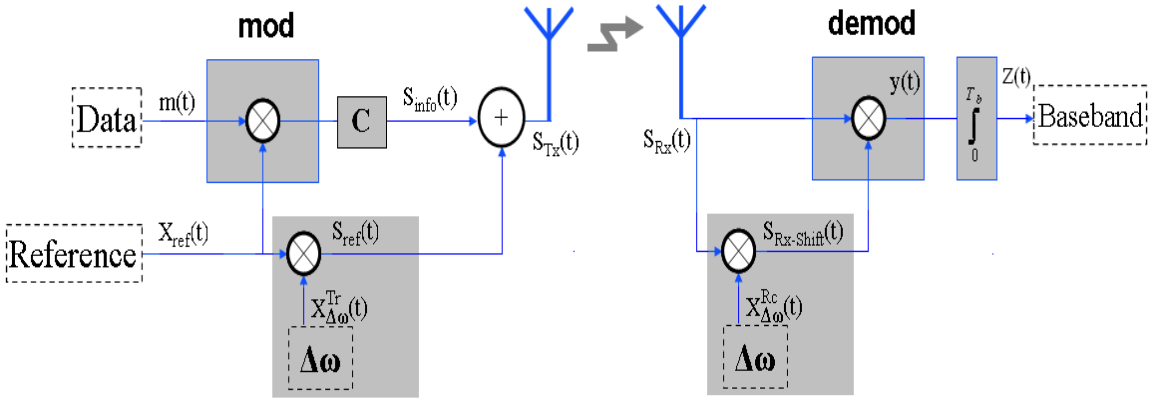

Figure 10: Noise Modulation transceiver

In the real world, the channel adds noise. Shang explained how this thermal noise will spread throw the receiver till it reaches the output of the low pass filter. The signal at the output of the low pass filter *Z(t)* constructs from a baseband polar NRZ *E{Z(t)}* and a noise $n_Z(t)$:

$$Z(t) = E\{Z(t)\} + n_Z(t) \qquad \textbf{Equation 2-13}$$

The quantification of the SNR at the output of the low pass filter is necessary to have an intuitive measure for describing the quality of the output signal, and to measure the Bit Error Rate (BER) of the system:

$$SNR = \frac{[E\{Z(t)\}]^2}{\sigma_{n_Z}^2} \qquad \textbf{Equation 2-14}$$

Shang made the derivation of the SNR of Equation 2-14 and found:

$$SNR = \frac{16\left(\frac{E_b}{N_O}\right)^2}{\left(8C^2 + 36 + \frac{5}{C^2}\right)\frac{1}{PG}\left(\frac{E_b}{N_O}\right)^2 + 2\left(8C^2 + 10 + \frac{3}{C^2}\right)\frac{E_b}{N_O} + 2\left(4C^2 + 4 + \frac{1}{C^2}\right)PG} \qquad \textbf{Equation 2-15}$$

Since the output signal *E{Z(t)}* is a baseband polar NRZ signal in Additive White Gaussian Noise (AWGN), and assuming symbols 1 and -1 occur with equal probability, one can find that BER of the FODMA system working in the baseband is (Haykin [4]):

$$P_e = \frac{1}{2} erfc\left(\sqrt{\frac{SNR}{2}}\right) \qquad \textbf{Equation 2-16}$$

Where erfc is the complimentary error function:

$$erfc(x) = \frac{2}{\sqrt{\pi}} \int_{-\infty}^{\infty} \exp(-y^2)\, dy$$

Differentiating the denominator of Equation 2-15 with respect to *C* and *PG*, gives the following two conditions in order to maximize the BER:

$$C = C_{optimum} = 0.77 \qquad \textbf{Equation 2-17}$$

$$PG = PG_{optimum} = \sqrt{\frac{8C^4 + 36C^2 + 5}{8C^4 + 8C^2 + 2}}\,\frac{E_b}{N_O} \qquad \textbf{Equation 2-18}$$

$$\xrightarrow{C = C_{optimum}} PG = PG_{optimum} = 1.75\frac{E_b}{N_O} \qquad \textbf{Equation 2-19}$$

Then the BER is:

$$P_{e\,\text{minimum}} = \frac{1}{2} erfc\left(\sqrt{0.083\,\frac{E_b}{N_O}}\right) \qquad \textbf{Equation 2-20}$$

Shang also explained that the communication performance is slightly degraded when the value of $C = 1$ and keeping the condition of Equation 2-18 to be still satisfied:

$$C = 1 \qquad \textbf{Equation 2-21}$$

$$\xrightarrow{C=1} PG = PG_{optimum} = 1.65\frac{E_b}{N_O} \qquad \textbf{Equation 2-22}$$

This makes the BER to be:

$$P_e = \frac{1}{2} erfc\left(\sqrt{0.079\,\frac{E_b}{N_O}}\right) \qquad \textbf{Equation 2-23}$$

Equation 2-18 shows that for a given E_b/N_O, the processing gain should be as close to $G_{optimum}$ for the low error rate. This means that PG should be adaptively optimized to different values of E_b/N_O For example, if $15\ dB < E_b/N_O < 20\ dB$, then $G = 20\ dB$ should be the best choice as shown in Figure 11.

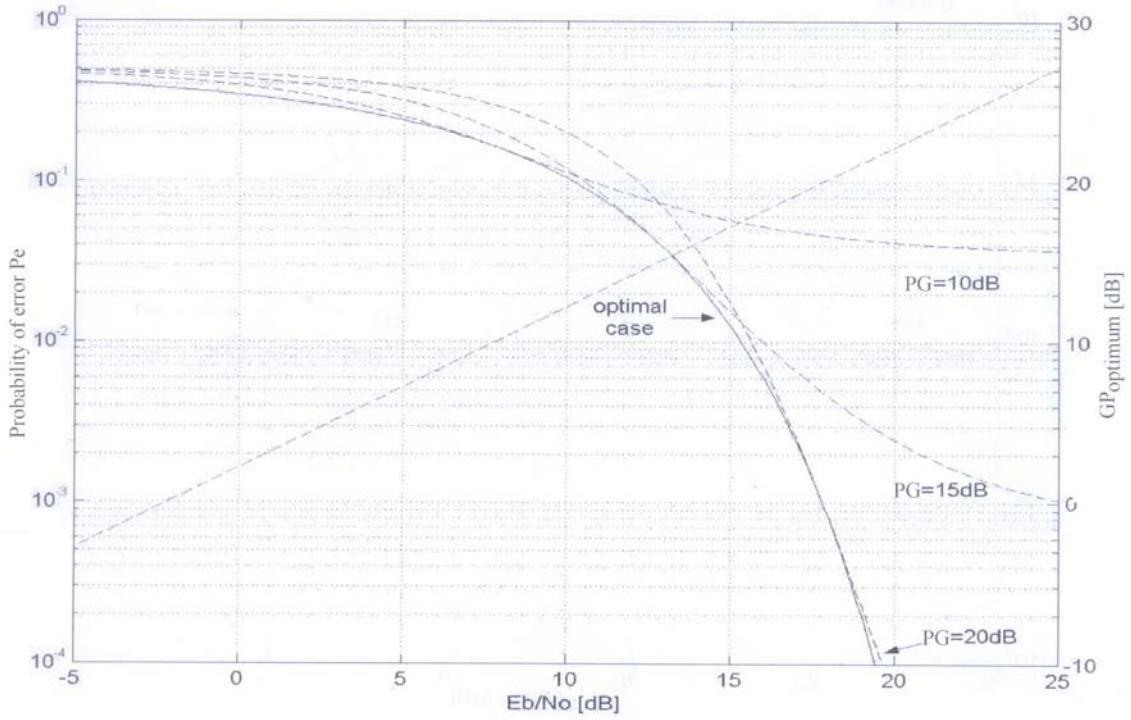

Figure 11: Single user performance transmitted in baseband when C=1

2.2.2 Passband Noise Modulation transceiver

In the RF application, the transmitted signal must be shifted to the RF domain as shown in Figure 12.

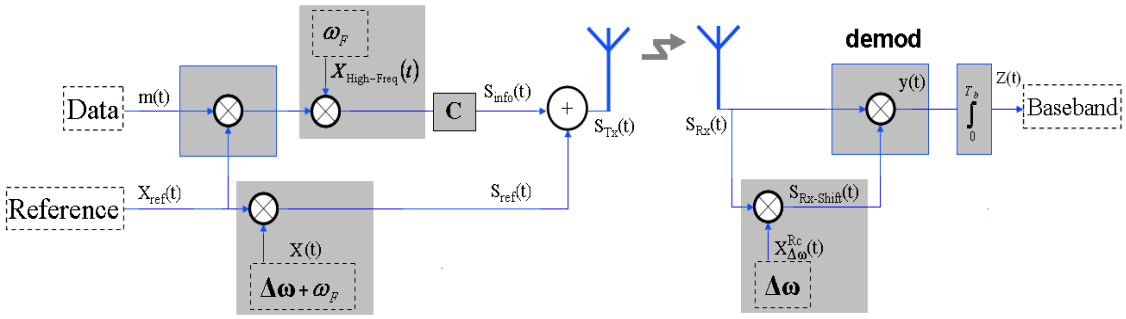

Figure 12: Passband Noise Modulation transceiver

The Passband transceiver is almost the same as a baseband transceiver, except that both the modulated information data and the reference signal are up-converted to the passband, by a cosine wave with a carrier frequency of ω_F, where $\omega_F >> B_X >> \Delta\omega >> B$. The concept of the noise modulation does not change because the same operation is done in the RF domain in stead of the baseband domain.

The output signal *E{Z(t)}* is again a baseband polar NRZ signal in AWGN, and assuming symbols 1 and -1 occur with equal probability, one can find that BER of the FODMA system working in the baseband is (Haykin [4]):

$$P_e = \frac{1}{2} erfc\left(\sqrt{\frac{SNR}{2}}\right) \qquad \textbf{Equation 2-24}$$

Shang made the derivation for the SNR:

$$SNR = \frac{[E\{Z(t)\}]^2}{\sigma_{n_Z}^2}$$

$$= \frac{\left(\frac{E_b}{N_O}\right)^2}{\left(\frac{C^4+5C^2+1}{2C^2}\right)\frac{1}{PG}\left(\frac{E_b}{N_O}\right)^2 + \frac{(C^2+1)^2}{C^2}\frac{E_b}{N_O} + \frac{(C^2+1)^2}{2C^2}PG} \qquad \textbf{Equation 2-25}$$

Differentiating the denominator of Equation 2-25 with respect to *C* and *PG*, gives the following two conditions in order to maximize the BER:

$$C = C_{optimum} = 1 \qquad \textbf{Equation 2-26}$$

$$PG = PG_{optimum} = 1.32\frac{E_b}{N_O} \qquad \textbf{Equation 2-27}$$

Then the BER is:

$$P_{e\,\text{minimum}} = \frac{1}{2} erfc\left(\sqrt{0.054\,\frac{E_b}{N_O}}\right) \qquad \textbf{Equation 2-28}$$

For a fixed bandwidth system with limited output power, the energy per bit can be controlled by changing the processing gain. The performance for various PG is plotted in Figure 13. It can be seen that for lower E_b/N_O, a lower PG is better.

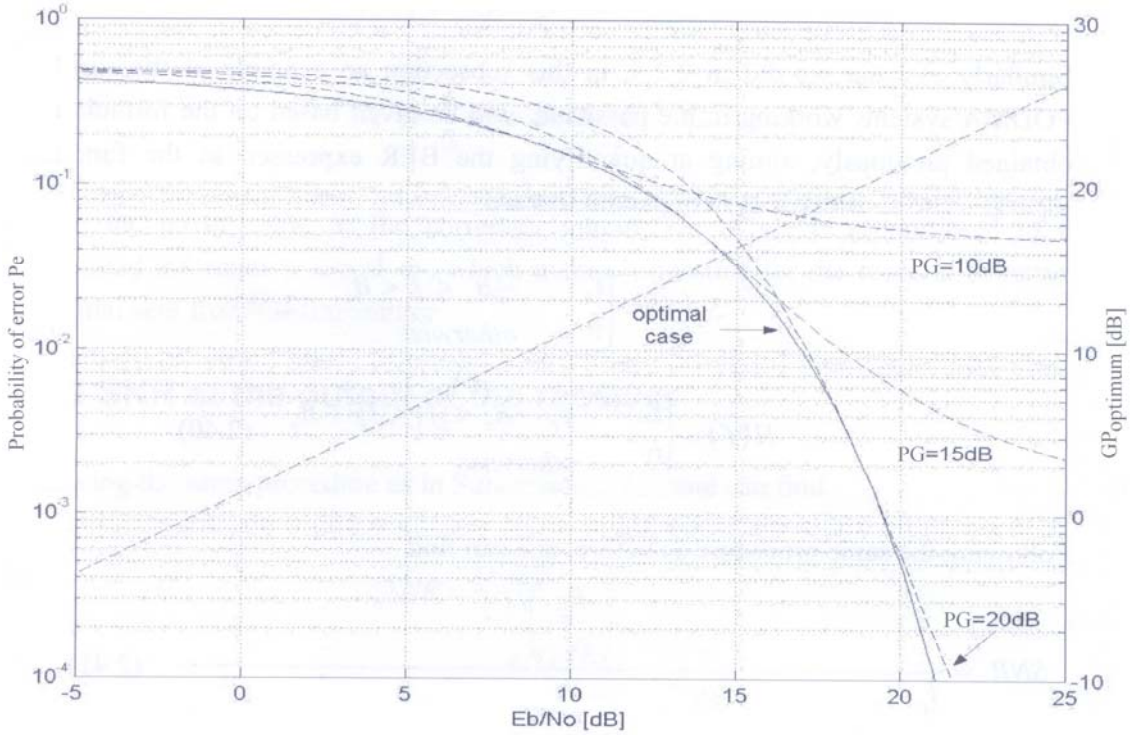

Figure 13: Single user performance transmitted in passband when C=1

Finally, by comparing Equation 2-23 with Equation 2-28, one can see that the link performance of the FODMA system in the baseband is better than the Passband. This is because with the same E_b/N_O, less power of the transmitted signal for the system working in the Passband is de-spread to the baseband in the receiver in compare with that working in the baseband (Shang [1]).

2.3 Time analysis

Visualizing the system operation in time domain leads to gain deep view into the concept of Noise Modulation. Let's assume, first that the ratio between the bit rate (R_b[4]) and the offset frequency ($R_b/\Delta\omega$) is an integer for instance, $R_b = 1MHz$ and $\Delta\omega = 2\ MHz$ (Next section deals with the situation where the ratio of ($R_b/\Delta\omega$) in not integer) and, second that the offset frequency signal at the receiver is synchronized to the offset frequency signal at the transmitter.

For the transmitter in Figure 14, the signals are visually analyzed in time domain.

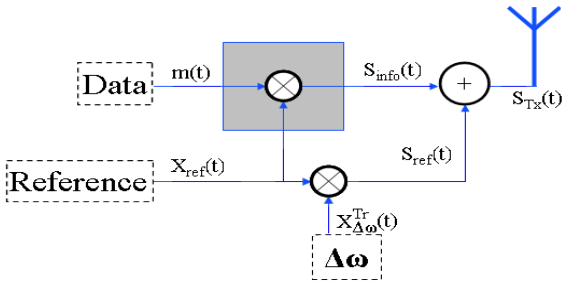

Figure 14: Noise Modulation transmitter

As depicted in Figure 15, $S_{info}(t)$ contains a Gaussian distributed random part, which is the reference signal $X_{ref}(t)$ and a deterministic part, which is the bit 1:

$$S_{info}(t) = X_{ref}(t) \times m(t)$$

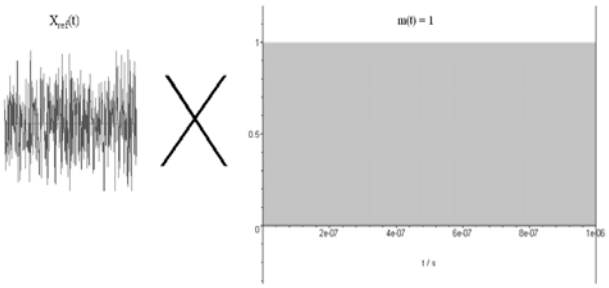

Figure 15: $S_{info}(t) = X_{ref}(t) \times m(t)$ where: $m(t) = 1$

As depicted in Figure 16, $S_{ref}(t)$ consists of a Gaussian distributed random part $X_{ref}(t)$ and a deterministic part, which is the offset frequency $X^{Tr}_{\Delta\omega}(t)$ signal:

$$S_{ref}(t) = X_{ref}(t) \times X^{Tr}_{\Delta\omega}(t)$$

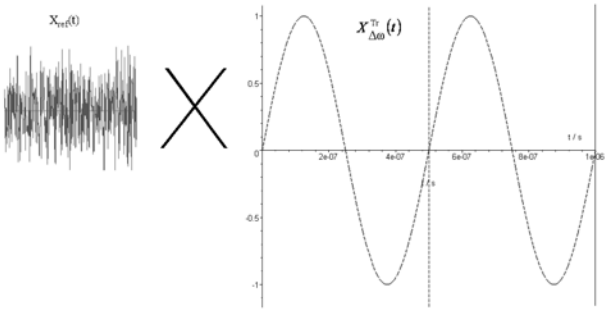

Figure 16: $S_{ref}(t) = X_{ref}(t) \times X^{Tr}_{\Delta\omega}(t)$

The transmitted signal $S_{Tx}(t)$ as shown in Figure 17 contains a Gaussian distributed random part $X_{ref}(t)$ and a deterministic part $X^{Tr}_{\Delta\omega}(t) + m(t)$.

The deterministic part shapes the random part so that the energy of the random part is distributed around the two peaks of the deterministic part. Thus, there are two active regions inside a bit time namely, the 1st and 3rd region.

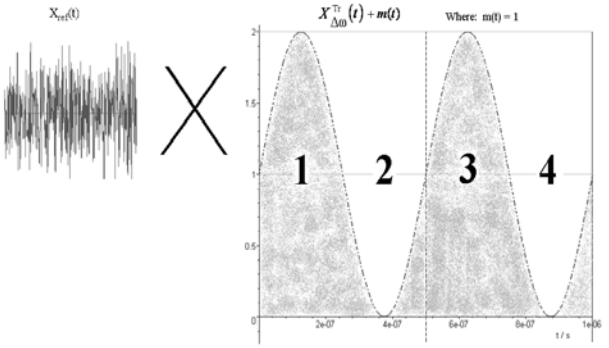

Figure 17: $S_{Tx}(t) = S_{info}(t) + S_{ref}(t)$ where: $m(t) = 1$

[4] R_b: bit rate. In this thesis, the number of symbols are equal to the number of bits therefore $R_b = B$.

For an ideal channel (noiseless), the received signal is equal to the transmitted signal. The receiver of Figure 18 multiplies the received signal with the shifted version of the received signal to produce *y(t)* as shown in Figure 19. The deterministic part of *y(t)* gathers the energy of the random part in the 1st and 3rd -quarter of the bit time. Thus, the integration operation of the baseband filter is active just in those two regions.

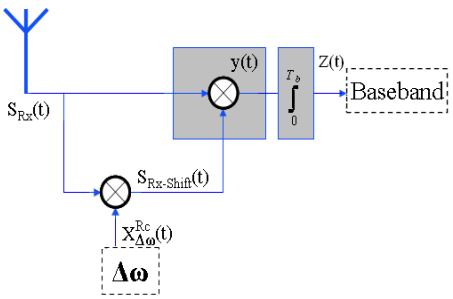

Figure 18: Noise Modulation receiver

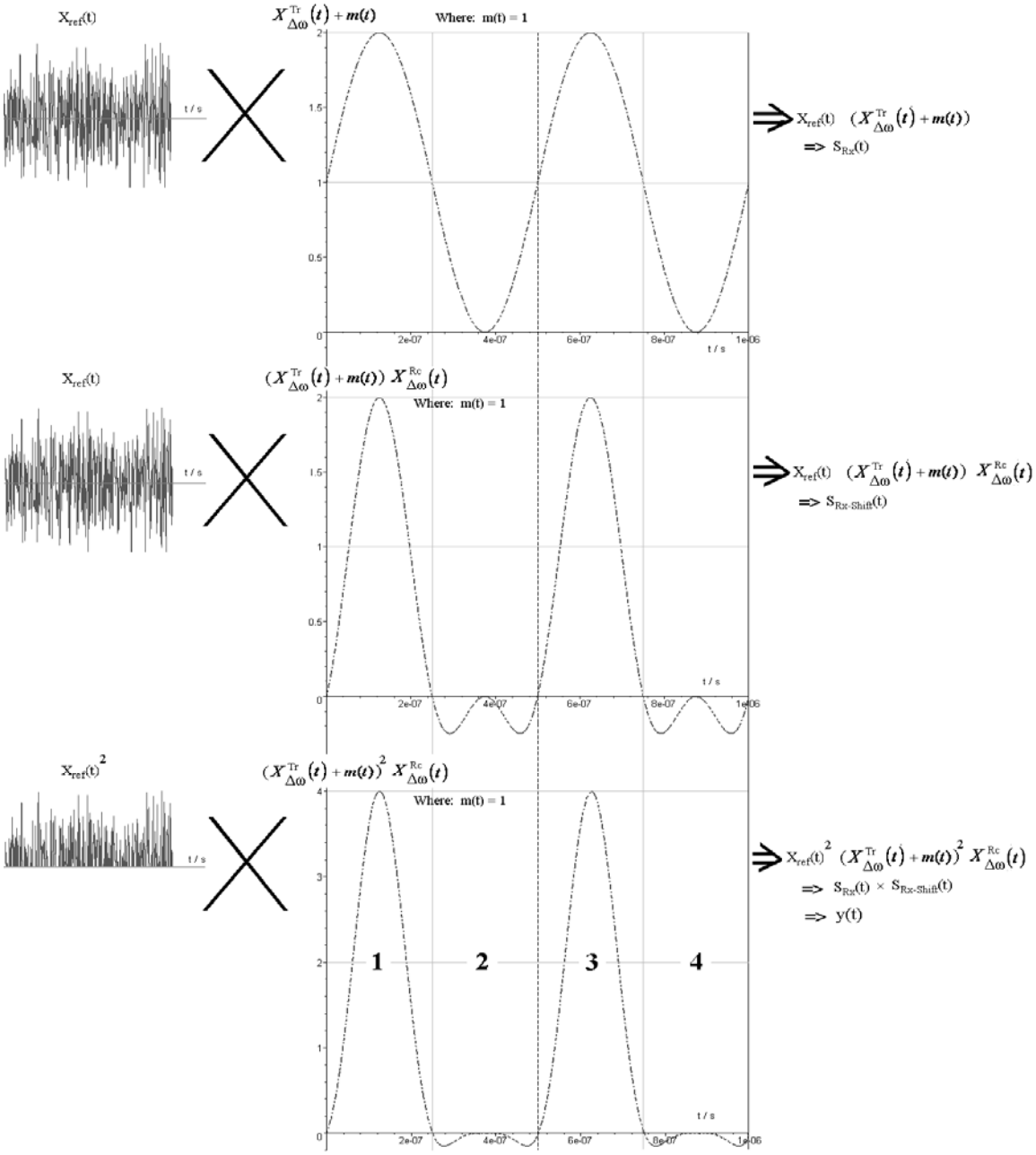

Figure 19: Receiver signal analysis

The same analysis can be applied when the bit is zero as shown in Figure 21, Figure 22, Figure 23 and Figure 24.

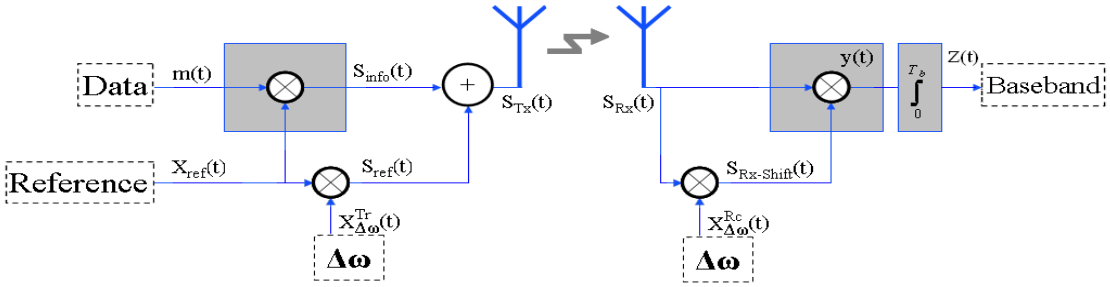

Figure 20: Noise Modulation transceiver

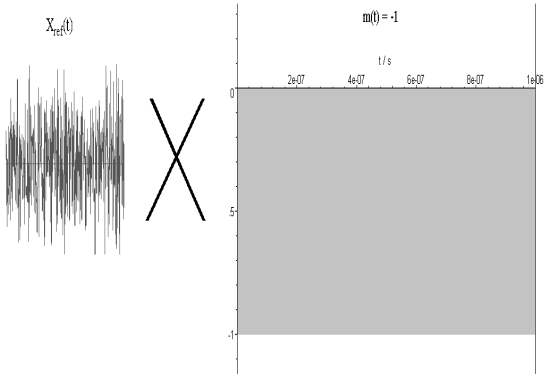

Figure 21: $S_{info}(t) = X_{ref}(t) \times m(t)$ where m(t) = -1

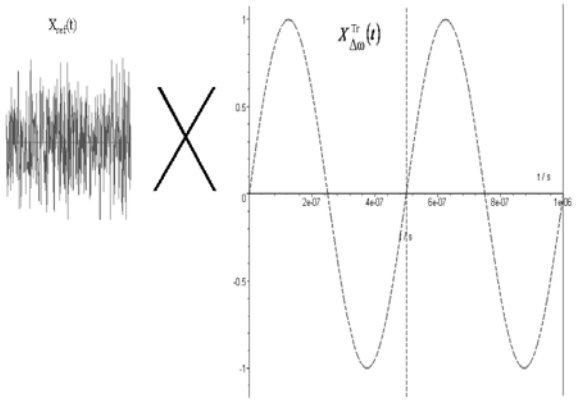

Figure 22: $S_{ref}(t) = X_{ref}(t) \times X^{Tr}_{\Delta\omega}(t)$

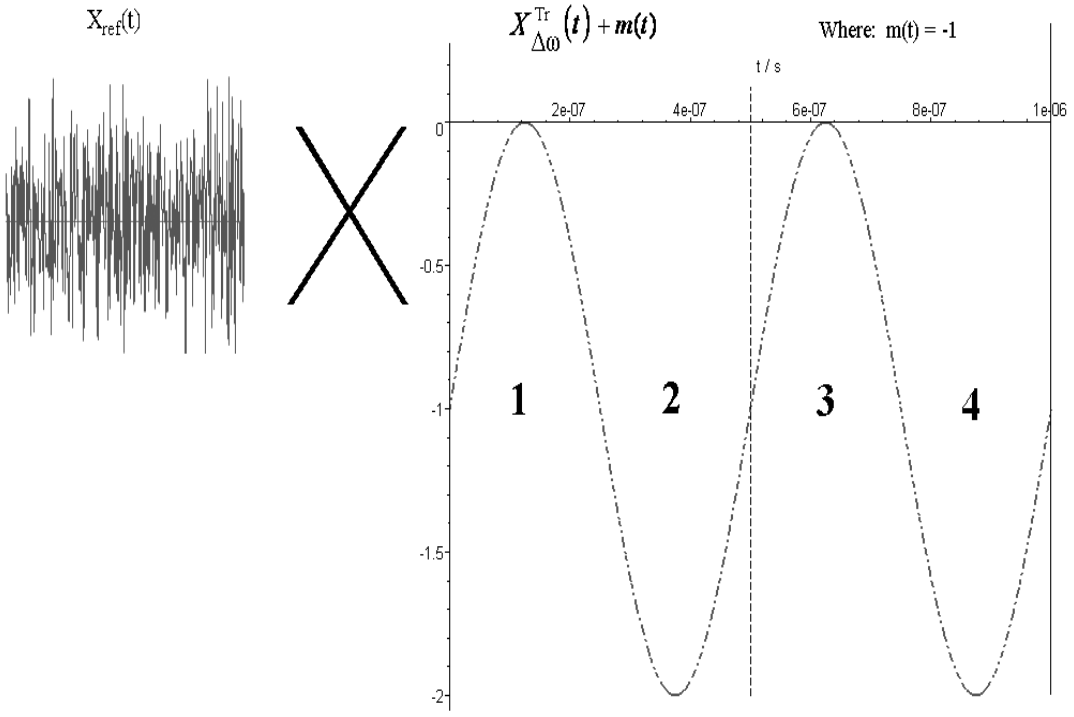

Figure 23: $S_{Tx}(t) = S_{info}(t) + S_{ref}(t)$ where m(t) = -1

As shown in Figure 24, the deterministic part of the signal *y(t)* gathers the energy of the random part in the 2nd and the 4th -quarter of the bit time. Thus, the integration operation of the filter is active just in those two regions.

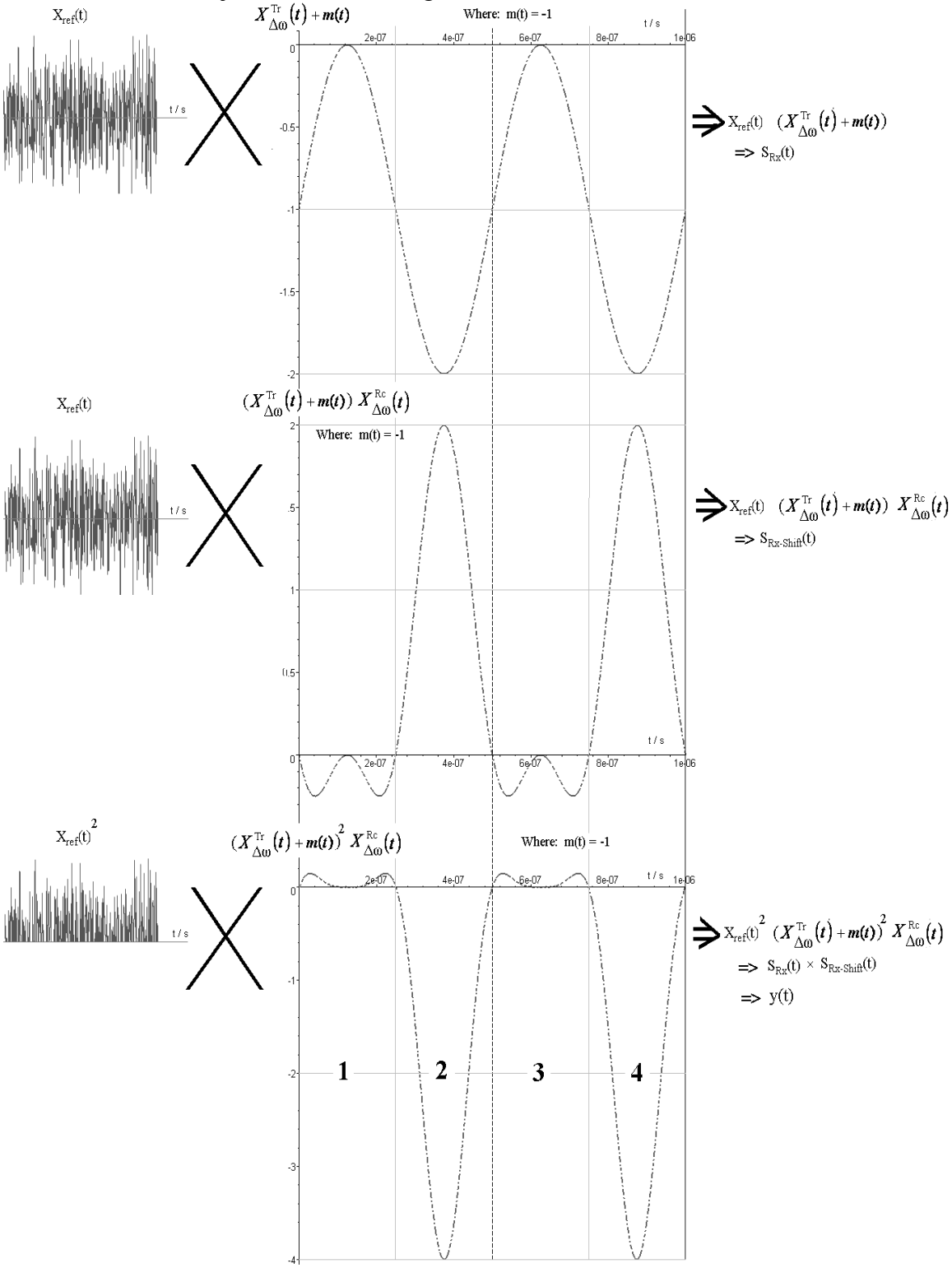

Figure 24: Receiver signal analysis

In the previous analysis, the role of the $X_{\Delta\omega}^{Rc}(t)$ in reconstructing the bit at the receiver is implicitly presented. To explain this role, let's write the equation of *y(t)*:

$$y(t) = \underbrace{X_{ref}^2(t)}_{\text{Random positive samples}} \underbrace{\left(X_{\Delta\omega}^{\text{Tx}}(t) + m(t)\right)^2 \times X_{\Delta\omega}^{\text{Rc}}(t)}_{\text{Deterministic Signal}} \qquad \textbf{Equation 2-29}$$

The deterministic part contains two Offset frequencies, one is generated at the transmitter and the other is generated at the receiver. Now let's draw the deterministic part of the signal *y(t)*:

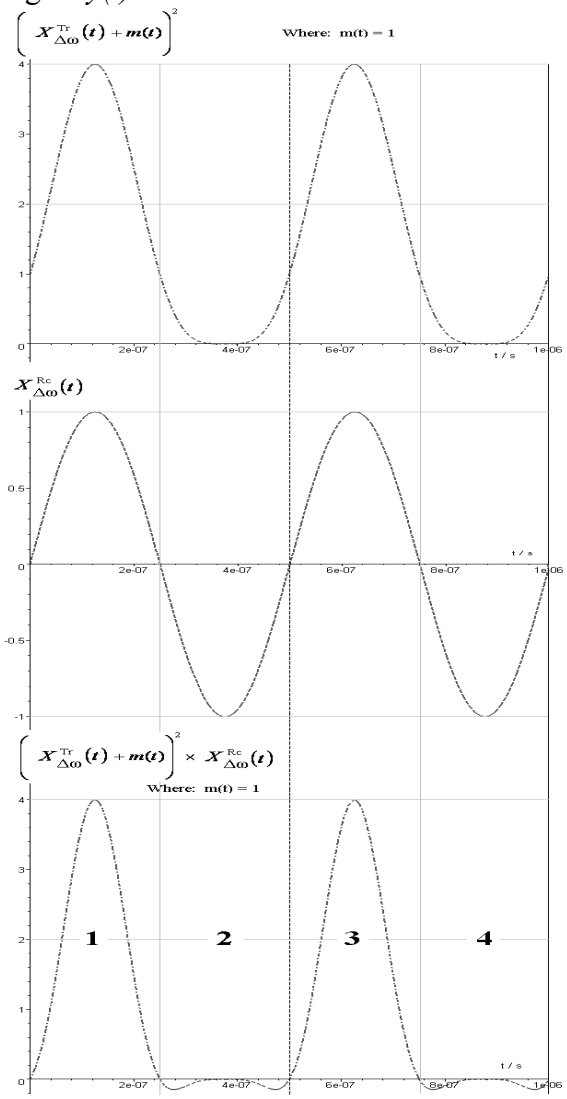

Figure 25: Receiver signal analysis for m(t) = 1

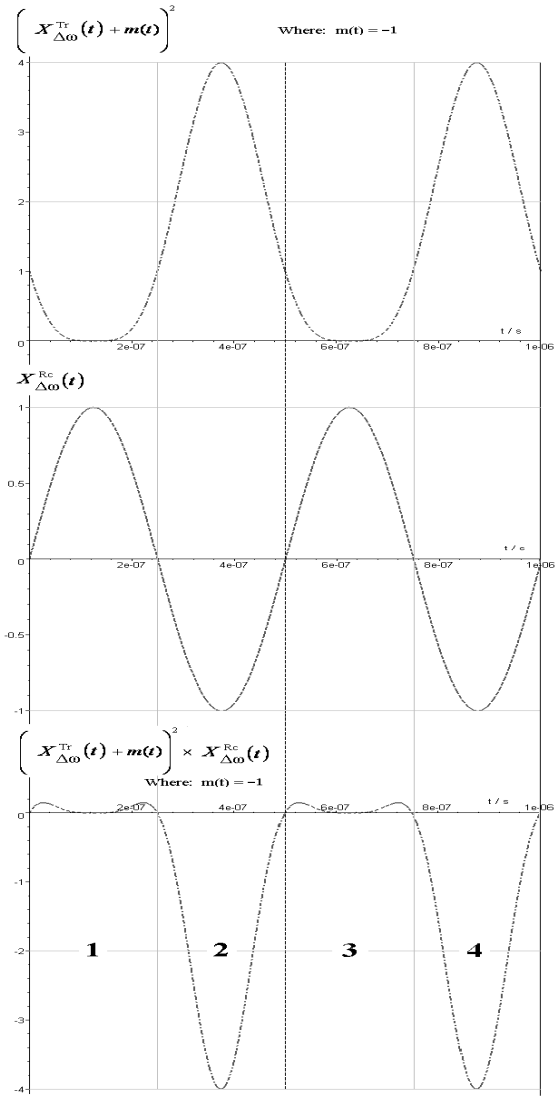

Figure 26: Receiver signal analysis for m(t) = -1

The signal $\left(X_{\Delta\omega}^{Tr}(t) + m(t)\right)^2$ is positive and concentrated in the 1st and 3rd quarter for the situation where Bit 1 is sent, and the 2nd and 4th quarter for the situation where Bit 0 is sent, as shown in Figure 25 and Figure 26. The $X_{\Delta\omega}^{Rc}(t)$ at the receiver determines if the signal $\left(X_{\Delta\omega}^{Tr}(t) + m(t)\right)^2$ must stay positive or flip to become negative. This way of analysis is practical to study the influence of the phase synchronization of $X_{\Delta\omega}^{Rc}(t)$ at the receiver to that $X_{\Delta\omega}^{Tr}(t)$ at the transmitter.

2.1.3 Channel noise contribution

In this section, the previous time analysis is extended to include the contribution of the AWGN channel noise. As mentioned before the channel noise process *n(t)* is modeled as an Additive, White and Gaussian Noise, whose mean power spectral is zero and whose power spectral density is constant. Assuming that there is no attenuation in the channel, the received signal is equal to the transmitted signal plus the channel noise *n(t)*:

$$\begin{aligned} y(t) &= \left(S_{Rx}(t)+n(t)\right)\times\left(S_{Rx}(t)+n(t)\right)X_{\Delta\omega}^{\mathrm{Rc}}(t) \\ &= \left(S_{Rx}(t)+n(t)\right)^2 X_{\Delta\omega}^{\mathrm{Rc}}(t) \\ &= S_{Rx}^2(t)X_{\Delta\omega}^{\mathrm{Rc}}(t)+\underbrace{2n(t)S_{Rx}(t)X_{\Delta\omega}^{\mathrm{Rc}}(t)+n^2(t)X_{\Delta\omega}^{\mathrm{Rc}}(t)}_{\text{Channel noise contribution}} \\ &= S_{Rx}^2(t)X_{\Delta\omega}^{\mathrm{Rc}}(t)+\underbrace{2n(t)X_{ref}(t)\left(X_{\Delta\omega}^{\mathrm{Tr}}(t)+m(t)\right)X_{\Delta\omega}^{\mathrm{Rc}}(t)+n^2(t)X_{\Delta\omega}^{\mathrm{Rc}}(t)}_{\text{Channel noise contribution}} \end{aligned} \qquad \textbf{Equation 2-30}$$

Assuming $X_{\Delta\omega}^{\mathrm{Rc}}(t)=X_{\Delta\omega}^{\mathrm{Tr}}(t)$

$$\begin{aligned} y(t) &= S_{Rx}^2(t)X_{\Delta\omega}^{\mathrm{Rc}}(t)+\underbrace{2n(t)X_{ref}(t)\left(X_{\Delta\omega}^{\mathrm{Rc}}(t)+m(t)\right)X_{\Delta\omega}^{\mathrm{Rc}}(t)+n^2(t)X_{\Delta\omega}^{\mathrm{Rc}}(t)}_{\text{Channel noise contribution}} \\ &= X_{ref}^2(t)\underbrace{\left(X_{\Delta\omega}^{\mathrm{Rc}}(t)+m(t)\right)^2 X_{\Delta\omega}^{\mathrm{Rc}}(t)}_{\text{Deterministic Signal}} \\ &\quad \underbrace{+2n(t)X_{ref}(t)\underbrace{\left(X_{\Delta\omega}^{\mathrm{Rc}}(t)+m(t)\right)X_{\Delta\omega}^{\mathrm{Rc}}(t)}_{\text{Deterministic Signal}}+n^2(t)\quad \underbrace{X_{\Delta\omega}^{\mathrm{Rc}}(t)}_{\text{Deterministic Signal}}}_{\text{Channel noise contribution}} \end{aligned} \qquad \textbf{Equation 2-31}$$

The dot-dashed red line in Figure 27 gathers the positive energy of $X_{ref}^2(t)$ in the 1st and 3rd region.

The two grey peaks is multiplied by the random part: $2n(t)X_{ref}(t)$, which consist of positive and negative samples. The results of this multiplication are positive and negative samples, which they will be concentrated in the 1st and 3rd region, where also the desired signal exists. The negative samples distort the desired signal, hence they distort the detection operation.

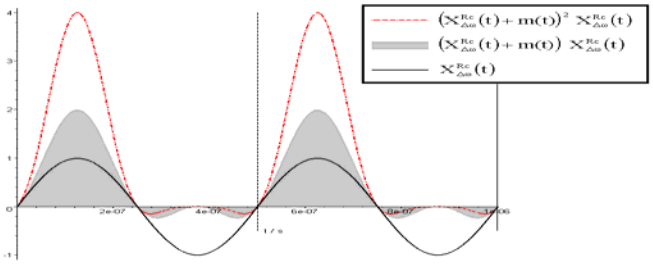

Figure 27: Deterministic parts of Equation 2-31 (m(t) = 1)

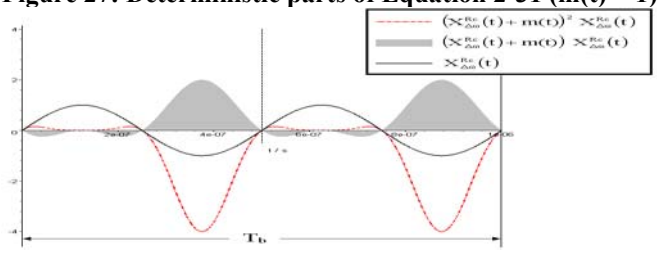

Figure 28: Deterministic parts of Equation 2-31 (m(t) = -1)

The positive samples of $n^2(t)$ are multiplied by two cycles of $X_{\Delta\omega}^{\mathrm{Rc}}(t)$, which consist of two positive and negative peaks. The results are 4 regions, namely two regions of positive samples and two regions of negative samples. The baseband filter will average those samples. If the energy of the channel noise *n(t)* is low, then the contribution of $n^2(t)X_{\Delta\omega}^{\mathrm{Rc}}(t)$ can be neglected. Figure 28 shows the deterministic parts of Equation 2-31 for the situation when bit 0 has been sent.

2.2.3 Non-Integer ratio of Δω en R_b Frequency offset

All the explinations and the examples that are till now presented, assume an integer ratio between Δω en R_b[5] Carefully inspecting Equation 2-31 and Figure 27, one can recognize the appearance of an inhomogeneous distribution of the signal and the noise per bit, if the ratio between Δω en R_b becomes non-integer as shown in the example of Figure 29, where Δω = 2.5 MHz and R_b = 1 M samples/s. In this example, two bit times must be drawn so that the $X_{\Delta\omega}^{Rc}(t)$ complete its cycle.

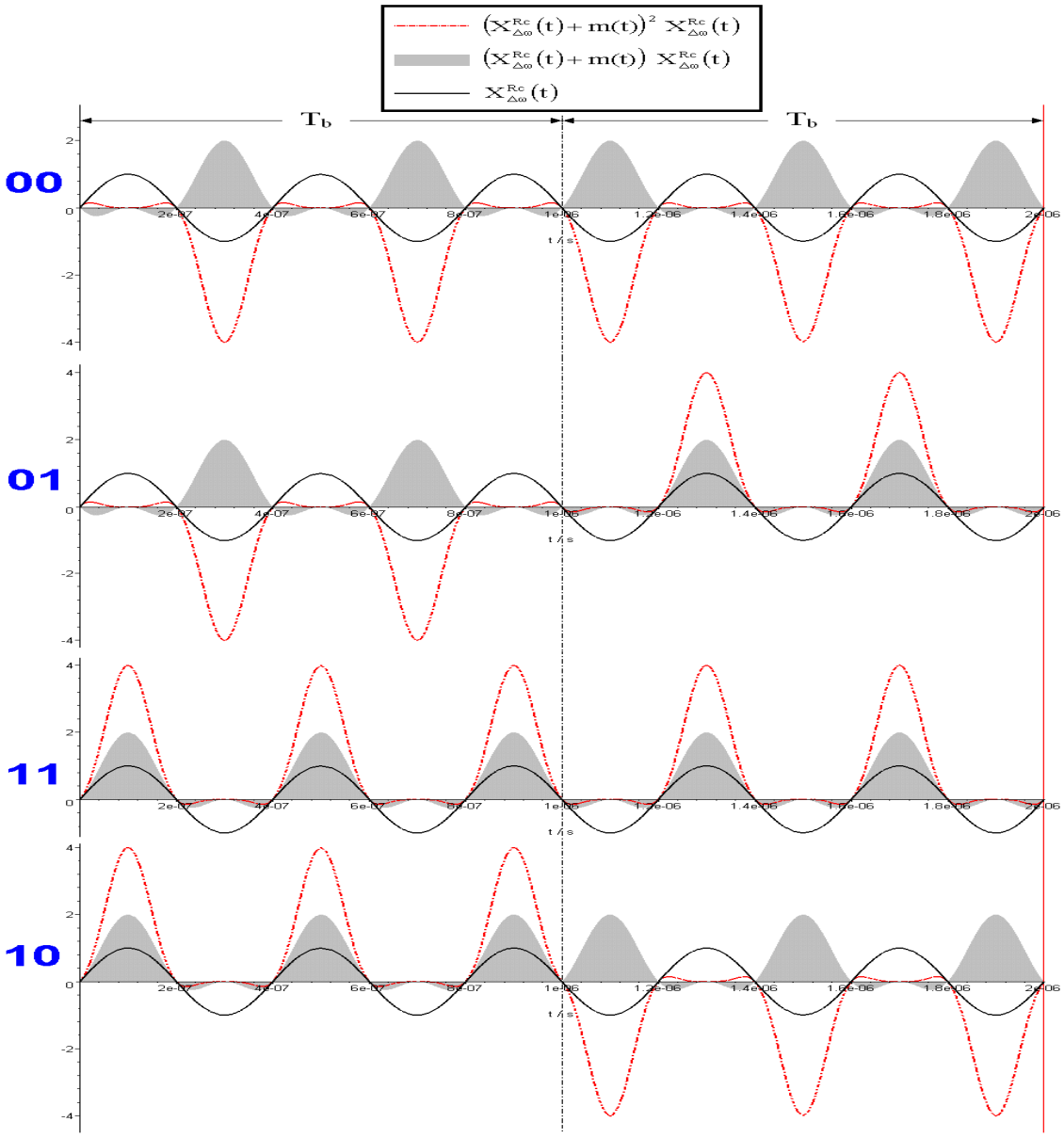

Figure 29: Bias issue for Δω = 2.5 MHz , Rb = 1 M samples/s

This inhomogeneous distribution of the signal and the noise per bit causes different probability in detecting the zero and one -bits in each pattern, namely 00, 01, 11 and 10. Thus, it degrades the performance of the system as it is shown later.

[5] R_b: bit rate. In this thesis, the number of symbols are equal to the number of bits therefore R_b = B.

The distribution can be made homogeneous by letting the filter of Figure 20 to integrate from 0 to 4/5 T_b as shown in Figure 30.

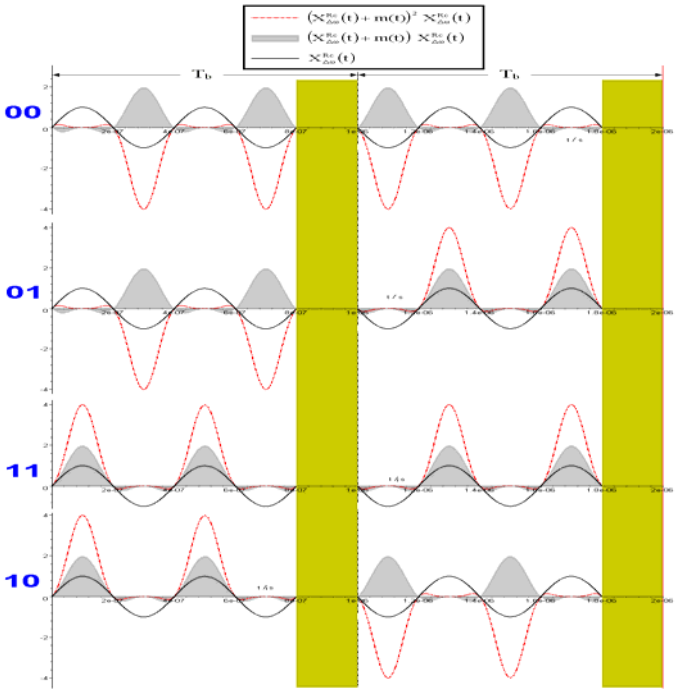

Figure 30: Solving the bias issue for Δω = 2.5 MHz , R_b = 1 M samples/s

A Simulink model as explained in Appendix 2 for the Noise Modulation system is built to inspect the effect of the bias issue on the BER. The results of our model are shown in Figure 31.

As you can observe in Figure 31 that when there exists a non-integer ratio between Δω en R_b (Δω = 2.5 MHz, R_b = 1 M samples/s) then the BER performance degrades, if the filter integrates over the whole bit time as shown by Curve 2. Using the solution depicted in Figure 30 improves the BER as shown by Curve 3. However even this solution is not enough to improve the BER to that degree shown by Curve 1, where there exist an integer ratio between Δω en R_b (Δω = 2 MHz, R_b = 1 M samples/s). This is because of an inefficient use of one bit time interval.

Thus, choosing an integer ratio between Δω en R_b provides the maximum performance, due to the maximum utilizing of one bit time interval.

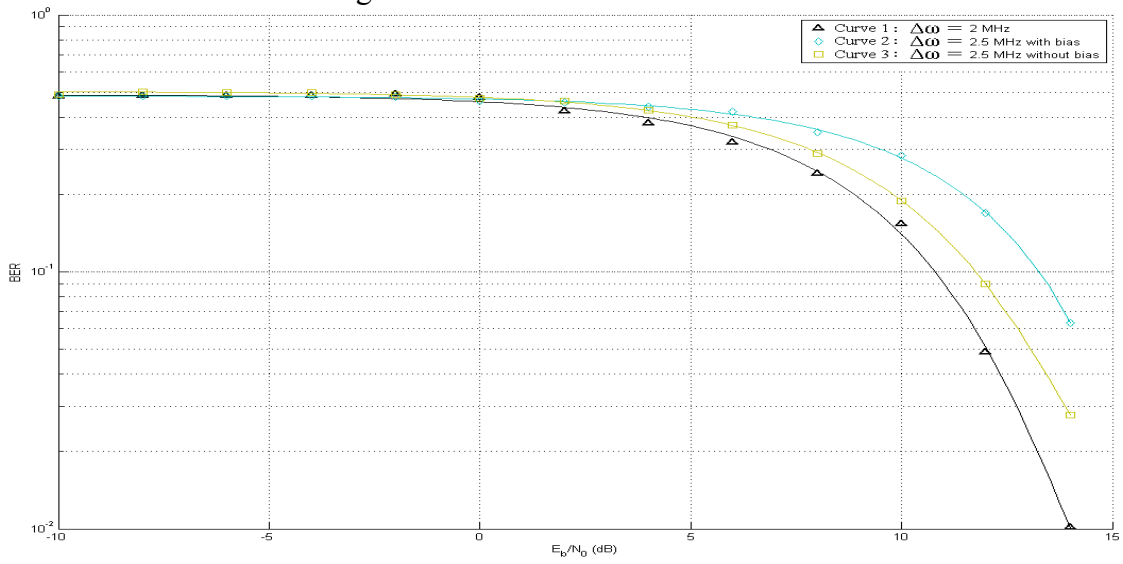

Figure 31: The effect of the bias issue on the performance

2.4 Frequency synchronization

In the ideal case, the receiver needs to be coherent in the sense that it requires two forms of synchronization for its operation:

1. Phase synchronization, which ensures that the local oscillator in the receiver is locked in phase with respect to that employed in the transmitter.
2. Timing synchronization, which ensures proper timing of the decision-making operation in the receiver with respect to the sampling instants (i.e. switching between bits 1 and 0)

The phase synchronization problem decreases the bit energy at the input of the filter. This can be explained by inspecting Equation 2-29, which is rewritten as follows:

$$y(t) = \underbrace{X_{ref}^2(t)}_{\text{Random positive samples}} \quad \underbrace{\left(X_{\Delta\omega}^{\text{Tx}}(t)+m(t)\right)^2 \times X_{\Delta\omega}^{\text{Rc}}(t)}_{\text{Deterministic Signal}}$$

As mentioned that $X_{ref}^2(t)$ represents a positive samples and that the deterministic part decide if those samples must stay positive or convert to become negative samples so that the filter will produce bit 1 or bit 0, respectively. In Figure 32, the deterministic part of the equation above are plotted for different phase differences φ between the local oscillators in the receiver and the transmitter:

$$X_{\Delta\omega}^{Tr}(t) = \sin(\Delta\omega t)$$
$$X_{\Delta\omega}^{Rc}(t) = \sin(\Delta\omega t + \varphi)$$

Figure 32 shows that the area under the deterministic signal for one bit time T_b is a cosine function of φ. This is the same results as what Chang found:

$$E\{Z(t)\}_{NotSynchronized} = E\{Z(t)\}_{Synchronized} \times \cos(\varphi)$$

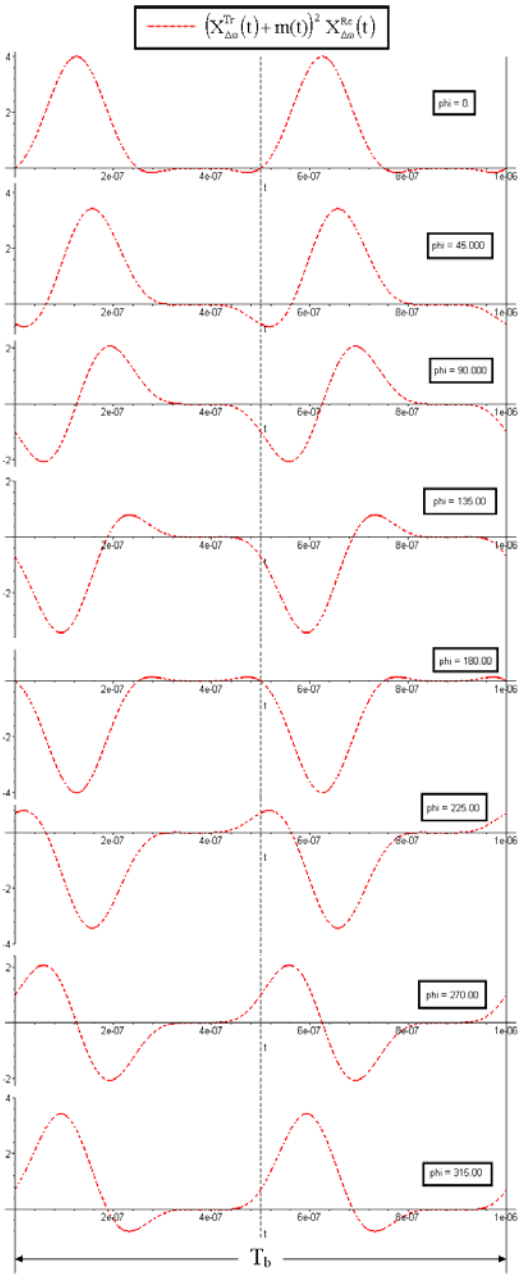

Figure 32: Phase synchronization problem

The conventional way to solve the phase synchronization problem is to use the IQ Costas loop as shown in Figure 33 . However, the Costas loop is just able to solve phase differences less than 45^{o}.

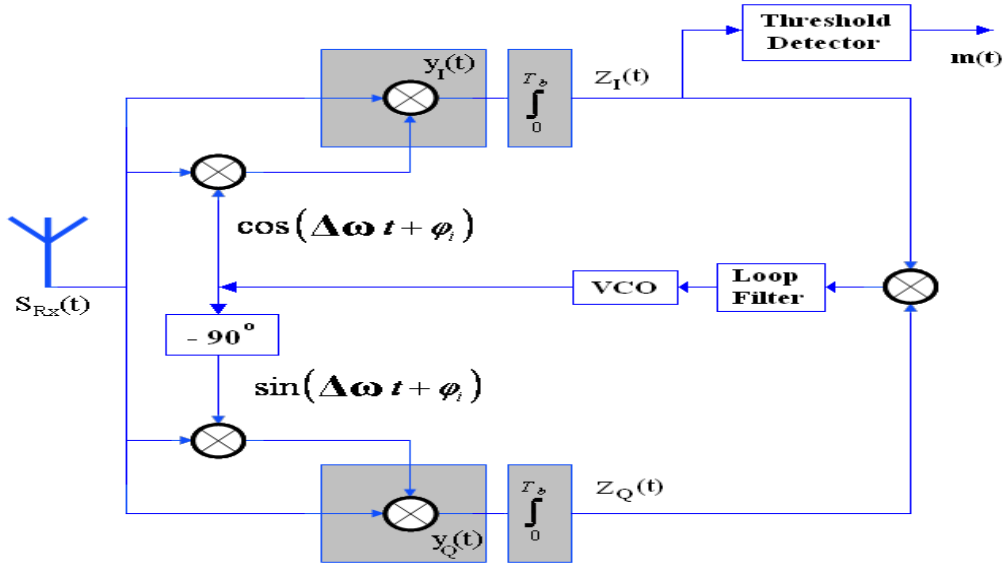

Figure 33: Costas loop receiver

Solving the phase synchronization issue in the analogue domain requires extra components to process the received signal. Mostly, the signal processing in digital domain, where flexible and accurate phase correction algorithms can be easily implemented, requires less energy than in analogue domain. Therefore, we suggest solving the synchronization issues in the digital domain as shown in Figure 34, where the IQ structure provides information about the complex plan of the received signal. The Analogue to Digital Converter (ADC) component samples the IQ signal and converter it to the digital domain.

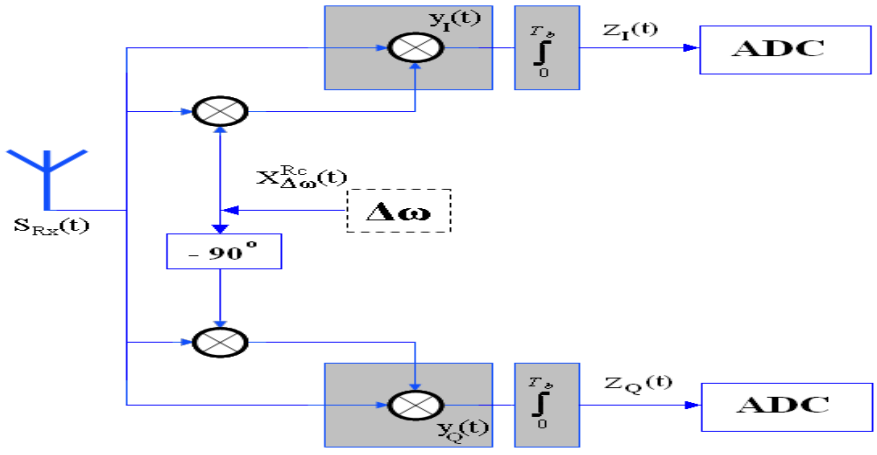

Figure 34: IQ receiver

Chapter 3 : System Design Optimization

After understanding the operation and the signal processing of the Noise Modulation system, this chapter optimizes the design choices at the system level. This optimization is necessary to characterize the system components. The chapter begins with studying the possibility of using Switch Mixers instead of Linear Multipliers to reduce the noise figure of the system. The next section is about the optimum design for the baseband filter in order to achieve a maximum BER performance. Then, the de-spreading block will be introduced and a simpler implementation of it will be explained. The chapter ends with the final schematic of the Noise Modulation system.

3.1 Multiplier vs. Mixer

Switch Mixers are preferable to Linear Multipliers because of their higher gain and lower noise contribution. Figure 35 shows four Linear Multipliers of 1, 2, 3 and 4. The aim of this section is to search the possibility to replace Linear Multipliers of 1, 2 and 3 with Switch Mixers. The 4th Multiplier is necessary to be as linear as possible, because it is responsible about the de-spreading process at the receiver, hence it has a critical influence on the quality of the detection operation.

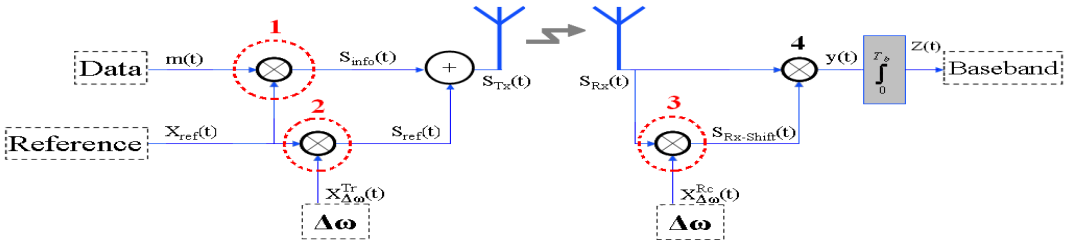

Figure 35: Noise Modulation transceiver

The linear Multiplier of 1 can easily be replaced by a Switch Mixer, because the data *m(t)* is a series of 1 and -1 signals (i.e. a polar NRZ signal). However the replacing of Linear Multipliers of 2 and 3 with Switch Mixers demands that the old $X_{\Delta\omega}^{Tr}(t) = A_{Sine}^{Tr} \times \sin(\Delta\omega t)$ and $X_{\Delta\omega}^{Rc}(t) = A_{Sine}^{Rc} \times \sin(\Delta\omega t)$ must become square signals, with a frequency of $\Delta\omega$ and amplitude of A_{Square}^{Tr} and A_{Square}^{Rc}, respectively as shown in Figure 37 and Figure 39.

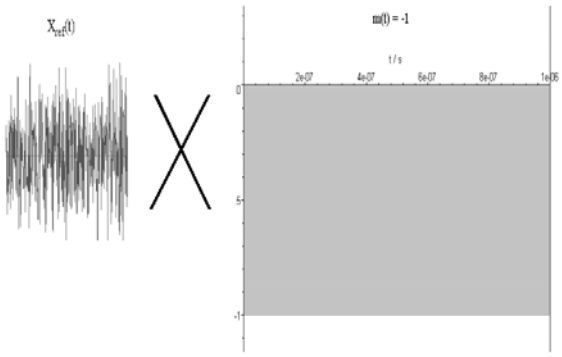

Figure 36: $S_{info}(t) = X_{ref}(t) \times m(t)$ where $m(t) = -1$

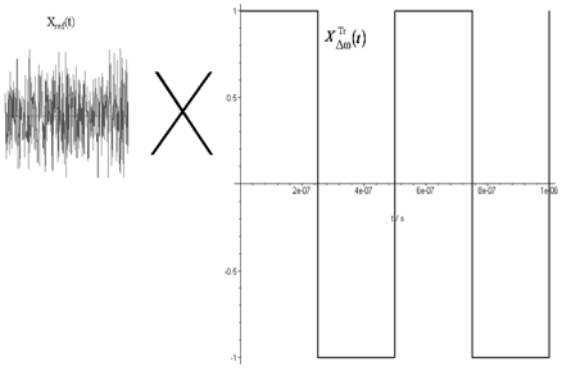

Figure 37: $S_{ref}(t) = X_{ref}(t) \times X_{\Delta\omega}^{Tr}(t)$

Figure 36, Figure 37, Figure 38 and Figure 39 present the time analysis.

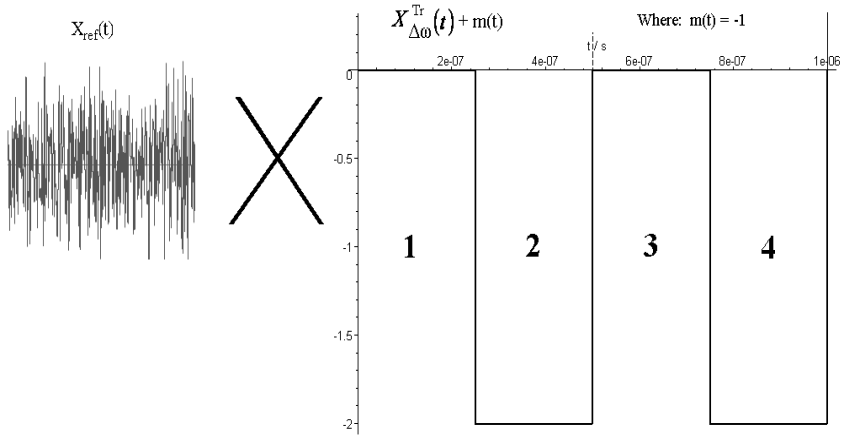

Figure 38: $S_{Tx}(t) = S_{info}(t) + S_{ref}(t)$
Where m(t) = -1

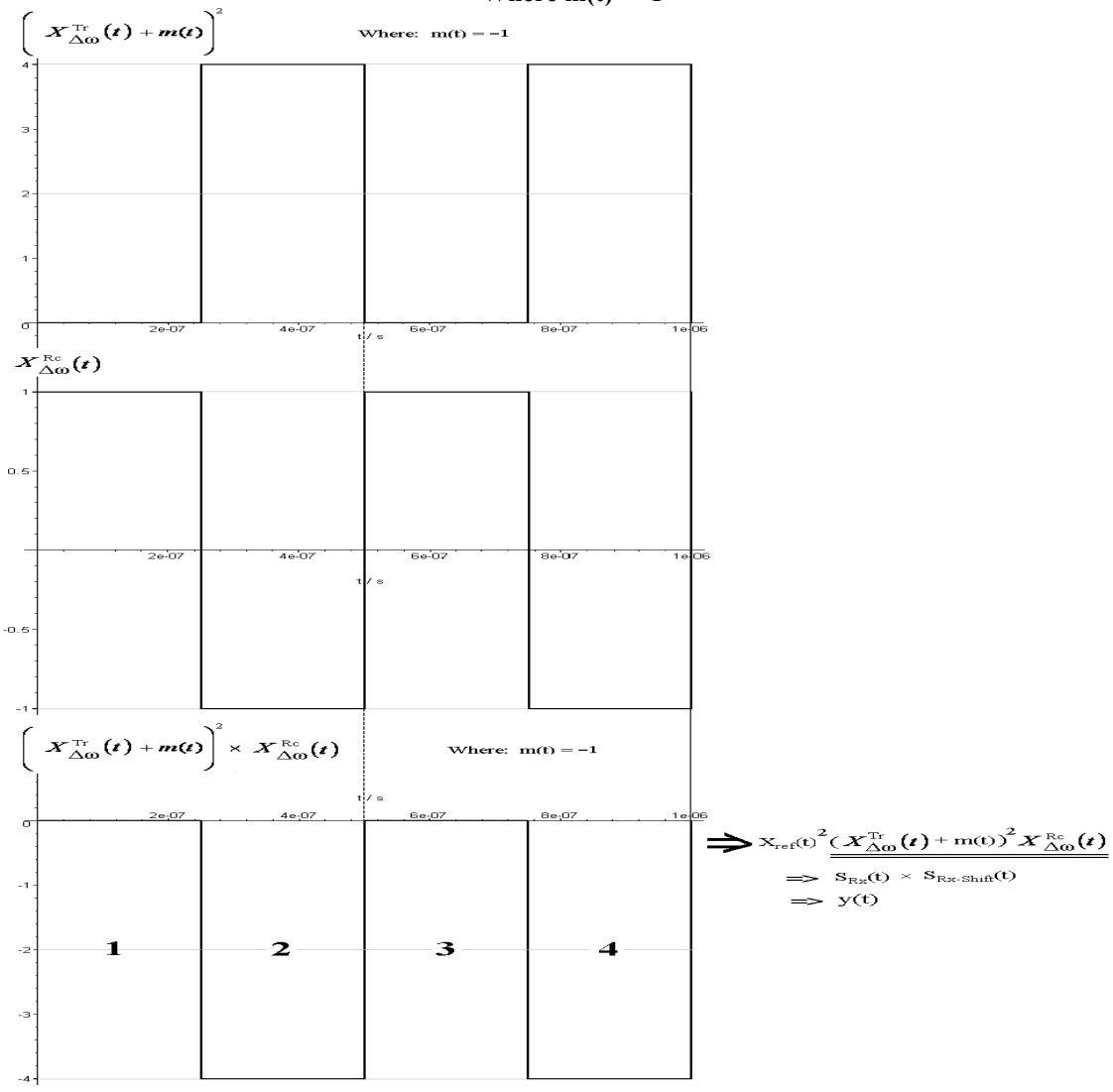

Figure 39: Receiver signal analysis

The interesting point appears when comparing regions 1 and 3 in the deterministic part of *y(t)* between Figure 24 and Figure 39. Figure 39 shows that the deterministic part of *y(t)* is zero in those regions, while Figure 24 shows that the deterministic part of *y(t)* contains a positive signal in those regions. This positive signal gathers the positive samples of $X_{ref}^2(t)$ and produces undesired positive samples (Only the negative samples of y(t) are useful for the detection of bit 0), hence they decrease the energy bit at the output of the baseband filter.
Therefore, by using switched mixers, we may expect an improvement of the performance.

As shown in the figures below, the same time analysis has been done when bit 1 is sent. Again one can observe that the whole energy are only concentrated in regions 1 and 3.

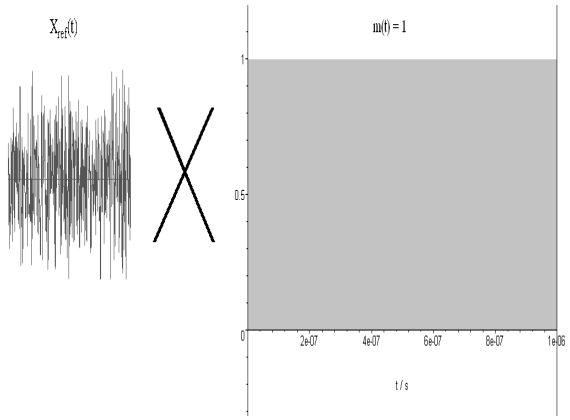

Figure 40: $S_{info}(t) = X_{ref}(t) \times m(t)$ where m(t) = 1

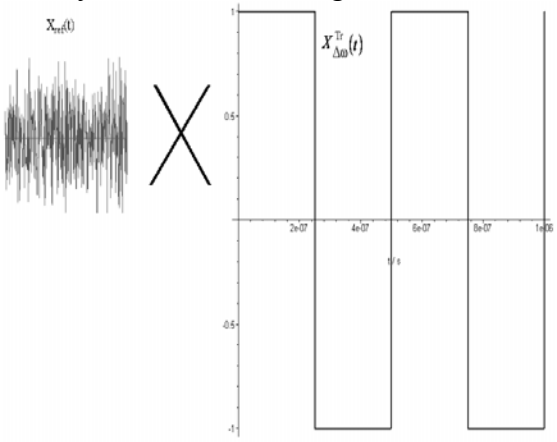

Figure 41: $S_{ref}(t) = X_{ref}(t) \times X_{\Delta\omega}^{Tr}(t)$

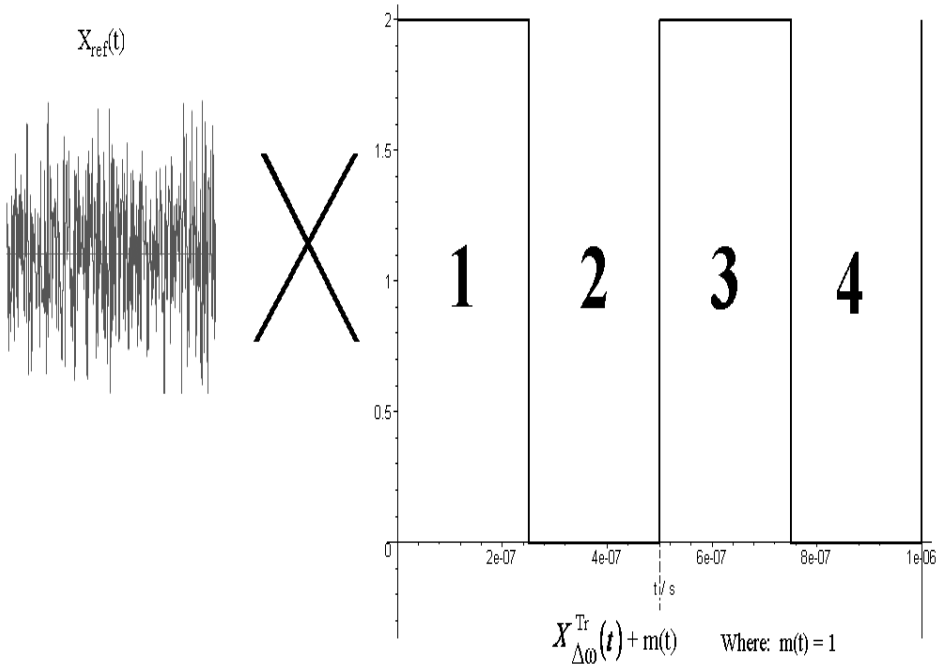

Figure 42: $S_{Tx}(t) = S_{info}(t) + S_{ref}(t)$ where m(t) = 1

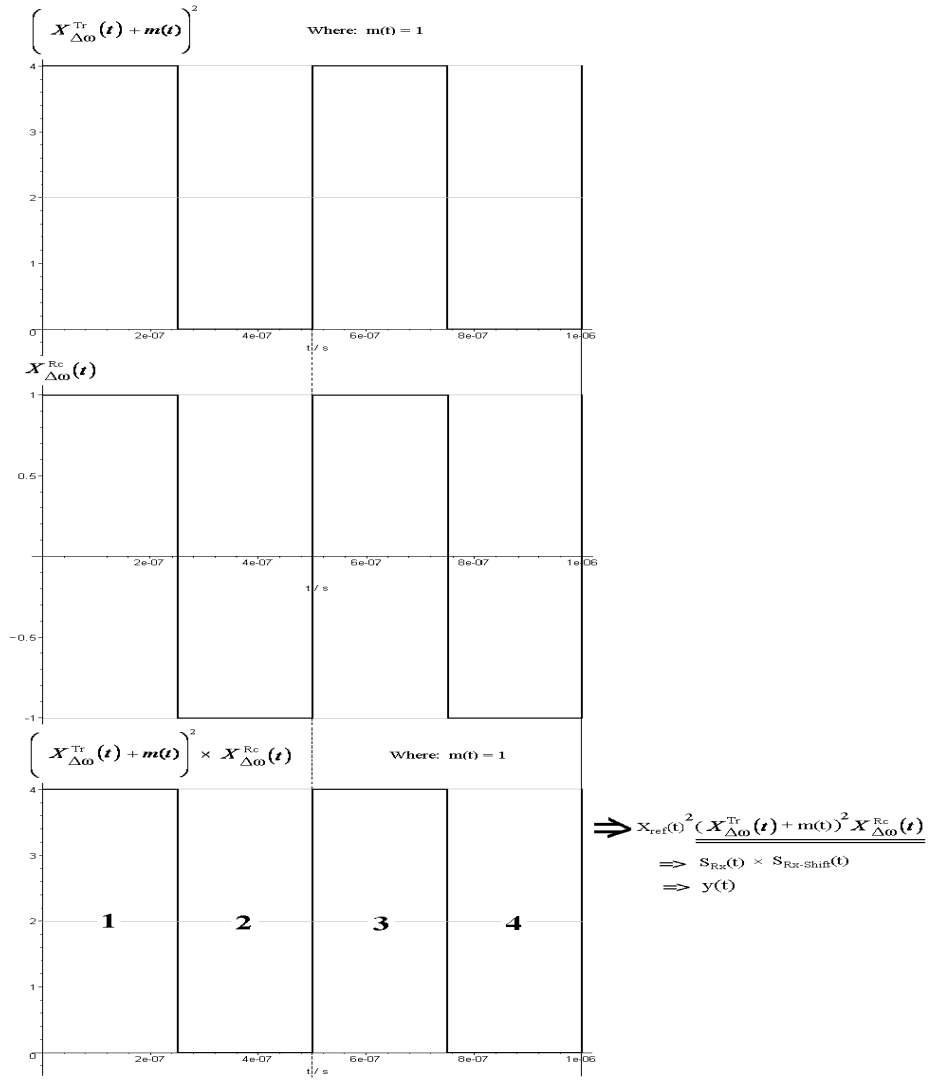

Figure 43: Receiver signal analysis

The Simulink model of chapter 2 has been used to measure the BER for this new system, where Linear Multipliers of 1,2, and 3 are replaced by Switch Mixers. The switch Mixer is modeled by using a multiplier and an oscillator that produce a square signal with a frequency of $\Delta\omega$ and unity amplitude. An ideal square wave does not exist in the reality, therefore a 6 level Fourier series version of the square signal is chosen (See Appendix 3). In order to have a fair BER comparison between this new system and the old one, the amount of power that those Switch Mixers produce must be equal to that produced by Linear Multipliers. This is achieved as follows:

$$A_{Sine}^{Tr} = A_{Sine}^{Rc} = \sqrt{2} \times \sqrt{\sum_{n=1}^{6} \left(\frac{B_n}{\sqrt{2}} \right)^2} = 1.39 \ [V] \qquad \textbf{Equation 3-1}$$

where $B_n = \dfrac{4A_{Square}^{Tr}}{n\pi} = \dfrac{4A_{Square}^{Rc}}{n\pi}$ is the amplitude of the nth element of the Fourier series of the square signal, which has an amplitude of $A_{Square}^{Tr} = A_{Square}^{Rc} = 1$

To complete the picture, the channel noise contribution must also be included. For this purpose Equation 2-31 has been rewritten below:

$$y(t) = X_{ref}^2(t)\underbrace{\left(X_{\Delta\omega}^{Rc}(t) + m(t)\right)^2 X_{\Delta\omega}^{Rc}(t)}_{\text{Deterministic Signal}} \qquad \textbf{Equation 3-2}$$

$$+ \underbrace{2n(t)X_{ref}(t)\underbrace{\left(X_{\Delta\omega}^{Rc}(t) + m(t)\right)X_{\Delta\omega}^{Rc}(t)}_{\text{Deterministic Signal}} + n^2(t)\quad \underbrace{X_{\Delta\omega}^{Rc}(t)}_{\text{Deterministic Signal}}}_{\text{Channel noise contribution}}$$

Figure 44 plot the deterministic parts of Equation 3-2. The BER performance depends on the SNR at the output of the baseband filter:

1. The signal is represented by the dash-dot red line in Figure 44 and Figure 45. In Figure 44, the area under this line in the 1st and 3rd region are approximately equal to that of Figure 45, while as mentioned before that regions 2 and 4 in Figure 44 do not have a negative effect on BER in comparison to the signal of the same regions in Figure 45. Thus, the quality of the signal will be improved by using Switch Mixers.

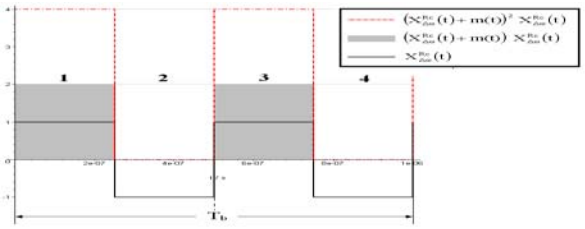

Figure 44: Deterministic parts of Equation 3-2 when Switch Mixers are used (m(t)=1)

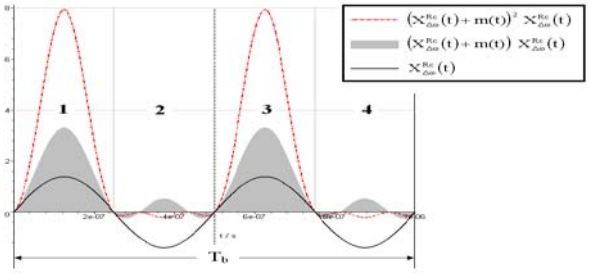

Figure 45: Deterministic parts of Equation 3-2 when Linear Multipliers are used (m(t)=1)

2. The noise is essentially represented by the grey curve in Figure 44 and Figure 45. The area under the grey curve in the 1st and 3rd region on Figure 44 is approximately equal to that of Figure 45. Interesting point is that the grey curve in the 2nd and 4th region in Figure 44 is zero, while those regions in Figure 45 contribute some noise. Thus, less channel noise contribution exists at y(t) by using Switch Mixers.

Therefore, the SNR will be improved by using Switch Mixers, which means a better BER performance. The Simulink model verifies our expectation as shown in Figure 46.

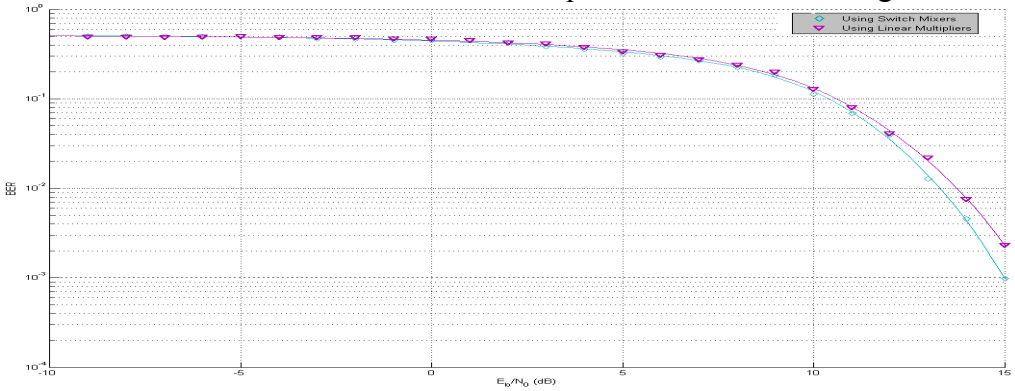

Figure 46: Comparing the BER performance between using Linear Multipliers or Switch Mixers

The conclusion is that replacing the linear Multiplier with Switch Mixer will improve the performance of the Noise Modulation system.

3.2 Baseband Filter

This section investigates the optimum design for the baseband filter (See Figure 47) to increase the bit energy with the assumption that the criterion of the phase synchronization is satisfied.

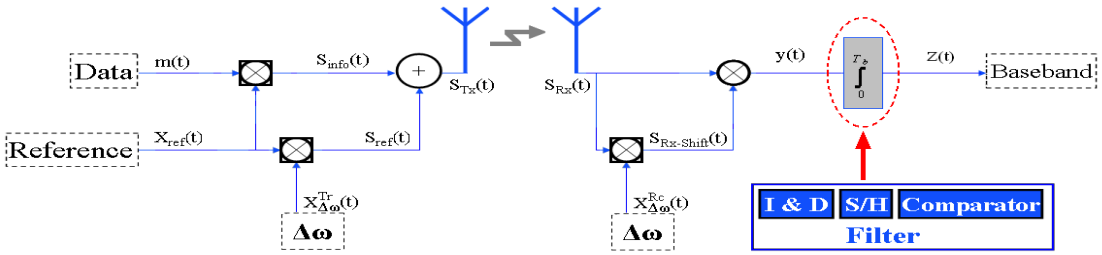

Figure 47: Noise Modulation transceiver, the linear Multiplier are replace by the Switch Mixers

The baseband filter integrates the energy for the duration of one bit time T_b. The result of the integration is compared to a threshold value so that a decision can made whether bit 1 or 0 has been sent. This block consists of three components:

- Integration and Dump (I&D): it creates a cumulative sum of the input signal, while resetting the sum to zero according to a fixed schedule at the end of T_b.
- Sample and Hold (S/H): it acquires the output signal of I&D component when it receives a trigger event before the resetting operation of I&D component. Then it holds the output at the acquired input value until the next triggering event occurs.
- Comparator: it balances the output of the S/H component to a threshold to make a decision about the transmitted bit.

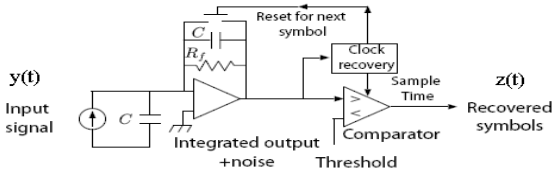

Figure 48: An example of baseband filter uses I&D

Figure 48 shows a simple example of this block, where the working principle is presented. The shape of y(t) is approximated by two blocks for each bit as depicted in Figure 49. The scenario of our example assumes that bit 1 and bit 0 have been sent.

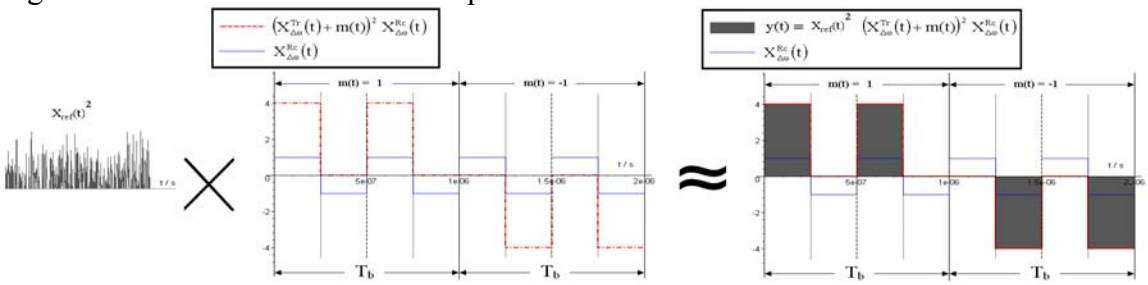

Figure 49: Approximate presentation of y(t)

As depicted in Figure 50, the integrated signal of I&D component will be sampled at T_b. The comparator compares the sample to the threshold signal, which is equal to zero in our system.

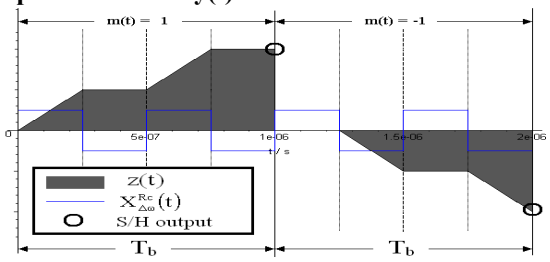

Figure 50:Approximate presentation of z(t)

The optimum design for the baseband is the Matching[6] Filter. The distribution of the energy for bit 0 is different than that for bit 1 as shown in Figure 49. Consequently, the impulse response of the optimum filter must match the shape of the input signal for bit 1 and bit 0 as depicted in Figure 51. As a result, the matching Filter has an impulse response of a block with unity amplitude and a width of T_b, which is a Sinc function in

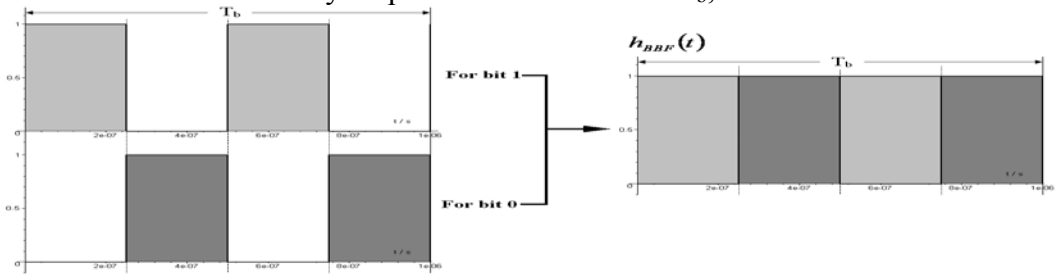

Figure 51: Impulse response of the Matching Filter

the frequency domain. The output of the Matching Filter is the convolution between its impulse response $h_{BBF}(t)$ and its input signal y(t) (See Figure 49):

$$z(t) = \int_{-\infty}^{+\infty} y(\rho) h_{BBF}(t-\rho) d\rho \qquad \textbf{Equation 3-3}$$

The result of the convolution operation is depicted in Figure 52. The S/H acquires a sample at T_b for each bit. Both bits 1 and 0 will have the same bit energy because the amplitudes of those two samples are equal. By replacing I&D component with the Matching Filter in our Simulink model, the BER performance does not change as shown in Figure 53.

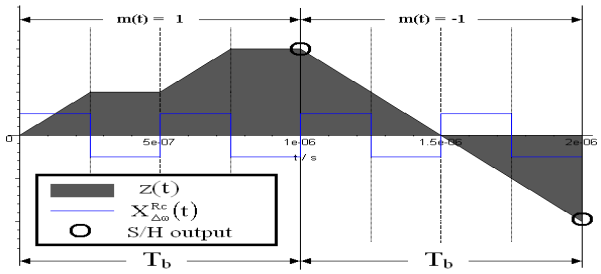

Figure 52: Approximate presentation of z(t), when Matching Filter is used

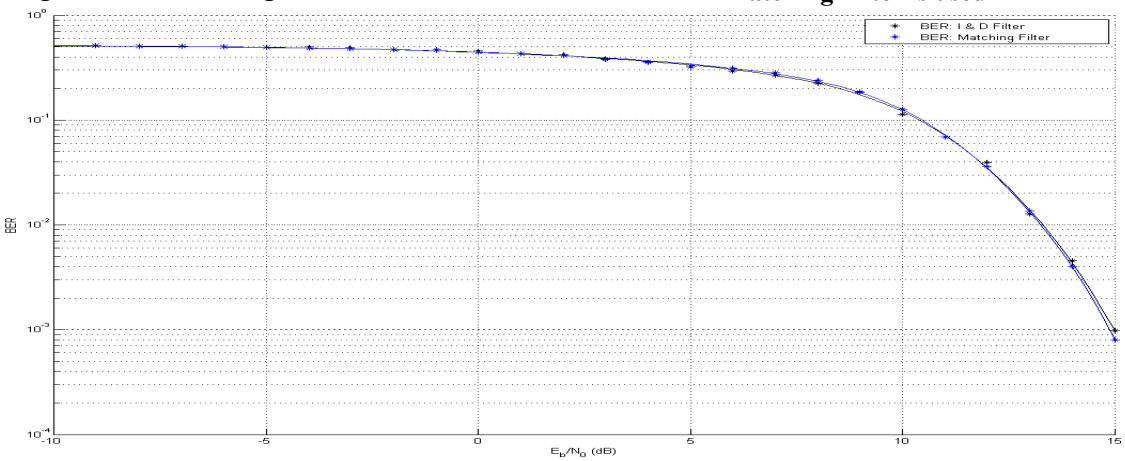

Figure 53: Comparing BER performances for different baseband Filter implementations

The conclusion is that I&D Filter is in fact the Matching filter for our system and can be replaced by a low pass filter + sampling at the proper times (determination of this proper sampling is done in the digital domain).

[6] Matching Filter theory states that in order to optimize the detection operation, the impulse response of the matching filter must be similar to the shape of the known input signal for the duration of T_b.

3.3 De-Spreading Block

The de-spreading block as shown in Figure 54 has the responsibility of de-spreading the received broadband signal at the antenna.

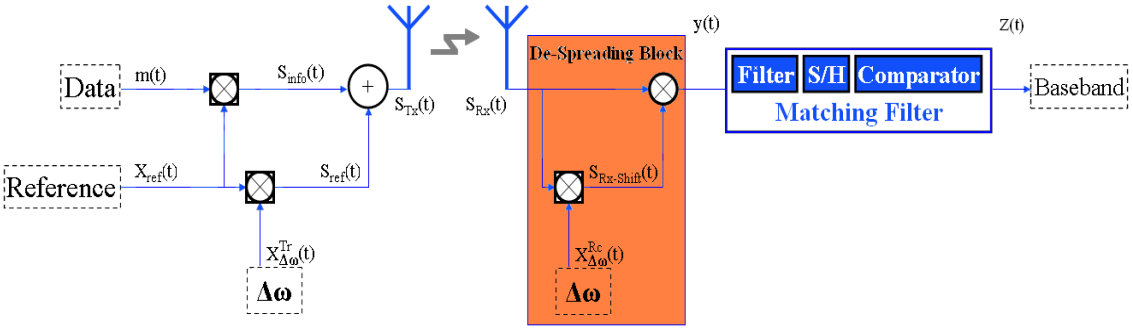

Figure 54: Noise Modulation transceiver

Since multiplication is a commutative operation, the receiver in Figure 54 can be drawn in more convenient form as given in Figure 55 (Massachusetts [5]).

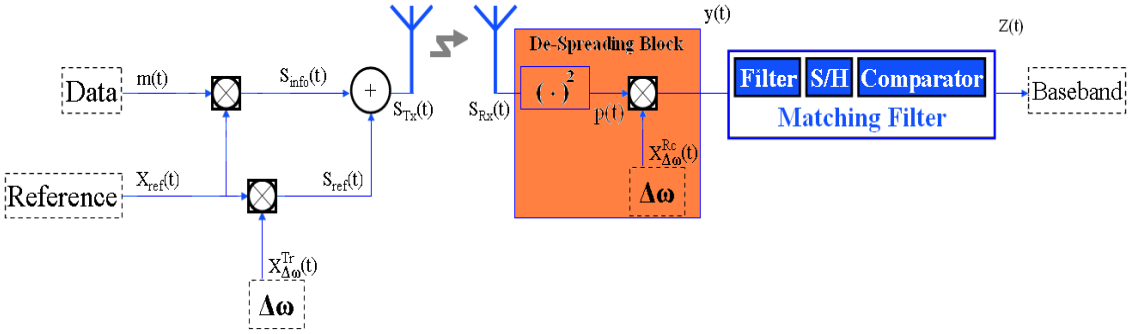

Figure 55: Noise Modulation transceiver

Although that our system uses the mentioned Switch Mixers, but it is interesting to redraw Figure 9 for our new system so that we get an approximate picture about the spectrum of signals *p(t)* and *y(t)*. This is done in Figure 56.

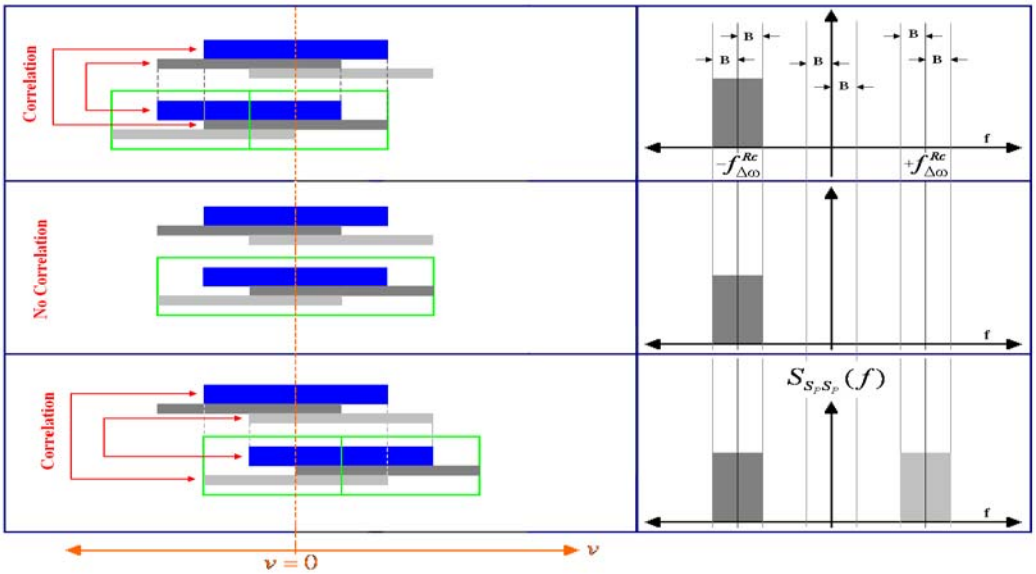

Figure 56: De-spreading operation at the Square component

The spectrum of *p(t)* will be concentrated at $\Delta\omega$ with a bandwidth of *B*. Multipling *p(t)* with $X_{\Delta\omega}^{\mathrm{Rc}}(t)$, which applies the frequency offset $\Delta\omega$ to the receiver, results in the spectrum shown in Figure 57, which is exactly equal to the spectrum of y(t) in Figure 9.

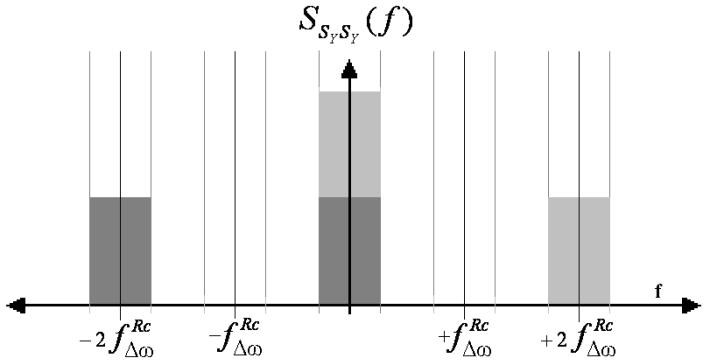

Figure 57: Spectrum of y(t)

Finally, the new schema for the de-spreading block is very useful for the work of chapter 4, where the RF specifications are distributed on each component. This is because in the new schema, the De-Spreading block consists of two components in series, whereas in the schema of Figure 54, the block is a complex structure, where you can not separately specify the influence of the NF of the Switch Mixer and the linear multiplier on the whole Front End specification.

3.4 Total schematic of the Noise Modulation system

In summary of the system analysis, Figure 58 presents the total schema for the Noise modulation system:

1. At the transmitter, a power amplifier is needed to amplify the power to the required level, which is *0 dBm*.
2. At the receiver, a Front End RF Filter is needed to filter the out of band signals as mentioned previously. The bandwidth of this filter is equal to the bandwidth of the broadband signal $S_{TX}(t)$, *100MHz* around *2.4 GHz*.
3. Three from four Linear Multipliers can be replaced by Switch Mixers. This improves the NF of the system, which means that there is no need to spend extra power consumption to raise the desired signal above the noise.
4. The de-spreading block can be implemented in a more convenient way by using a square component and a Switch Mixer in place of using a Linear Multiplier and a Switch Mixer.
5. Finally, I&D is the matching filter for our system. It can be replaced by a low pass filter + sampling at the proper times (determination of this proper sampling is done in the digital domain).

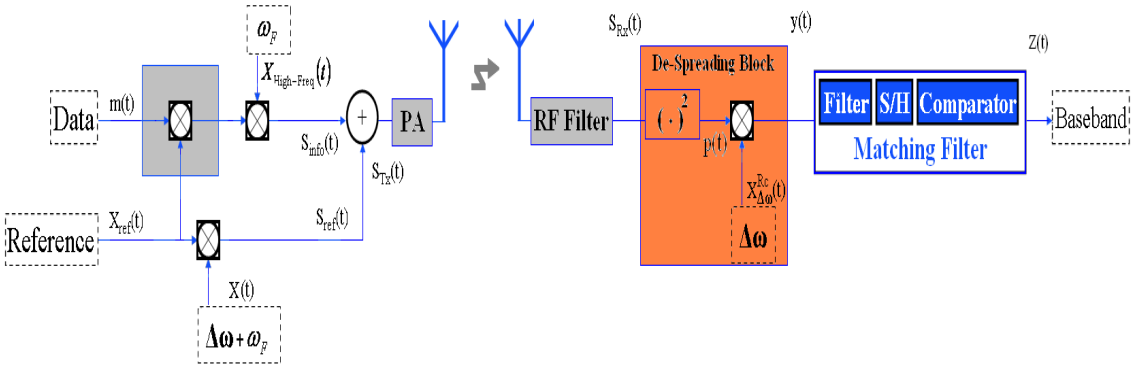

Figure 58: Total schema of the Passband Noise Modulation

Chapter 4 Receiver requirements & Optimization

After optimizing the design choices on the system level, it is the time to map the system requirements to block requirements of the receiver. This is necessary to specify some important requirements for the receiver integration on a chip, and also to estimate the required power consumption. The chapter begins to calculate the required voltage gain and the noise figure (*NF*) of the receiver. After designing the squarer component, those gain and NF are distributed over receiver's components. Finally, the chapter ends with a discussion.

4.1 System requirements (NF and Gain)

The fundamental blocks, which are necessary for the signal processing operation in the receiver, are plotted in Figure 59. The Front End components, namely RF Filter, Squarer block, Switch Mixer and the Baseband filter, needs to amplify the received signal at the antenna to an appropriate level above the noise so that the ADC can process it. Therefore it is necessary to specify the required voltage gain and NF for the receiver.

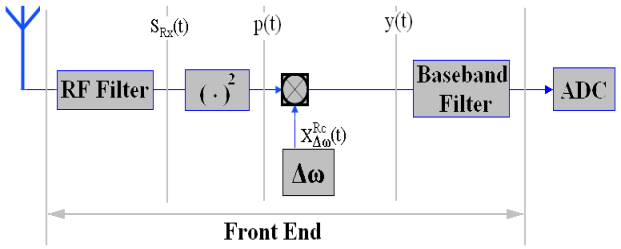

Figure 59: Noise Modulation transceiver

In our derivations, an ideal case is assumed, where the transmitting and receiving antennas are in a free space without boundaries or obstructions. The received signal power at the antenna is given by Rappaport [6]:

$$P_R = \frac{P_T G_T G_R \lambda^2}{(4\pi)^2 d_O^2 L} \qquad \textbf{Equation 4-1}$$

This equation is known Fiis Free space equation, where:

P_T : Transmitted signal power

G : Antenna gain (transmitter and receiver side)

d_O : is a distance of 1m between the transmitter and the receiver

L : The system loss

λ : Signal wave length, which is equal to $\lambda = c / f_{RF} = \frac{3\times10^8}{2.4\ GHz} = 125\ mm$

For isotropic[7] antennas and no system loss, the ratio between transmitted signal power and received signal power is called Path Loss ($PL(d_O)$):

$$PL(d_O) = \frac{P_T}{P_R} = \left(\frac{4\pi d_O}{\lambda}\right)^2 \qquad \textbf{Equation 4-2}$$

[7] For isotropic antennas the antenna gain is equal to one.

By using the Log-distance Path Loss Model [6], Equation 4-2 can be extended to calculate PL for higher distances than just 1m:

$$PL = PL(d_O) + 10\,n \log\left(\frac{d}{d_O}\right)$$
$$= 10 \log\left(\frac{4\pi d_O}{\lambda}\right)^2 + 10\,n \log\left(\frac{d}{d_O}\right) \qquad \textbf{Equation 4-3}$$

where *n* depends on the specific propagation environment. As an example for an urban area cellar radio n is in the range *2.7* to *3.5*. For our calculation *n* is assumed to equal to *3*. In addition to that the chosen distance range (*d*) will be from 1m to *25m*. This range is a good start to investigate the feasibility of designing our receiver in CMOS technology. For this range, *PL* varies from *40 dB* to *82 dB*. The desired transmitted signal power is specified by $P_T = 0\ dBm$. Thus, the received signal power is in the range *-40 dBm* (*2.22 mV*) to *-82 dBm* (*17.8 μV*).

From one side, the signal with *-40 dBm* is the maximum signal that can be expected at the antenna. The Front End amplifies this signal to a level, which is in some radio receivers below the full scale of the ADC with few dB's. Leaving those dB's below the full scale can serve as margin for power from other nearby strong signals. However, our system does not need this margin due to that the received signal is a spread[8] spectrum signal. Therefore, the Front End amplifies the signal with -40 dBm to the level of the full scale (V_{max}) of the ADC. In most typical ADC, the full scale is around 300 mV. Consequently, the required voltage gain is:

$$G_{FE} = \left.\frac{V_{\max}}{\sqrt{0.001 * 50 * 10^{P_{R\max}/10}}}\right|_{dB}$$
$$= 42.5\,dB$$

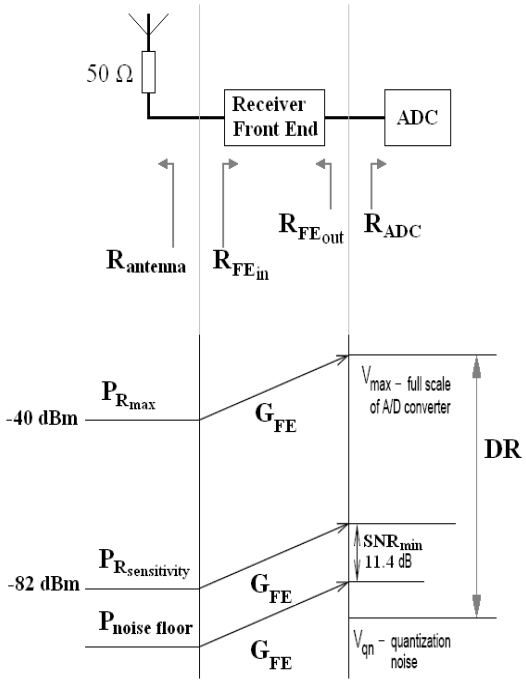

Figure 60: Mapping the applied signal level into the AD Converter

From the other hand, the signal with *-82 dBm* is the minimum signal level that the system can detect with achieving an acceptable signal to noise ratio (*SNR*) as shown in Figure 60. The acceptable *SNR* is related to a desired *BER*. For our system the desired BER must be less or equal than 10^{-4}, which according to Chang [1] the required SNR must be larger or equal to 11.4 dB:

$$BER \leq 0^{-4} \rightarrow SNR \geq 11.4\ dB.$$

[8] Spread spectrum communication system has a high immunity against the interference signals. This is because of that those interference signals are not correlated with the spread spectrum signal. Thus, by the de-spreading operation at the receiver those signals are almost "filtered".

$P_{R\,sensitivity}$ specifies the maximum allowed *NF* for the Front End [8]:

$$NF_{FE} \le P_{R\,sensitivity}\,[\text{dBm}] + 174\,[\text{dbm/Hz}] - 10\log(B)[\text{dB}] - SNR_{\min}\,[\text{dB}] \quad \textbf{Equation 4-4}$$

where:
SNR_{min} : the minimum signal to noise ratio that achieves the desired *BER*. In our system, this SNR_{min} is equal to *11.4 dB* as shown in Figure 60.
With $P_{Rsensitivity}$ = *-82 dBm*, SNR_{min}=*11.4 dB* and *B=1 MHz*, the maximum allowed *NF* must be *20.5 dB*.
The noise floor of the ADC needs to be below the noise floor of the front-end, so that the ADC noise does not contribute in an observable way to the overall NF of the receiver. As the ADC noise begins to contribute to the floor of the receiver, nonlinearities can adversely impact receiver performance, especially when it comes to signal power estimation. Therefore, the ADC noise floor should be as small as reasonable by tuning its sample frequency and number of needed bits.

Thus, the Front End requirements for the front End are as follows:

- G_{FE} = *42.5 dB*
- *NF = 20.5 dB*

For achieving the mentioned voltage gain and *NF*, the receiver architecture needs Low noise amplifiers at the RF side (before the Switch Mixer) and/or amplifier at the Baseband side. However it is not possible to make any decision about the receiver architecture without first investigating the design of the Square block. This is the subject of the next section.

4.2 Squarer Block

As mention previously, the Square component is responsible for the dispreading operation, which makes it to be the core of our receiver. Therefore the main criteria in designing this block must be high performance:

1. High performance: The desired output signal must be a lot larger than the distortion, which is generated by the Squarer block.
2. High conversion gain
3. Low power consumption, as the emphasis inside this project is to design low power receiver using the Noise Modulation concept.

Optimum design choice

We want to implement the square function using a CMOS process with MOSFET transistors. A MOSFET transistor has three operating regions, namely the Saturation, Triode and Subthreshold–region. Each operation region provides the possibility to realize the square function as follows:

Saturation Multiplier

The basic condition for a transistor to operate in the triode region is $V_{GS} - V_{TH} \le V_{DS}$. The drain current has the following equation:

$$I_D = \frac{\beta}{2}\left(V_{GS} - V_{TH}\right)^2 \qquad \textbf{Equation 4-5}$$

Where $\beta = \mu_n C_{OX} \frac{W}{L}$

By adding the desired RF signal to the gate voltage: $V_{GS} = V_G + V_{RF}$, the drain current becomes:

$$\begin{aligned} I_D &= \frac{\beta}{2}\left(\left(V_G + V_{RF}\right) - V_{TH}\right)^2 \\ &= \frac{\beta}{2}\left(V_{GT}^2 + 2V_{RF}V_{GT} + V_{RF}^2\right) \\ &= \frac{\beta}{2}\left(V_{GT}^2 + 2V_{RF}V_{GT}\right) + \frac{\beta}{2}V_{RF}^2 \end{aligned} \qquad \textbf{Equation 4-6}$$

Where $V_{GT} = V_G - V_{TH}$

Although the drain current contains the squaring term $V_{RF}^2\,\beta/2$, the circuit still needs to cancel the first two terms from Equation 4-6.

Linear (Triode) Multiplier

The basic condition to operate in the triode region is $V_{GS} - V_{TH} \ge V_{DS}$. The drain current has the following equation:

$$I_D = \beta\left(\left(V_{GS} - V_{TH}\right)V_{DS} - \frac{1}{2}V_{DS}^2\right) \qquad \textbf{Equation 4-7}$$

By making $V_{DS} = V_{RF}$, the drain current becomes:

$$\begin{aligned} I_D &= \beta\left(\left(V_{GS} - V_{TH}\right)V_{RF} - \frac{1}{2}V_{RF}^2\right) \\ &= \beta\left(V_{GS} - V_{TH}\right)V_{RF} - \frac{\beta}{2}V_{RF}^2 \end{aligned} \qquad \textbf{Equation 4-8}$$

The drain current contains the desired squarer term $V_{RF}^2\,\beta/2$, but again the circuit still needs to cancel the first two terms from Equation 4-8.

Subthreshold Multiplier

A transistor operates in Subthreshold region has $V_{GS} \approx V_{TH}$. The drain current has the following equation:

$$I_D = I_O e^{\frac{V_{GS}}{\zeta V_T}} \qquad \textbf{Equation 4-9}$$

Where ζ >1 is a nonlinearity factor and $V_T = kT/q = 25$ mV

By making $V_{GS} = V_G + V_{RF}$, the drain current becomes:

$$I_D = I_O e^{\frac{V_G + V_{RF}}{\zeta V_T}} = \underbrace{I_O e^{\frac{V_G}{\zeta V_T}}}_{I_O''} e^{\frac{V_{RF}}{\zeta V_T}} = I_O'' e^{\frac{V_{RF}}{\zeta V_T}} \qquad \textbf{Equation 4-10}$$

Taking the Taylor expansion for e^x around x = 0:

$$e^x = 1 + \frac{x}{1!} + \frac{x^2}{2!} + ... \qquad \textbf{Equation 4-11}$$

for Equation 4-10 gives:

$$I_D = a_0 + a_1 V_{RF} + a_2 V_{RF}^2 + ... \qquad \textbf{Equation 4-12}$$

As it can be observed that the drain current contains the desired square element $a_2 V_{RF}^2$,

where $a_2 = \frac{I_O''}{2} \frac{1}{(\zeta V_T)^2}$

In this situation, the circuit needs to cancel a lot of elements from Equation 4-12 that distorts the desired output signal.

The optimum selection between those three choices will be based on our criteria:

1. The performance of the 1st and the 2nd choice are better than the 3rd choice, because their drain current contains less distortion terms. The distortion terms in Equation 4-6 and Equation 4-8 are additive, hence it is easier to cancel them in comparison to those in Equation 4-12, because of the exponential character of Equation 4-10.
2. All the three choices can have higher conversion gain, for example by increasing the width of the transistor.
3. The 2nd choice consumes no DC current in compare to the 1st one. Consequently, the 2nd choice satisfies all our targets as summarized in Table 2:

	Saturation	**Linear**	**Subthreshold**
Unwanted distortion terms	Good	Good	Bad
Power consumption	Bad	Good	Medium
Conversion gain	Good	Good	Good

Table 2: Optimum choice to design the Square Multiplier

Component Design

Although the previous section proposes the triode operation region as the optimum choice for building the Square component, there are still terms that must be canceled from Equation 4-8. Figure 61 shows the implementation of Equation 4-8 on a circuit level. The 2.4 GHz RF voltage signal is supplied to terminals (a) and (b) of the MOSFET

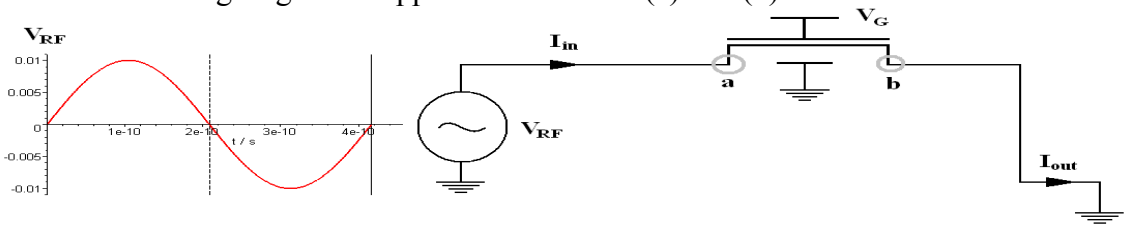

Figure 61: Begin concept to build the Square component

transistor. The source terminal alternates between terminals (b) and (a) as the input voltage signal alternates between positive and negative, respectively:

$$V_{RF} > 0 \rightarrow I_D = I_{in} \rightarrow \text{Terminal (b) is the Source}$$

$$V_{RF} < 0 \rightarrow I_D = -I_{in} \rightarrow \text{Terminal (a) is the Source}$$

Where I_D: the drain current

Let's take the scenario when $V_{RF} > 0$:

$$I_{out} = I_{in} = I_D = \beta\left(V_{GS} - V_{TH}\right)V_{DS} - \frac{\beta}{2}V_{DS}^2 \qquad \textbf{Equation 4-13}$$

$$= \underbrace{\beta\left(V_{GS} - V_{TH}\right)V_{RF}}_{\text{RF current}} - \underbrace{\frac{\beta}{2}V_{RF}^2}_{\text{Square current}}$$

To cancel the RF current from Equation 4-13, the differential structure is used as it is depicted in Figure 62, where $V_{RF} = V_{RF1} - V_{RF2}$. The terminals (b1) and (a2) are the source terminal for the top and bottom transistor, respectively.

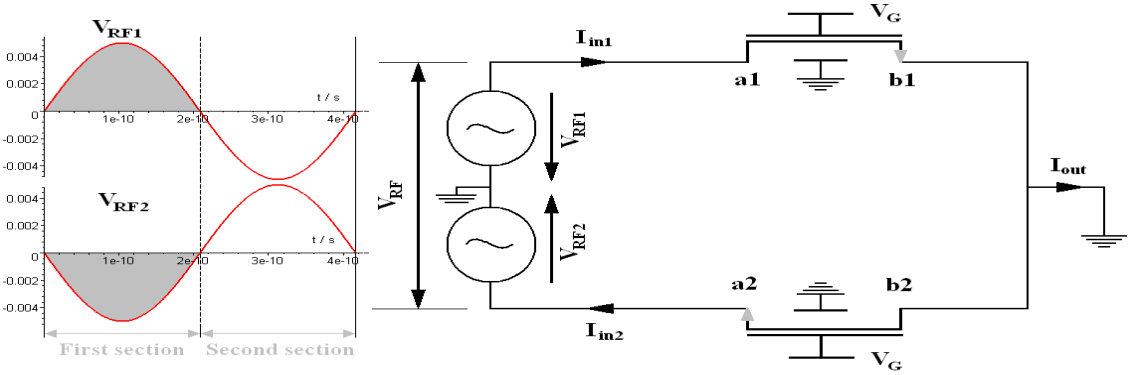

Figure 62: Canceling the nonlinear terms in the output of the Square component

The equation of the top transistor is:

$$I_{in1} = I_{D1} = \beta\left(V_{GS1} - V_{TH}\right)V_{DS1} - \frac{\beta}{2}V_{DS1}^2$$

$$= \beta\left(V_{GS1} - V_{TH}\right)V_{RF1} - \frac{\beta}{2}V_{RF1}^2$$

$$= \beta\left(V_G - V_{TH}\right)V_{RF1} - \frac{\beta}{2}V_{RF1}^2$$

$$= \beta V_{GT} V_{RF1} - \frac{\beta}{2} V_{RF1}^2 \qquad \textbf{Equation 4-14}$$

The equation of the bottom transistor is:

$$I_{in2} = I_{D2} = \beta\left(V_{GS2} - V_{TH}\right)V_{DS2} - \frac{\beta}{2}V_{DS2}^2$$

$$= \beta\left(V_{GS2} - V_{TH}\right)\left(-V_{RF2}\right) - \frac{\beta}{2}\left(-V_{RF2}\right)^2$$

$$= \beta\left(V_G - V_{S2} - V_{TH}\right)\left(-V_{RF2}\right) - \frac{\beta}{2}V_{RF2}^2$$

$$= \beta\left(V_G - V_{TH}\right)\left(-V_{RF2}\right) + \beta V_{S2} V_{RF2} - \frac{\beta}{2}V_{RF2}^2 \qquad \textbf{Equation 4-15}$$

As $V_{S2} = V_{RF2}$ then:

$$I_{in2} = \beta V_{GT}\left(-V_{RF2}\right) + \beta V_{RF2}^2 - \frac{\beta}{2}V_{RF2}^2$$

$$= \beta V_{GT}\left(-V_{RF2}\right) - \frac{\beta}{2}V_{RF2}^2 + \beta V_{RF2}^2 \qquad \textbf{Equation 4-16}$$

Finally: $I_{out} = I_{in1} - I_{in2}$

$$I_{out} = \left[\beta V_{GT} V_{RF1} - \frac{\beta}{2}V_{RF1}^2\right] - \left[\beta V_{GT}\left(-V_{RF2}\right) - \frac{\beta}{2}V_{RF2}^2 + \beta V_{RF2}^2\right] \qquad \textbf{Equation 4-17}$$

But $V_{RF2} = -V_{RF1}$ then:

$$I_{out} = \left[\beta V_{GT} V_{RF1} - \frac{\beta}{2}V_{RF1}^2\right] - \left[\beta V_{RF1} - \frac{\beta}{2}V_{RF1}^2 + \beta V_{RF1}^2\right]$$

$$= -\beta V_{RF1}^2 \qquad \textbf{Equation 4-18}$$

The previous derivations show that the squarer circuit redrawn in Figure 63 produces partly symmetrical terms which stay inside the loop of the Square component, while the asymmetrical current terms flow outside the loop from the output terminal to the negative RF-input.

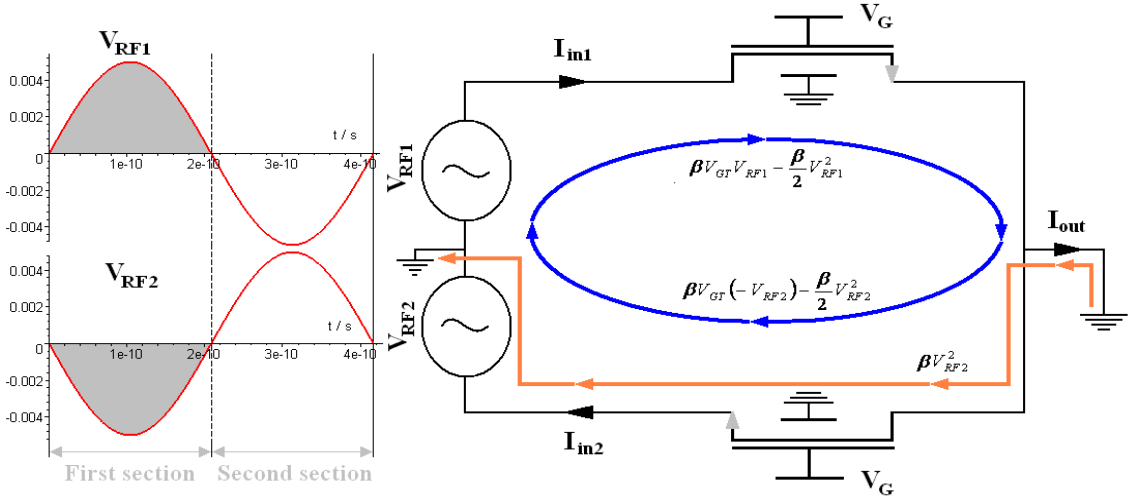

Figure 63: The current flow for the first section of the RF signal period

Till now the operation of the Square component has been analyzed for the first section of the RF signal period. For the second section, similar analysis can be derived to proof the

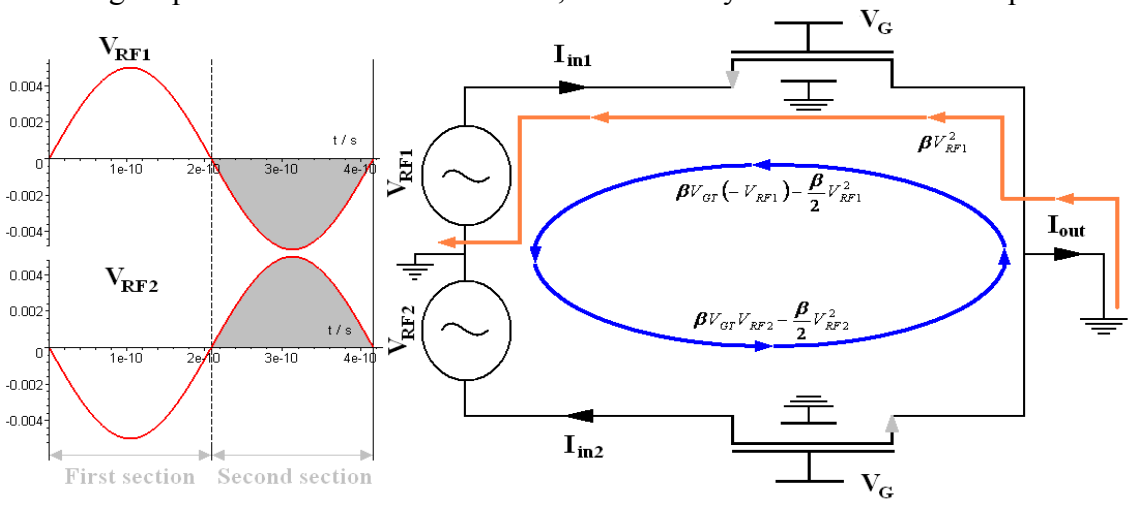

Figure 64: The current flow for the second section of the RF signal period

results shown in Figure 64. Consequently, in each section of the RF signal period, only one transistor will provide the desired current to the output terminal. In addition, this same transistor that provides the desired current will also generate an extra current due to the bulk effect. This extra current belongs to the group of asymmetrical currents. Therefore it flows towards the output. Fortunately, it is much smaller than the desired square current:

$$\frac{\text{Square current}}{\text{Bulk effect current distortion}} = \frac{1}{V_{RF1}}\left(\frac{8}{\gamma}\sqrt{(2\Phi_F)^3} + 4(2\Phi_F)\right) \qquad \textbf{Equation 4-19}$$

Where: $\Phi_F = \frac{kT}{q}\ln\left(\frac{N_{sub}}{n_i}\right)$ [V]

N_{sub} : Dopping concentration of the substrate

γ : body effect coefficient [$\sqrt{\text{V}}$]

Equation 4-19 has been derived in Appendix 4. For example a 0.5 µm transistor has $2\Phi_F = 0.9$ V and $\gamma = 0.45\ (\text{V})^{1/2}$:

$V_{RF1} = 5$ mV then $\frac{\text{Square current}}{\text{Bulk effect current distortion}} = 3.76\times10^3$

Hence, the bulk effects can be neglected in our analysis.

The differential input voltage V_{RF1} and V_{RF2} is actually the balance side of a BalUn (BalUn with a centre tap) or the output terminal of a LNA (in case, the receiver needs the utility of a LNA). In either situation, both V_{RF1} and V_{RF2} will have their own internal impedance. For simplicity, let's assume that they are two resistances *R1* and *R2* as shown

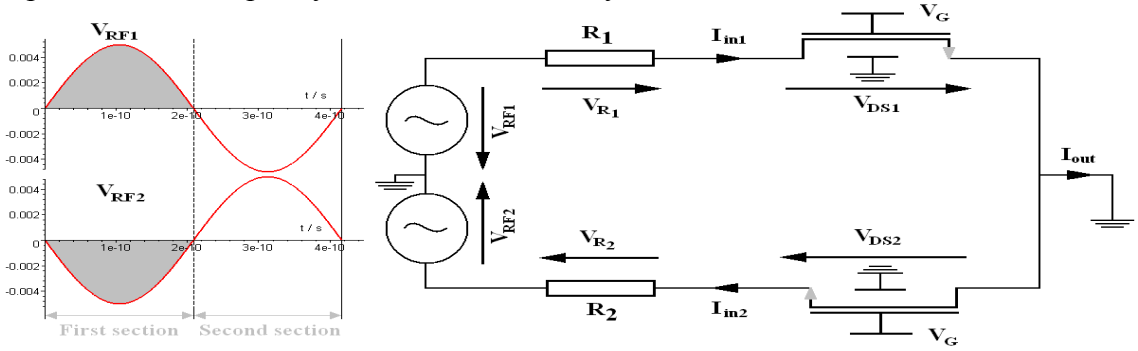

Figure 65: Square component

in Figure 65. The existence of those internal resistances complicates the analysis of the output current. For the first section of the RF signal period as shown in Figure 65:

$$I_{in1} = I_{D1} = \beta\left(V_{GS1} - V_{TH}\right)V_{DS1} - \frac{\beta}{2}V_{DS1}^2$$

$$= \beta V_{GT} V_{DS1} - \frac{\beta}{2}V_{DS1}^2$$

But $V_{DS1} = V_{RF1} - V_{R_1}$:

$$I_{in1} = \beta V_{GT}\left(V_{RF1} - V_{R_1}\right) - \frac{\beta}{2}\left(V_{RF1} - V_{R_1}\right)^2$$

$$= -\frac{\beta}{2}V_{R_1}^2 - \beta V_{R_1}\left(V_{GT} - V_{RF1}\right) - \frac{\beta}{2}V_{RF1}^2 + \beta V_{GT} V_{RF1}$$

And $V_{R1} = I_{in1}R1$:

$$I_{in1} = -\frac{\beta}{2}\left(I_{in1}R_1\right)^2 - \beta\left(I_{in1}R_1\right)\left(V_{GT} - V_{RF1}\right) - \frac{\beta}{2}V_{RF1}^2 + \beta V_{GT} V_{RF1}$$

$$= \left[-\frac{\beta}{2}R_1^2\right]I_{in1}^2 - \left[\beta R_1\left(V_{GT} - V_{RF1}\right)\right]I_{in1} - \left[\frac{\beta}{2}V_{RF1}^2 - \beta V_{GT} V_{RF1}\right]$$

$$\Rightarrow \left[\frac{\beta}{2}R_1^2\right]I_{in1}^2 + \left[1 + \beta R_1\left(V_{GT} - V_{RF1}\right)\right]I_{in1} + \left[\frac{\beta}{2}V_{RF1}^2 - \beta V_{GT} V_{RF1}\right] = 0$$

Solving this equation with respect to I_{in1} results in:

$$I_{in1} = \frac{-\left[1 + \beta R_1\left(V_{GT} - V_{RF1}\right)\right] \pm \sqrt{1 - 2\beta R_1 V_{RF1} + 2\beta R_1 V_{GT} + \left(\beta R_1 V_{GT}\right)^2}}{\beta R_1^2} \qquad \textbf{Equation 4-20}$$

The same analysis will be done for I_{in2}:

$$I_{in2} = I_{D2} = \beta\left(V_{GS2} - V_{TH}\right)V_{DS2} - \frac{\beta}{2}V_{DS2}^2$$

$$= \beta\left(V_G - V_{S2} - V_{TH}\right)V_{DS2} - \frac{\beta}{2}V_{DS2}^2$$

$$= \beta V_{GT} V_{DS2} - \beta V_{S2} V_{DS2} - \frac{\beta}{2}V_{DS2}^2$$

But $V_{S2} = -V_{DS2}$

$$I_{in\,2} = \beta V_{GT} V_{DS\,2} - \beta\left(-V_{DS\,2}\right)V_{DS\,2} - \frac{\beta}{2}V_{DS\,2}^2 = \beta V_{GT} V_{DS\,2} + \beta V_{DS\,2}^2 - \frac{\beta}{2}V_{DS\,2}^2$$

$$= \beta V_{GT} V_{DS\,2} + \frac{\beta}{2}V_{DS\,2}^2$$

But $V_{DS2} = -V_{RF2} - V_{R_2}$:

$$I_{in\,1} = \beta V_{GT}\left(-V_{RF\,2} - V_{R_2}\right) + \frac{\beta}{2}\left(-V_{RF\,2} - V_{R_2}\right)^2$$

$$= \frac{\beta}{2}V_{R_2}^2 - \beta V_{R_2}\left(V_{GT} - V_{RF\,2}\right) + \frac{\beta}{2}V_{RF\,2}^2 - \beta V_{GT} V_{RF\,2}$$

And $V_{R2} = I_{in2}R_2$:

$$I_{in\,2} = \frac{\beta}{2}\left(I_{in\,2}R_2\right)^2 - \beta\left(I_{in\,2}R_2\right)\left(V_{GT} - V_{RF\,2}\right) + \frac{\beta}{2}V_{RF\,2}^2 - \beta V_{GT} V_{RF\,2}$$

$$= \left[\frac{\beta}{2}R_2^2\right]I_{in\,2}^2 - \left[\beta R_2\left(V_{GT} - V_{RF\,2}\right)\right]I_{in\,2} + \left[\frac{\beta}{2}V_{RF\,2}^2 - \beta V_{GT} V_{RF\,2}\right]$$

$$\Rightarrow \left[-\frac{\beta}{2}R_2^2\right]I_{in\,2}^2 + \left[1 + \beta R_2\left(V_{GT} - V_{RF\,2}\right)\right]I_{in\,2} + \left[-\frac{\beta}{2}V_{RF\,2}^2 + \beta V_{GT} V_{RF\,2}\right] = 0$$

Solving this equation with respect to I_{in2} results in:

$$I_{in\,2} = \frac{\left[1 + \beta R_2\left(V_{GT} - V_{RF\,2}\right)\right] \mp \sqrt{1 - 2\beta R_2 V_{RF\,2} + 2\beta R_2 V_{GT} + \left(\beta R_2 V_{GT}\right)^2}}{\beta R_2^2} \qquad \textbf{Equation 4-21}$$

Finally, the output current becomes:

$$I_{out} = I_{in\,1} - I_{in\,2}$$

$$= \frac{-\left[1 + \beta R_1\left(V_{GT} - V_{RF\,1}\right)\right] + \sqrt{1 - 2\beta R_1 V_{RF\,1} + 2\beta R_1 V_{GT} + \left(\beta R_1 V_{GT}\right)^2}}{\beta R_1^2}$$

$$- \frac{\left[1 + \beta R_2\left(V_{GT} - V_{RF\,2}\right)\right] - \sqrt{1 - 2\beta R_2 V_{RF\,2} + 2\beta R_2 V_{GT} + \left(\beta R_2 V_{GT}\right)^2}}{\beta R_2^2}$$

To have a simple expression, let's assume that $R_2 = R_1 = R_S$ and $V_{RF2} = -V_{RF1}$ then the output current is:

$$I_{out} = \frac{-2 - 2\beta R_S V_{GT} + \sqrt{1 - 2\beta R_S V_{RF1} + 2\beta R_S V_{GT} + \left(\beta R_S V_{GT}\right)^2} + \sqrt{1 + 2\beta R_S V_{RF1} + 2\beta R_S V_{GT} + \left(\beta R_S V_{GT}\right)^2}}{\beta R_S^2} \qquad \textbf{Equation 4-22}$$

The same analysis and results hold for the second section of the RF signal period. Maple[9] program has been used to compute the limiting value of I_{out} as R_S approaches zero:

$$\lim_{R_S \to 0}\left(I_{out}\right) = -\beta V_{RF\,1}^2 \qquad \textbf{Equation 4-23}$$

As expected that the result is equal to Equation 4-18. Although this may be an indication that Equation 4-22 is correct, but it is difficult to recognize how the output current is still a square function of V_{RF1}. Taking the Taylor expansion for the square roots in Equation 4-22 shows the following result (See Appendix 5 for the derivation):

$$I_{out} = -\frac{\beta}{\left(1 + \beta R_S V_{GT}\right)^3}V_{RF\,1}^2 \qquad \textbf{Equation 4-24}$$

[9] Maple is a software for exploring and applying mathematics

Comparing Equation 4-24 to Equation 4-18, shows that the existence of R_S will reduce the output current of the Square component by factor of $(1+\beta R_S V_{GT})^3$. In fact, the existence of R_S will also bring V_{GT} to the picture, where small V_{GT} increases the transconductance. To plot this equation, let's take the following example:

$$\text{Transistor}: 0.35\ \mu\text{m with } \mu_n C_{OX} = 178.65\ \mu\text{A/V}^2$$

$$W = 75\ \mu\text{m and } L = 0.35\ \mu\text{m} \Rightarrow \beta = 38.3\ \text{mA/V}^2$$

$$R_S = 35\ \Omega,\ V_G = 1\ \text{V},$$

$$V_{RF1} = 5\times10^{-3}\sin(2\pi f_{RF} t),\ \text{where } f_{RF} = 2.4\ \text{GHz}$$

The output current is plotted in Figure 66. Obviously, the shown output current is a square function of the input signal:

$$\text{Input voltage signal} = A\sin(\omega_{RF} t)$$

$$\Rightarrow I_{out} \propto (A\sin(\omega_{RF} t))^2 = \frac{A^2}{2}(1-\cos(2\omega_{RF} t))$$

The peak value of the output current is 289 nA.

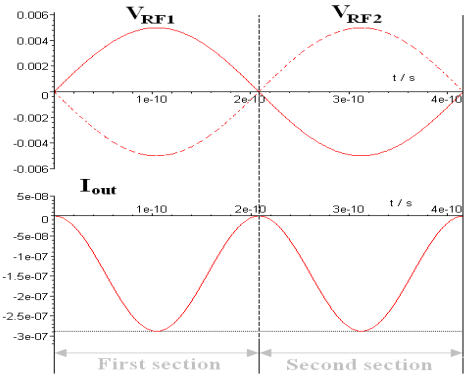

Figure 66: The output current of the Square component (Theory)

Cadence/SpectraRF has been used to verify our theory, where Model 11 of a 0.35 µm transistor with a gate oxide thickness equal to 6.5 nm have been used to build the Square component. The same values of the previous example have been used in our simulation circuit. The simulation results are depicted in Figure 67. As you can observe that the peak value of the output current is 321.64 nA, which is almost equal to our theory result.

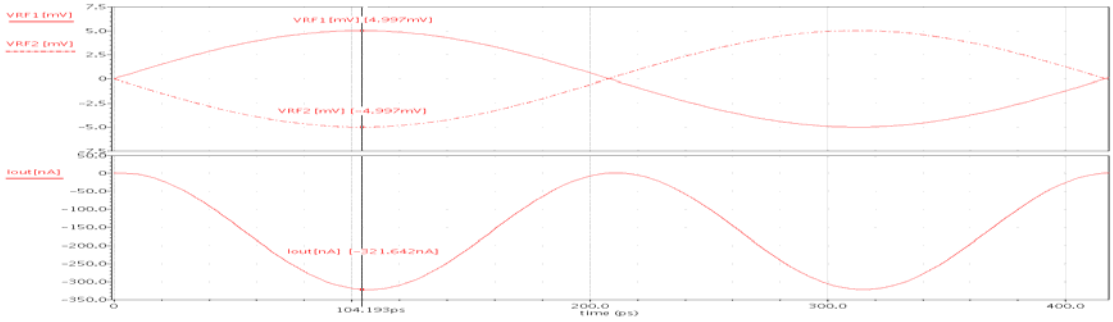

Figure 67: The output current of the Square component (Cadence simulation)

The simulation plot shows a high performance with respect to unwanted spectral components of the Squarer. To check this point in an accurate way, the Discreet Fourier Transform (DFT) of the output current has been plotted in Figure 68. It shows that the

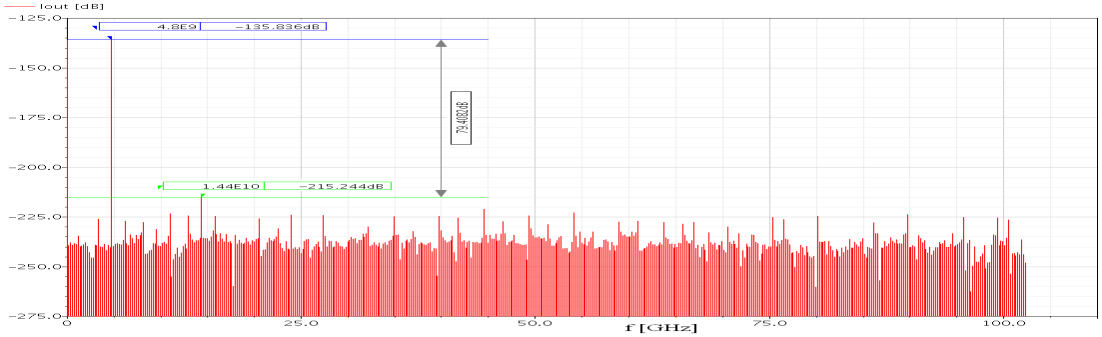

Figure 68: The frequency spectrum of the output current (Cadence simulation)

ratio between the desired and undesired signal is approximately 80 dB.

Hence, the Square component achieves a high performance and consumes almost zero power. Actually, there is a very small DC leakage current that is supplied from V_G. The leakage current crosses the gate oxide and flows towards the drain and the source of the transistors. This current limits the sensitivity of our component to process small input signals and its value depends on the gate oxide thickness and the gate-voltage. Hence, increasing the gate oxide thickness will increase the sensitivity. In the simulation of our previous example (gate oxide thickness is equal to 6.5 nm), the smallest input signal is around 100 pV that the Square component can still process without having distortions from this leakage current. The simulation also shows that decreasing the thickness to 2 nm will reduce the sensitivity to 500 µV and the leakage current is around 200 pA (Cadence simulation).

Optimum W to Maximizing the output current

Let's now investigate the optimum transistor's width (W) to maximize the output current for a specific R_S value, hence maximizing the conversion gain. Optimizing the transistor's width is the same as optimizing β, because β is a function of W ($\beta = \mu_n C_{OX} W/L$). The optimization procedure begins with differentiating the output current (see Equation 4-24) with respect to β and equating the result to zero:

$\frac{dI_{out}}{d\beta} = 0$ From this equation the optimum β is derived:

$$\Rightarrow \beta_{I_{out}\text{-max}} = \frac{1}{2R_S V_{GT}} \Rightarrow W_{I_{out}\text{-max}} = \frac{1}{2R_S \frac{\mu_n C_{OX}}{L} V_{GT}} \qquad \textbf{Equation 4-25}$$

Substituting Equation 4-25 in Equation 4-24 gives:

$$I_{out\_\text{maxmimu}} = \frac{4}{27}\frac{1}{R_S V_{GT}} V_{RF1}^2 \qquad \textbf{Equation 4-26}$$

The derivation of Equation 4-25 has been done with the Maple program. For our previous example, the optimum W must be 76.2 µm for R_S = 35 Ω as shown in Figure 69. This result is verified with the cadence simulation as depicted in Figure 70. $H_O(I_{out})$ is the DC component of the simulated output current, which is half of I_{out}. The dependency of I_{out} on β in the numerator and denominator of Equation 4-24 is also proved by observing Figure 70. Thus, our theory predicts the optimum W accurately.

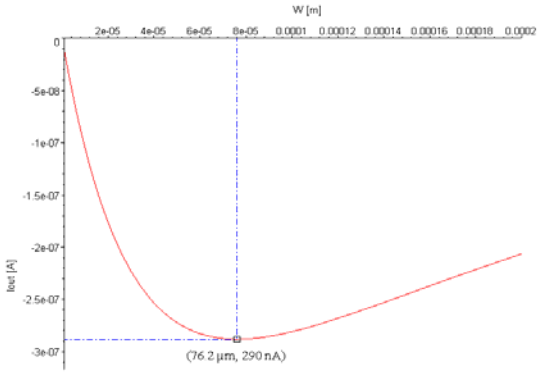

Figure 69: The optimum W to maximize I_{out} (Theory)

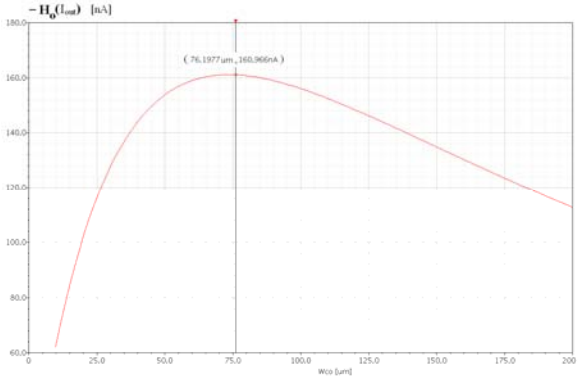

Figure 70: The optimum W to maximize I_{out} (Cadence)

Noise Figure calculations

After investigating the optimum W to maximize the output current for a specific R_S, the next interesting investigation is to derive the optimum W to minimize the noise figure for a specific R_S. The physical meaning of the Noise Figure (NF) is a measure of how much the Signal to Noise Ratio (SNR) degrades as the signal passes through a component:

$$NF = \frac{SNR_{in}}{SNR_{out}}$$ **Equation 4-27**

As you know that our MOSFET transistors operate as resistor (R_{on}) in the triode region:

$$R_{on} = \frac{1}{\beta V_{GS}} \approx \frac{1}{\beta V_{GT}}$$ **Equation 4-28**

Thus, the transistors can be replaced by R_{on} as shown in Figure 71. Consequently, there are four resistors, which means four sources of thermal noise, where $\overline{V_{RS}^2} = 4kTR_S$ and $\overline{V_{R_{on}}^2} = 4kTR_{on}$:

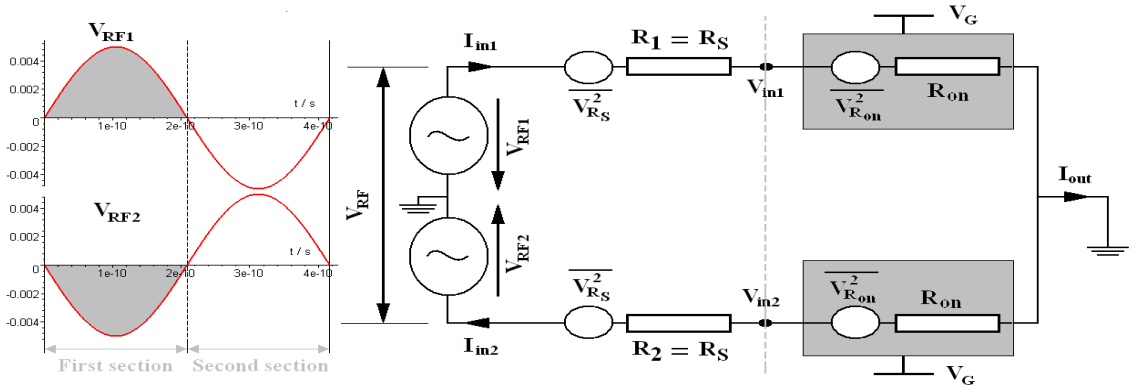

Figure 71: Square component including the noise sources

In our previous analysis it is shown that for each half of the RF signal period, only one of the transistors will operate to deliver the desired output current. This means that:

$$SNR_{in} = \frac{V_{RF1}^2 \dfrac{R_{on}}{R_{on}+R_S}}{\overline{V_{R_S}^2} \dfrac{R_{on}}{R_{on}+R_S}} = \frac{V_{RF1}^2}{\overline{V_{R_S}^2}}$$ **Equation 4-29**

However both top and bottom branch contribute noise to the output signal I_{out}:

$$SNR_{out} = \frac{I_{out}^2}{\left(\dfrac{\overline{V_{R_1}^2}+\overline{V_{R_{on}}^2}}{(R_1+R_{on})^2}\right)+\left(\dfrac{\overline{V_{R2}^2}+\overline{V_{R_{on}}^2}}{(R_2+R_{on})^2}\right)} = \frac{I_{out}^2}{2\left(\dfrac{\overline{V_{R_S}^2}+\overline{V_{R_{on}}^2}}{(R_S+R_{on})^2}\right)}$$ **Equation 4-30**

Substituting Equation 4-29 and Equation 4-30 in Equation 4-27 results in:

$$NF = \frac{\dfrac{V_{RF1}^2}{\overline{V_{R_S}^2}}}{2\left(\dfrac{\overline{V_{R_S}^2}+\overline{V_{R_{on}}^2}}{(R_S+R_{on})^2}\right)}$$

$$NF = \frac{V_{RF1}^2}{\overline{V_{R_S}^2}} 2\left(\frac{\overline{V_{R_S}^2}+\overline{V_{R_{on}}^2}}{(R_S+R_{on})^2}\right)\frac{1}{I_{out}^2} = 2\left(\frac{V_{RF1}}{I_{out}}\right)^2 \frac{R_S+R_{on}}{R_S(R_S+R_{on})^2}$$

$$= 2\left(\frac{V_{RF1}}{I_{out}}\right)^2 \frac{1}{R_S(R_S+R_{on})} = 2\left(\frac{V_{RF1}}{-\frac{\beta}{(1+\beta R_S V_{GT})^3}V_{RF1}^2}\right)^2 \frac{1}{R_S(R_S+R_{on})}$$

$$= 2\frac{(1+\beta R_S V_{GT})^6}{(\beta V_{RF1})^2}\frac{1}{R_S(R_S+R_{on})}$$

Equation 4-31

Equation 4-31 indicates an inverse relation between NF and V_{RF1} as shown in Figure 72. This is really different than the conventional form of the NF for different types of components like amplifiers, where the NF only depends on the internal elements like gm and internal resistances.

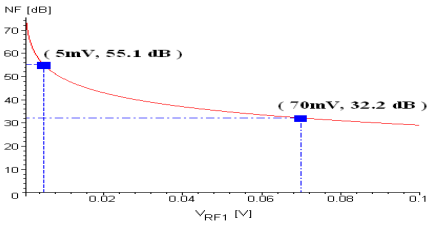

Figure 72: NF vs V_{RF1}

To verify our analysis, the circuit shown in Figure 73 has been used, where $V_{RF} = V_{RF1} - V_{RF2}$. The combination of an ideal transformer, $2R_S$ and V_{RF} in Figure 73 replaces the combination of R_1, R_2, V_{RF1} and V_{RF2} in Figure 71.

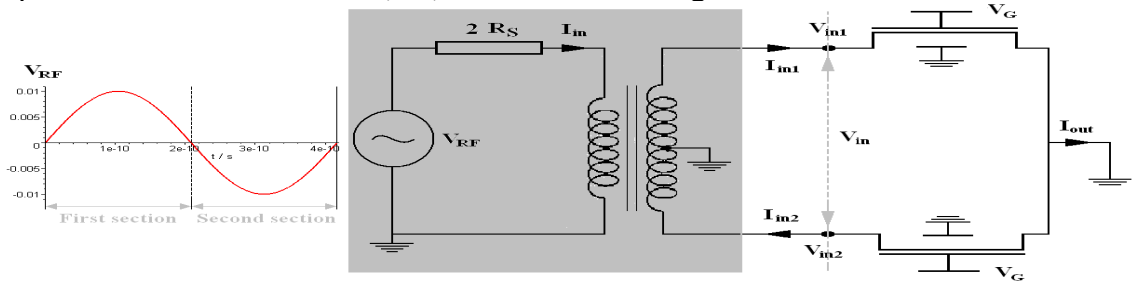

Figure 73: The used schematic to simulate the NF in cadence

This ideal transformer does not contribute any noise to our circuit. The results of the simulation are shown in Figure 74, where the inverse relation between the NF and V_{RF1} is very clear.

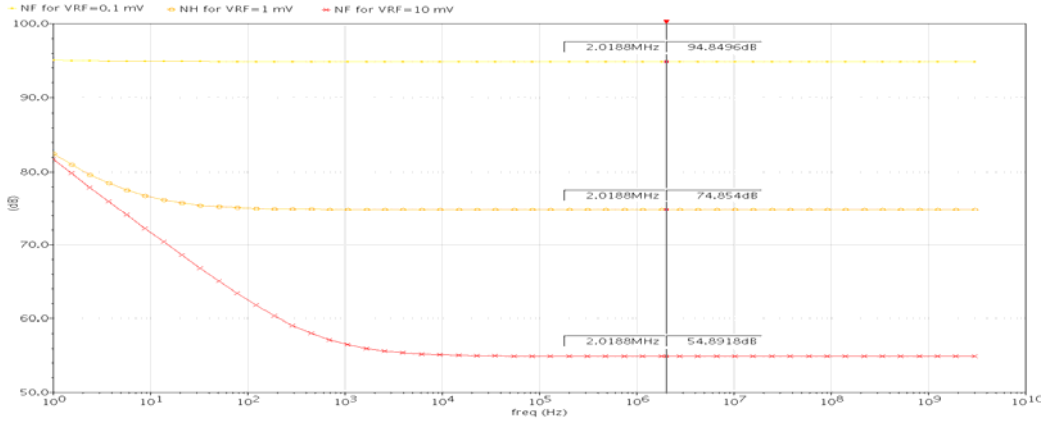

Figure 74: Cadence simulation results

The measured points in Figure 74 are at 2 MHz, which is equal to the offset frequency $\Delta\omega$, where our desired signal with bandwidth equal to 2B (B = 1 MHz) exists as mentioned at the end of Chapter 3. You can also observe the 1/f noise, for which its corner frequency increases with increasing V_{RF1}. For our system, there is no need to be worry strongly about the 1/f noise because its boundary is much smaller than the region where the desired signal exists. In Table 3, a comparison between our theory and the simulation results for different V_{RF} has been shown:

VRF [mV]	NF [dB]	
	Theory	Simulation
0.1	95.1	94.85
1	75.1	74.85
10	55.1	54.89
100	35.1	35.33

Table 3 NF comparison between the theory and the cadence simulation

Observing Equation 4-31 and Equation 2-24 shows that minimizing V_{GT} will improve both NF and the conversion gain of our Square component.

Optimum W to minimizing the NF

Now that we are confident about the NF equation, it is important to investigate the optimum W for a specific R_S to minimize the NF. The optimization procedure again begins with differentiating NF (see Equation 4-31) with respect to β and equating the result to zero:

$$\frac{dNF}{d\beta}=0 \quad \text{From this equation the optimum } \beta \text{ is derived: } \beta_{NF\,\min}=\frac{1}{4R_S V_{GT}} \qquad \textbf{Equation 4-32}$$

$$\Rightarrow W_{NF\,\min}=\frac{1}{4R_S\dfrac{\mu_n C_{OX}}{L}V_{GT}} \qquad \textbf{Equation 4-33}$$

Which also means $R_{on} = 4R_S$. Substituting Equation 4-32 in Equation 4-31 gives:

$$NF_{\text{minimum}}=2\frac{(1+\beta R_S V_{GT})^6}{(\beta V_{RF1})^2}\frac{1}{R_S(R_S+R_{on})}=2\frac{(1+1/4)^6}{\left(\dfrac{1}{4R_S V_{GT}}V_{RF1}\right)^2}\frac{1}{5R_S^2}$$

$$=\frac{2}{5}16\left(\frac{5}{4}\right)^6\left(\frac{V_{GT}}{V_{RF1}}\right)^2=24.4\left(\frac{V_{GT}}{V_{RF1}}\right)^2 \qquad \textbf{Equation 4-34}$$

The derivation of Equation 4-32 has been done with the Maple program. For our example of page 45, the optimum W must be 38.1 µm for R_S = 35 Ω as shown in Figure 75. Equation 4-34 says that once the matching condition for minimizing NF is satisfied then $NF_{minimum}$ only depends on V_{GT} and V_{RF1}.

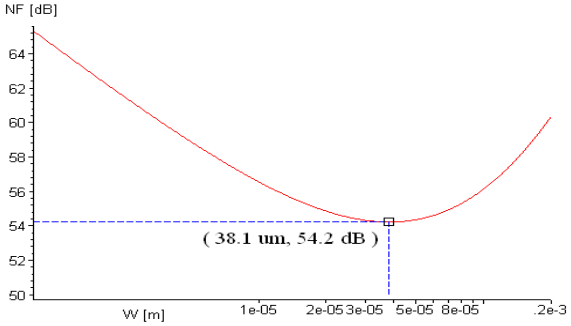

Figure 75: The optimum W to maximize NF (Theory)

Now, the question is: which optimum W is the best choice for our design? As you can observe in Figure 76, for $W = W_{NF\,\min}$ the output current will be reduced by more than 13% compared to the output current for $W = W_{I_{out}\,\max}$. On the other hand as shown in Figure 77, choosing $W = W_{I_{out}\,\max}$ increases the NF by less than 2%. Thus, the best choice is $W = W_{I_{out}\,\max}$.

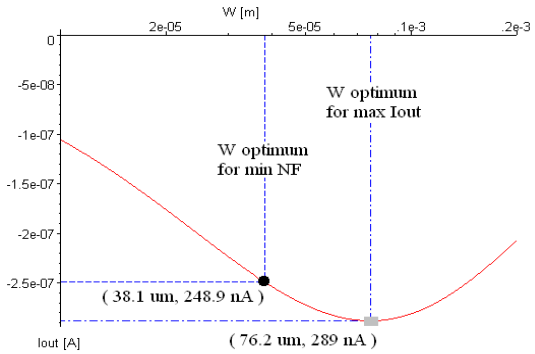

Figure 76: I_{out} Comparison to choose W

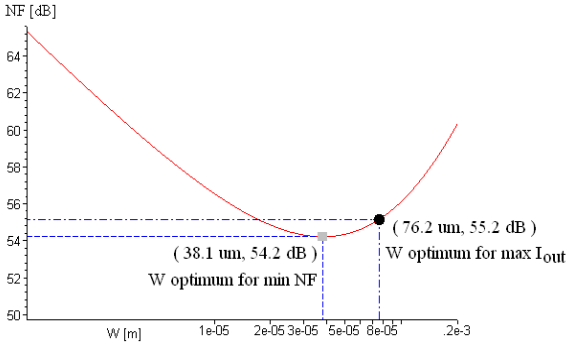

Figure 77: NF Comparison to choose W

The Squarer based on triode transistors still needs an extra component as shown in Figure 78, because of the following reasons:

- The output terminal of the Squarer component needs to be a virtual ground. If this condition is not satisfied and there is some resistance at the output gate, then there will be a voltage drop across this resistance. As a consequence, the voltage drop across R_S and the transistor will decrease, hence I_{out} decreases.
- The next block in the Front End chain is a Switch Mixer with a voltage as input signal. Therefore, the Square component needs an IV converter so that the desired information which is in I_{out} can be further processed.
- As you know that the transconductance of the Squarer component is $GT = I_{out}/V_{in}$. The existence of the IV converter will increase the gain of the whole Square block by factor of R_{IV}: $Av_{SQ\text{-}IV} = I_{out}\,R_{IV}/V_{in}$.

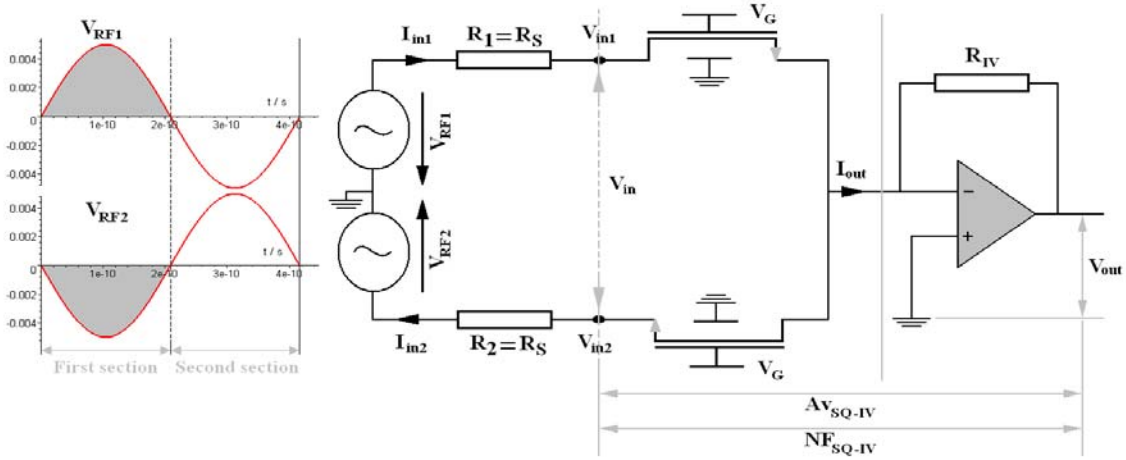

Figure 78: Square Block

The whole combination of the Square component and the IV converter will be called The Squarer Block. Before using the specifications of the Squarer Block in the mentioned mapping procedure, it is necessary to see the effect of adding the IV converter on the *NF* of the Squarer component (NF_{SQ}). In Figure 79, the expected noise sources inside our block are plotted. $\overline{V^2_{n-OpAmp}}$ is the noise of the operation amplifier. Its value depends inversely on the transconductance (g_m) of its input transistors. A typical value for $V_{n-OpAmp}$ is around 1nV/√Hz.

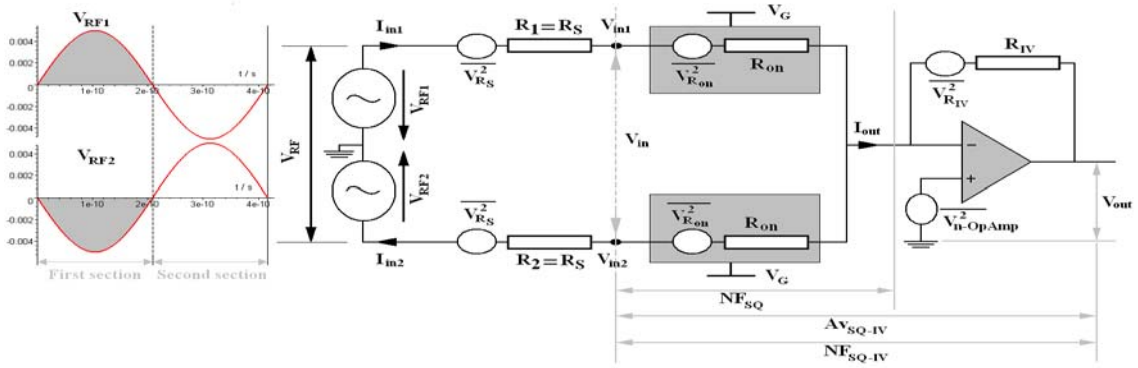

Figure 79: Square component with the IV converter

The input signal to noise ratio is equal to that SNR_{in} of Equation 4-29:

$$SNR_{in} = \frac{V_{RF1}^2 \dfrac{R_{on}}{R_{on}+R_S}}{\overline{V_{R_S}^2}\dfrac{R_{on}}{R_{on}+R_S}} = \frac{V_{RF1}^2}{\overline{V_{R_S}^2}} \qquad \textbf{Equation 4-35}$$

The output noise is the supper position of the all noise sources referred to output:

$$SNR_{out} = \frac{(I_{out}R_{IV})^2}{\left[\left(\dfrac{\overline{V_{R_1}^2}+\overline{V_{R_{on}}^2}}{(R_1+R_{on})^2}\right)+\left(\dfrac{\overline{V_{R2}^2}+\overline{V_{R_{on}}^2}}{(R_2+R_{on})^2}\right)\right]R_{IV}^2 + \overline{V_{R_{IV}}^2} + \overline{V_{n-Op}^2}\left(\dfrac{2R_{IV}}{R_S+R_{on}}\right)^2}$$

$$= \frac{(I_{out}R_{IV})^2}{2\left(\dfrac{\overline{V_{R_S}^2}+\overline{V_{R_{on}}^2}}{(R_S+R_{on})^2}\right)R_{IV}^2 + \overline{V_{R_{IV}}^2} + \overline{V_{n-OpAmp}^2}\left(\dfrac{2R_{IV}}{R_S+R_{on}}\right)^2} \qquad \textbf{Equation 4-36}$$

Then:

$$NF_{SQ-IV} = \frac{V_{RF1}^2}{\overline{V_{R_S}^2}} \frac{\left[2\left(\dfrac{\overline{V_{R_S}^2}+\overline{V_{R_{on}}^2}}{(R_S+R_{on})^2}\right)R_{IV}^2 + \overline{V_{R_{IV}}^2} + \overline{V_{n-OpAmp}^2}\left(\dfrac{2R_{IV}}{R_S+R_{on}}\right)^2\right]}{(I_{out}R_{IV})^2}$$

The *NF* equation has been processed in Appendix 6 to produce the following result:

$$NF_{SQ-IV} = NF_{SQ} + \frac{9}{16}\frac{\dfrac{R_{IV}}{R_S}}{Av_{QS-IV}^2} + \frac{1}{4}\frac{\dfrac{\overline{V_{n-OpAmp}^2}}{\overline{V_{R_S}^2}}\left(\dfrac{R_{IV}}{R_S}\right)^2}{Av_{QS-IV}^2} \qquad \textbf{Equation 4-37}$$

where NF_{SQ} is the *NF* of the Squarer component.

The NF equation can further be simplified to the basic parameters (see Appendix 6):

$$NF_{SQ-IV} = \frac{(1+\beta R_S V_{GT})^6}{\beta^2}\left(\frac{1}{V_{RF1}^2}\right)\left[\frac{2}{3}\frac{1}{R_S^2} + \frac{1}{R_S R_{IV}} + \frac{4}{9}\frac{\overline{V_{n-OpAmp}^2}}{\overline{V_{R_S}^2}}\frac{1}{R_S^2}\right]$$

But: $\beta R_S V_{GT} = \frac{R_S}{R_{on}} = \frac{R_S}{2R_S} = 0.5 \rightarrow$ optimum W to maximize I_{out}.

And: $\beta = \frac{1}{R_{on}V_{GT}} = \frac{1}{2R_S V_{GT}}$

$$NF_{SQ-IV} = \frac{(1+0.5)^6}{\left(\frac{1}{2R_S V_{GT}}\right)^2}\left(\frac{1}{V_{RF1}^2}\right)\left[\frac{2}{3}\frac{1}{R_S^2} + \frac{1}{R_S R_{IV}} + \frac{4}{9}\frac{\overline{V_{n-OpAmp}^2}}{\overline{V_{R_S}^2}}\frac{1}{R_S^2}\right]$$

$$= \frac{81}{4}\left(\frac{V_{GT}}{V_{RF1}}\right)^2\left[\frac{3}{2} + \frac{9}{4}\frac{R_S}{R_{IV}} + \frac{\overline{V_{n-OpAmp}^2}}{\overline{V_{R_S}^2}}\right] \qquad \textbf{Equation 4-38}$$

The 1st term in Equation 4-38 is the NF_{SQ}. Despite that the existence of the IV converter will increase NF_{SQ} by two extra terms, however the 2nd term can still be reduced by increasing R_{IV} and the 3rd term can only be reduced by designing operation amplifier (Op Amp) with very low noise figure, but of course this must not cost high power consumption inside the Op Amp. Finally, you can observe that decreasing V_{GT} helps to improve *NF* and Av_{SQ-IV}.

Conclusion:

- The optimum W for of Square component transistors is $W_{\text{optimum}} = W_{I_{out}\text{-max}} = 1/\left(2R_S\frac{\mu_n C_{OX}}{L}V_{GT}\right)$. This condition gives: $R_{on}=2R_S$
- The gain of the Square block is (See Appendix 7 for the derivation):

$$Av_{SQ-IV} = \frac{I_{out}R_{IV}}{V_{in}} = \frac{2}{9}\beta R_{IV}\, V_{RF1} \qquad \textbf{Equation 4-39}$$

- The Square block also has a high *NF*, which inversely depends on the input signal:

$$NF_{SQ-IV} = \frac{81}{4}\left(\frac{V_{GT}}{V_{RF1}}\right)^2\left[\frac{3}{2} + \frac{9}{4}\frac{R_S}{R_{IV}} + \frac{\overline{V_{n-OpAmp}^2}}{\overline{V_{R_S}^2}}\right] \qquad \textbf{Equation 4-40}$$

- Decreasing V_{GT} helps to improves *NF* and the voltage gain of the Square block.

4.3 Mapping system requirement to block requirements

As calculated previously , the Front End section requires to have $G_{FE} = 42.5\ dB$ and $NF_{FE} = 20.5\ dB$ for a distance range (d) between $1m$ to $25m$. The Squarer block has a very large NF. Consequently, it is necessary to utilize an LNA in our receiver as shown in

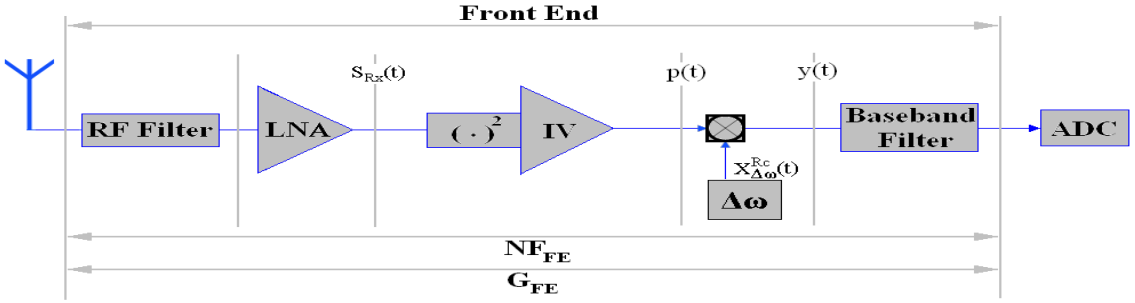

Figure 80: Receiver of the Noise Modulation

Figure 80. A powerful tool used to illustrate the effect of each stage in a cascade upon the signal and noise is the "level diagram" as shown in Table 4. Using the excel sheet is the easiest way to apply the level diagram (See Appendix 9). Note that in addition to the parameters of each stage, inter stage quantities are indicated so as to represent the levels at the interface between consecutive stages. For detailed information about building such level diagram, we refer to Razavi [8]. In Appendix 8, a summarized version is presented about this subject.

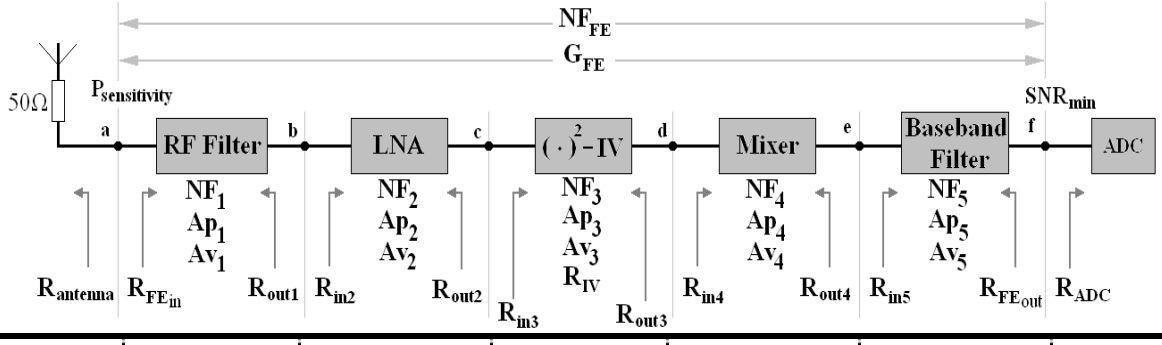

Stage Gain (dB)								
Voltage : *Av*		4	51.4	12	-4	2		
Power : *Ap*		-2	42.3	11.4	-10	-4		
Input resistance R_{in}		50	50	200	50	50	200	
Ouput resistance R_{out}	50	50	100	50	50	50		
Input voltage division $= \frac{R_{out}}{R_{out}+R_{in}}$		0.5	0.5	2/3	0.5	0.5	0.8	
Inter Stage Voltage Gain (V)			-2	46	52	42	42	
Stage NF (dB)		2	8	60.4	10	4		
NF contribution of all later stages (dB)	20.4		18.4	60.4	14	4	0	

Table 4: Level diagram calculations for the Frond End with LNA

The shown parameters namely, *Av*, *Ap* and *NF*, for the RF Filter, Mixer and Baseband Filter are typical values. R_{FEin} needs to be matched to $R_{antenna}$, so that no reflections occur at R_{FEin}. On chip there is no need to match the input impedance of a stage with the output

impedance of the preceding stage, because dimensions inside the chip is less than tenth of $\lambda = 125\ mm$, which is the wave length of *2.4 GHz*. R_{in3} and R_{out2} are the input and output impedance of differential terminals[10], where $R_{in3} = 2\ R_{out2}$ as mentioned previously ($R_{on}=2R_S$). Therefore, the input voltage division at point C is 2/3. The ADC has high input impedance; a typical value is *200* Ω. As this thesis is the early stage of designing a complete transceiver for Noise Modulation concept, we assign *50* Ω as a neutral value to the rest of input and output impedances of the blocks of our Front End. Changing those parameters does not change the picture in a dramatic way that we need to be concern about it. The transistor that is used to build the Squarer component is the *0.35 μm CMOS* with $\mu_n C_{OX} = 178.65\ \mu A/V^2$ and $V_{TH} = 0.6327\ V$ and V_G is equal to *1V*. What is important to recognize, is the dependency of NF_3, Av_3 and Ap_3 on the input voltage of the Squarer block. This puts a heavy weight on the gain of the LNA so that the required NF_{FE} can be achieved for $d = 25m$. R_{IV} has a large impact on the G_{FE} but it does not have a significant effect on NF_{FE}. With $R_{IV} = 250\ k\Omega$, $R_S = 50\Omega$ ($R_{on} = 100\Omega \rightarrow W_{Transistor} = 53\ \mu m$), $V_{n-OpAmp}$ = 1nV/√Hz and Av_2 = 51.4 dB (370 times), the following specifications can be achieved: $G_{FE}=42$ and $NF_{FE}=20.4$ as shown in Table 4. Thus, very large gain is demanded from the LNA, hence very large current consumption.
If the distance between the transmitter and the receiver decreases below 25m, then $Av_{SQ\text{-}IV}$ will increase, because V_{RF1} will increase. As a consequence of that, with fixed Av_2 = 51.4 dB and $R_{IV} = 250\ k\Omega$ the signal at the input terminals of ADC (See Figure 60) will be larger than V_{max}, hence wasting information. Therefore our receiver needs a block to control G_{FE}. This block can do that by controlling Av_2 so that the LNA does not waste extra not needed energy.

Designing a Low Noise Amplifier with a voltage gain of *51 dB* needs to use a lot of stages, where each stage typically consumes power more than *1mW*. Decreasing the maximum distance between the Transmitter and the receiver will increase the required NF_{FE}, which means that our Front End is allowed to contribute more noise to the signal. As a consequence of that the needed LNA gain can be reduced, hence decreasing its current consumption. Therefore it is interesting to investigate the following two points:

1. What is the relation between the distance (d) and the current consumption of the Front End, when the LNA exist?
2. What is the situation, when the LNA is removed?

[10] $R_{in3} = 2\ R_{on}$ and $R_{out2} = 2\ R_S$

Distance (d) vs. current consumption at the Front End

This section describes the relation between the current consumption of the Front End and the distance (d), when a LNA is used with acceptable voltage gain *5…20dB*. The LNA and the Squarer block are the two fundamental blocks that play the major role in relation to the Front End noise figure. Therefore the Friis equation can be simplified to just include those two blocks as follows[11]:

$$NF_{FE} = NF_{LNA} + \frac{NF_{SQ-IV} - 1}{Ap_{LNA}} \qquad \textbf{Equation 4-41}$$

NF_{LNA}, Ap_{LNA} and Av_{LNA} are all functions of the LNA current consumption (I_{LNA}). The interesting point is that $NF_{SQ\text{-}IV}$ is not just a function of the Op Amp current (I_{OpAmp}) but also (I_{LNA}). This is due to that I_{LNA} controls the amount of the input voltage of the Squarer block, hence controlling $NF_{SQ\text{-}IV}$ (See Equation 4-40). Thus:

$$NF_{FE}(d) = NF_{LNA}(I_{LNA}) + \frac{NF_{SQ-IV}(I_{OpAmp}, I_{LNA}) - 1}{Ap_{LNA}(I_{LNA})} \approx \frac{NF_{SQ-IV}(I_{OpAmp}, I_{LNA}) - 1}{Ap_{LNA}(I_{LNA})} \qquad \textbf{Equation 4-42}$$

The last step has been done because NF_{LNA} with a typical range of *2* to *6 dB* is much less than the second part.

In our derivations, some rough assumptions will be taken to present coarse estimations of the power consumption in the OpAmp and in the LNA, as follows:

By the OpAmp, we assume that its input transistor has the major noise contribution, therefore the relation between I_{OpAmp} and $V_{n-OpAmp}$ is:

$$\overline{V^2_{\text{n-OpAmp}}} = \frac{4kT}{g_{m\_\text{OpAmp}}} \text{ and } g_{m\_\text{OpAmp}} = \frac{2I_{\text{OpAmp}}}{V_{GT\_\text{OpAmp}}}$$

Therefore:

$$I_{\text{OpAmp}} = \frac{2kTV_{GT\_\text{OpAmp}}}{\overline{V^2_{\text{n-OpAmp}}}} \qquad \textbf{Equation 4-43}$$

Equation 4-43 can be further simplified if $V_{n-OpAmp}$ is replaced by its equivalent resistance ($R_{n-OpAmp}$), where $\overline{V^2_{\text{n-OpAmp}}} = 4kTR_{n-OpAmp}$. Then:

$$I_{\text{OpAmp}} = \frac{V_{GT\_\text{OpAmp}}}{2R_{n-OpAmp}} \qquad \textbf{Equation 4-44}$$

Replacing $V_{n-OpAmp}$ with $R_{n-OpAmp}$ allows to present Equation 4-40 in easier way:

$$NF_{SQ-IV} = \frac{81}{4}\left(\frac{V_{GT}}{V_{RF1}}\right)^2\left[\frac{3}{2} + \frac{9}{4}\frac{R_S}{R_{IV}} + \frac{R_{n-OpAmp}}{R_S}\right]$$
$$\approx \frac{81}{4}\left(\frac{V_{GT}}{V_{RF1}}\right)^2\left[\frac{3}{2} + \frac{R_{n-OpAmp}}{R_S}\right] \qquad \textbf{Equation 4-45}$$

The last step has been done because with R_{IV} *=250 k*Ω and R_S *= 50*Ω, the ratio of R_S/R_{IV} can be neglected.

[11] The NF parameters in Friis equation is not in dB.

For the LNA, we assume that its input transistor has a major influence on the voltage gain as follows:

$$Av_{LNA} = g_{m\_LNA} \times R_{LNA} \quad \text{and} \quad g_{m\_LNA} = \frac{2I_{LNA}}{V_{GT\_LNA}}$$

Therefore:

$$Av_{LNA} = \left(\frac{2R_{LNA}}{V_{GT\_LNA}}\right) I_{LNA} \qquad \textbf{Equation 4-46}$$

In Appendix 10, Equation 4-4, Equation 4-45, Equation 4-43 and Equation 4-46 have been used in Equation 4-42 to derive the following equation:

$$d = \left(51\times 10^{6} \frac{\lambda^4}{kTB \times SNR_{\min}} \frac{P_T^2}{V_{GT}^2} \frac{I_{LNA}^4}{\left[1+\frac{2\times 10^{-3}}{I_{OpAmp}}\right]} \right)^{\frac{1}{2n}} \qquad \textbf{Equation 4-47}$$

For: $\lambda = 125mm$, $B = 1MHz$, $V_{GT} = 67mV$ and $SNR_{\min} = 13.8 \rightarrow 11.4dB$:

$$d = 1910 \times \left(\frac{P_T^2 I_{LNA}^4}{1+\frac{2\times 10^{-3}}{I_{OpAmp}}} \right)^{\frac{1}{6}} \qquad \textbf{Equation 4-48}$$

Plotting Equation 4-48 for $P_T = 1\ mW$:

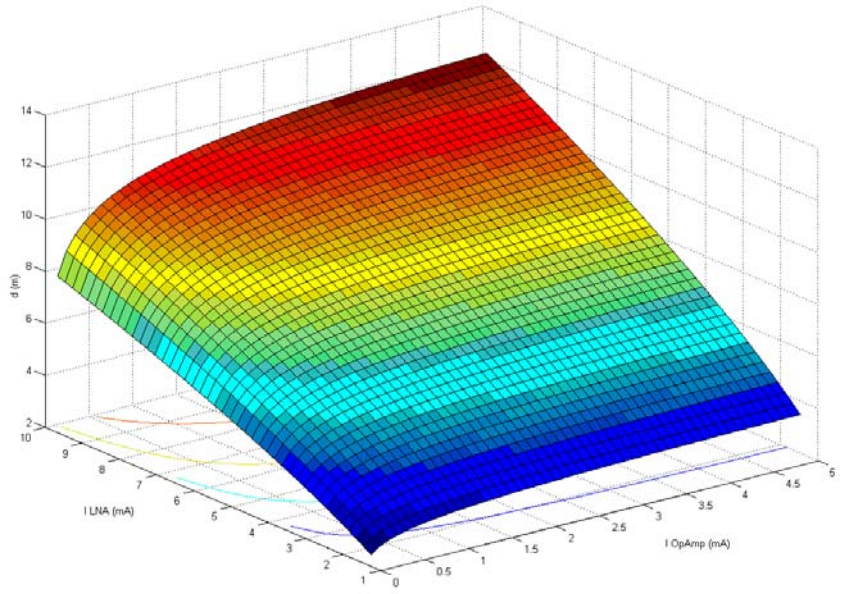

Figure 81: d vs. current consumptions, I_{LNA} and I_{OpAmp}

As example, let's assume that the current consumption of both LNA and the Op Amp is 2.5 mA (See Figure 82 and Figure 83). Then by fixing I_{LNA} and increasing I_{OpAmp} with 1 mA, the distance can just be increased by 2.3%, while fixing I_{OpAmp} and increasing I_{LNA} with 1 mA, the distance can be increased by 25.2%, hence approximately 10 times than the previous situation.

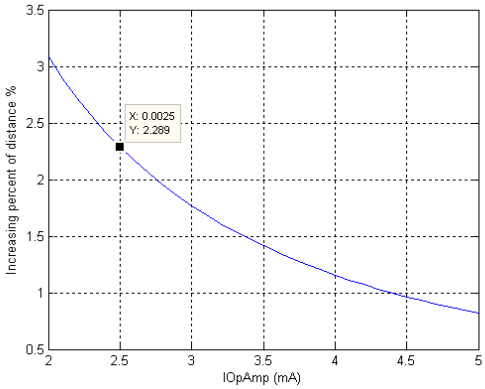

Figure 82: Increase in radio range for 1mA additional current of I_{OpAmp}, expressed as a percentage of the range for the original current.

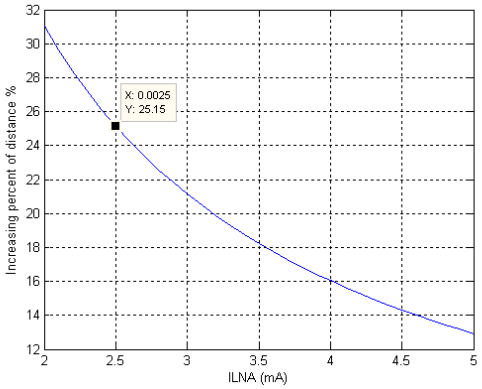

Figure 83: Increase in radio range for 1mA additional current of I_{LNA}, expressed as a percentage of the range for the original current.

Conclusion:

It is more efficient to increase the current consumption of the LNA than increasing the current consumption of the Op Amp.

Removing the LNA from the Front End

In the situation when the LNA is removed, the Transmitted power must be increased in order to increase the reachable distance between the Transmitter and the Receiver. This is because by increasing P_T, the needed NF_{FE} increases and also the NF of the Squarer block decreases. V_{GT} is another important factor in reducing $NF_{SQ\text{-}IV}$ as mentioned previously. By reducing V_{GT} and increasing P_T, the reachable distance (d) can be increased as shown in Figure 84 . For this figure, the current consumption of the Op Amp is 2.3 mA.

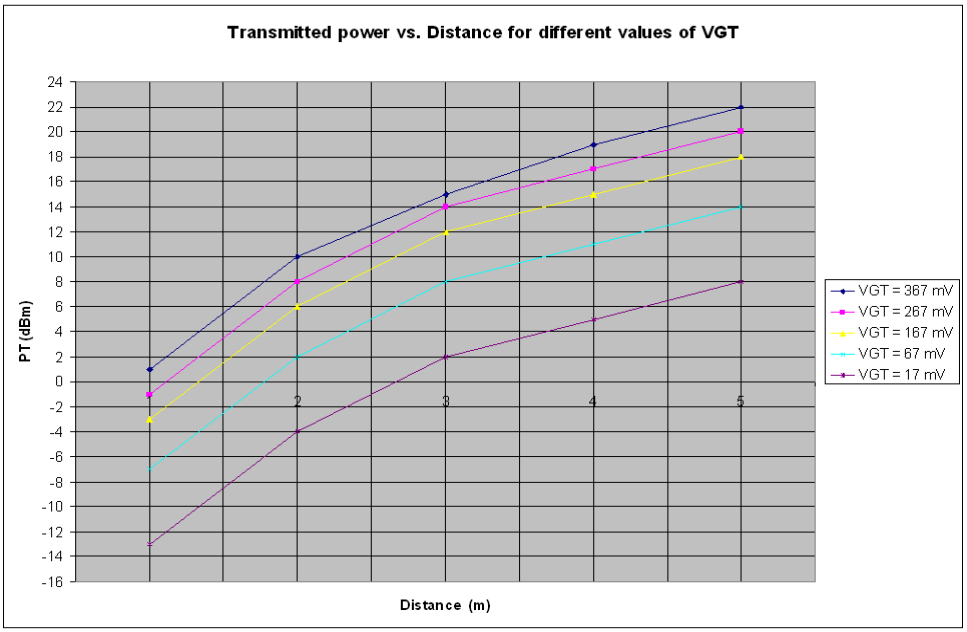

Figure 84: Transmitted power vs. Distance (d) for different V_{GT}

If the current consumption of the Op Amp is reduced then the transmitted power must be increased as shown in Figure 85. For this figure V_{GT} = 17 mV.

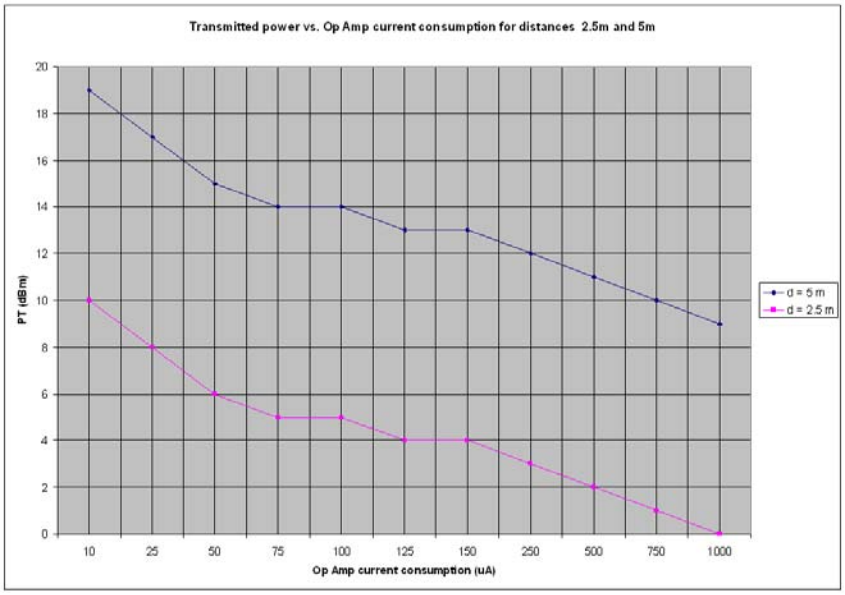

Figure 85: Transmitted power vs. I_{OpAmp} for distances 2.5m and 5 m

Chapter 5 Conclusions

The goal of our project was to build a low power sensor network for low throughput applications. Accordingly, the transmitter of the reporting node needs to be ON just for low "duty cycle", while the receiver of the listening node requires being ON most of the time. This is because the listening node does not know when a message will be sent. Thus, the power consumption at the receiver has been our major concern in this project.

In Noise Modulation systems, the information data is spread by a reference signal, which is a broadband noise signal with bandwidth of 100 MHz around 2.4 GHz (ISM frequency band). The modulated data is transmitted together with the reference signal on the same band, therefore there is no need to regenerate and synchronize the phase of the reference signal at the receiver. This attractive property gives the motivation to utilize the Noise Modulation in building low power receivers in CMOS technology.

To gain an intuitive understanding about the transceiver operation, a time analysis of the signal processing was presented. Based on this time analysis, the following design choices have been made and a Simulink model has verified our understanding:

1. The ratio between $\Delta\omega$ and the bit rate (R_b) must be integer to maximize the communication performance, *BER*.
2. Three linear multipliers are replaced by Switch Mixers: Switch mixers are preferable to linear multipliers because mixers have higher gain and lower noise contribution.
3. The I&D filter is in fact the matching filter for our system and can be replaced by a low pass filter + sampling at the proper times (determination of this proper sampling is done in the digital domain).
4. The 4th linear multiplier is replaced by a Squarer block.

After finishing the design choices at the system level for our transceiver, we moved our concern to the receiver design with the emphasis on low power consumption. First, we calculated the link budget requirements, NF_{FE} = 20.5 dB and G_{FE} = 42.5 dB, which is needed to achieve a distance between the Transmitter and the Receiver of approximately *1m* to *25m*. Then those requirements needed to be mapped to the block specifications at the Receiver. The most critical receiver block was the squarer performing the correlation. The main criteria to design this block was low power consumption and high functionality (correlation). According to those criteria, CMOS that works in the linear (Triode) region is the optimum choice. A differential CMOS structure was designed to remove the unwanted distortions from the output terminals. However, the output terminal needed to see a (virtual) ground. Consequently, an IV converter is used. The IV converter contains an Operation Amplifier that contributes noise to the whole Squarer block. The amount of the noise contribution depends inversely with the current consumption of this Operation Amplifier, I_{OpAmp} = 0.5 mA → ΔNF = 7 dB and I_{OpAmp} = 2 mA → ΔNF = 3 dB. Finally, the voltage gain and the noise figure of the whole Squarer block were derived. The NF of this block depends inversely on the square of its input signal. For an input voltage of 3.5 mV a NF = 60 dB is found at I_{OpAmp} = 2.3 mA.

With such NF performance, the receiver definitely needs a LNA to achieve a sensitivity for d=25 m. Such LNA must provide a voltage gain of around 50 dB (370 times), which means very large current consumption, 10...20 mA. Therefore, we had to review the important parameters in our system. The mentioned dependency brought our attention to the following parameters:

1. d: distance between the Transmitter and the Receiver.
2. P_T: the transmitted power.
3. Av_{LNA}: Voltage gain of the LNA which depends on its current consumption I_{LNA}.
4. $\overline{V^2_{n\text{-}OpAmp}}$: the noise contribution of the Operation Amplifier, which depends on its current consumption I_{OpAmp}.
5. V_{GT}: the derive voltage of the differential transistors of the Squarer block.

The last two parameters can help in decreasing the noise figure of the Squarer block.

Based on the effect of those parameters on the noise figure of our Front End, Two important points were investigated:

1. What is the situation, when the LNA is removed?
   Result: Even by decreasing V_{GT} to 17 mV, P_T still must be larger than 8 dBm (6 mW) to achieve a distance of 5m.
2. What is the relation between the distance (d) and the current consumption at the Front End, when the LNA exist?
   Result: This relation shows that it is much more efficient to increase the current consumption of the LNA than to increase the current consumption of the Op Amp. This is due to the fact that increasing the current consumption of the LNA increases the voltage gain of the LNA as well as it reduces the noise figure of the Squarer block in an efficient way. Increasing P_T helps to decrease the current consumption of LNA.

In conclusion: It is clear that in order to achieve a low power receiver, where the power consumption of the Op Amp must be less than 100 µA, then the LNA must be removed. This puts a heavy weight on the transmitted power P_T. Increasing the current consumption of the OP Amp does not help that much in reducing P_T:

D = 2.5 m		D = 5 m	
P_T (dBm)	I_{OpAmp} (µA)	P_T (dBm)	I_{OpAmp} (µA)
5	100	14	100
5	75	14	75
6	50	15	50
8	25	17	25
10	10	19	10

Table 5: Transmitted power vs. IOpAmp for distances 2.5m and 5 m

Therefore, in order to reduce the current consumption of the receiver below 100 µA the transmitted power must be higher than 14 dB to achieve a radio range of 5m. Decreasing the radio range to 2.5m relaxes the P_T.

References:

[1] Xiaoxin Shang. “New radio multiple access technique based on Frequency Offset Division Multiple Access (FODMA). Master’s thesis, University of Twente, April 2004.

[2] J.W. Balkema. “Realization and characterization of a 2.4 GHz radio system based on Frequency Offset Division Multiple Access”. Master’s thesis, University of Twente, August 2004.

[3] J.C. Haartsen, X. Shang, J.W. Balkema, A. Meijerink, J.L. Tauritz, “A new wireless modulation scheme based on frequency-offset,” Proc. of IEEE 12th Symp. on Communications and Vehicular Technology in the Benelux (SCVT 2005), Enschede, the Netherlands, Nov. 3, 2005.

[4] Simon Haykin. “An Introduction to Analog and Digital Communications”. John Wiley & Sons, 1989.

[5] Qu Zhang and Dennis L. Goeckel. “Multi-Differential slightly Frequency-Shifted reference Ultra-Wideband (UWB) Radio”. University of Massachusetts at Amherst. 2005.

[6] Theodore S. Rappaport. “Wireless Communication: Principles and Practice”. Prentice Hall, 2002.

[7] Paradiso, J.A.; Starner, T., "Energy scavenging for mobile and wireless electronics," Pervasive Computing, IEEE , vol.4, no.1, pp. 18-27, Jan.-March 2005

[8] Behzad Razavi. “RF Microelectronics”. Prentice Hall, 1998

Appendixes:

1. The power spectral density of $S_{Tx}(t)$

In order to calculate the power spectral density of $S_{Tx}(t)$, its autocorrelation must be calculated first (the derivation is done for Figure 6. The role of block C will be explained later):

$$
\begin{aligned}
E\left[S_{\mathrm{Tx}}(t)\times S_{\mathrm{Tx}}(t+\tau)\right] &= E\left[\left\{S_{\mathrm{ref}}(t)+S_{\mathrm{info}}(t)\right\}\times\left\{S_{\mathrm{ref}}(t+\tau)+S_{\mathrm{info}}(t+\tau)\right\}\right] \\
&= E\left[\left\{X_{\mathrm{ref}}(t)\times X_{\Delta\omega}^{\mathrm{Rc}}(t)+C*m\times X_{\mathrm{ref}}(t)\right\}\right. \\
&\quad \left.\times\left\{X_{\mathrm{ref}}(t+\tau)\times X_{\Delta\omega}^{\mathrm{Rc}}(t+\tau)+C*m\times X_{\mathrm{ref}}(t+\tau)\right\}\right] \\
&= \underbrace{E\left[X_{\mathrm{ref}}(t)\times X_{\mathrm{ref}}(t+\tau)\right]}_{R_{X_{ref}X_{ref}}(t,t+\tau)}\times E\left[\cos(\Delta\omega t+\phi)\cos(\Delta\omega(t+\tau)+\phi)\right] \\
&\quad +\mathrm{C}\times\mathrm{m}\times E\left[X_{\mathrm{ref}}(t)X_{\mathrm{ref}}(t+\tau)\right]\times\underbrace{E\left[\cos(\Delta\omega t+\phi)\right]}_{=0} \\
&\quad +\mathrm{C}\times\mathrm{m}\times E\left[X_{\mathrm{ref}}(t)X_{\mathrm{ref}}(t+\tau)\right]\times\underbrace{E\left[\cos(\Delta\omega(t+\tau)+\phi)\right]}_{=0} \\
&\quad +\mathrm{C}^2\times\mathrm{m}^2\times E\left[X_{\mathrm{ref}}(t)X_{\mathrm{ref}}(t+\tau)\right] \\
&= \frac{1}{2}R_{X_{ref}X_{ref}}(t,t+\tau)\cos(\Delta\omega\tau)+\mathrm{C}^2\mathrm{m}^2R_{X_{ref}X_{ref}}(t,t+\tau)
\end{aligned}
$$

But: $R_{X_{ref}X_{ref}}(t,t+\tau)=R_{X_{ref}X_{ref}}(\tau)$, because $\mathrm{X_{ref}}$ is a wide stationary process and $\mathrm{m}^2=1$:

$$
E\left[S_{\mathrm{Tx}}(t)\times S_{\mathrm{Tx}}(t+\tau)\right]=\mathrm{C}^2R_{X_{ref}X_{ref}}(\tau)+\frac{1}{2}R_{X_{ref}X_{ref}}(\tau)\cos(\Delta\omega\tau)
$$

2. Simulink Model for the Noise Modulation

The reason to build a Simulink model for the baseband Noise Modulation is to verify our expectations about the signal processing of our system. Figure 86 illustrates the simulation model structure. The information signal *m(t)* is generated at the output of the Unipolar to Bipolar Converter block. A noise samples with a length of T_b/T_S , where T_S is the sampling frequency, are generated in the workspace and let's call it X_{refbit}. Its bandwidth has been fixed to be equal to $B_X = 50\ MHz$. The reference signal $X_{ref}(t)$ is made to be a repetitive source of X_{refbit}. The reason behind building $X_{ref}(t)$ in that way is to hold the energy bit (E_b) constant for each bit so that AWGN block will just control the amount of the channel noise contribution (N_O) in the E_b/N_O parameter. The Sine Wave block, which applies the frequency offset $\Delta\omega$ to the system, is connected to both the multiplier in the transmitter and the receiver. In that way, the phase synchronization has been satisfied. The combination of the Integrate and Dump (I&D) block, the Discrete Pulse Generator (DPG) block and the Sample (S/H) and Hold block presents the integrator (baseband filter) of Figure 20. The output signal of S/H block is then sent to the IF block to be compared to the threshold of aero, and the receiver chooses bit 1 or 0 accordingly. The values of the Transmitted block and the Received block are put into and compared by the Error Rate Calculation block. The Bit Error Rate (BER) of the transmission system will then be calculated and shown in the Display block.

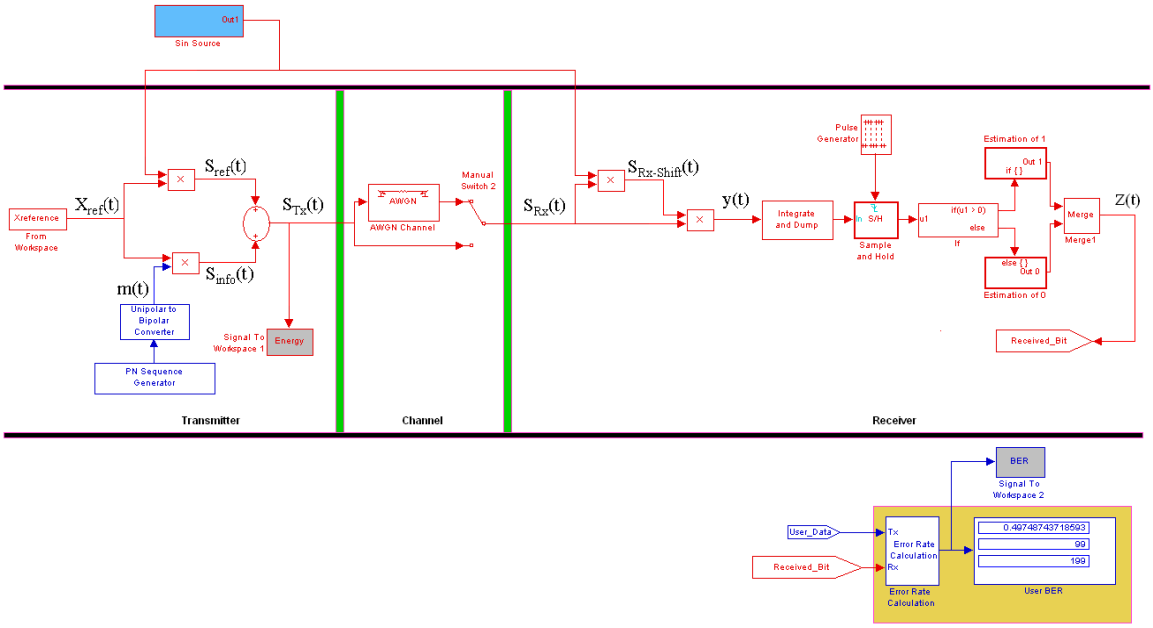

Figure 86: Baseband Noise Modulation Simulink Model

Matlab has a handy tool called "bertool". This tool sweeps E_b/N_O for a range that we can specify it and record BER for each E_b/N_O. Then, it automatically produces the plot of BER vs. E_b/N_O. As an example:

$$PG = 10\log\left(\frac{B_X}{B}\right) = 10\log\left(\frac{50\times10^6}{1\times10^6}\right) = 17\ dB$$

And $\Delta\omega = 2\ MHz$

In Figure 87, you can observe that the results of our Simulink Model coincide approximately with the analytical work of Shang.

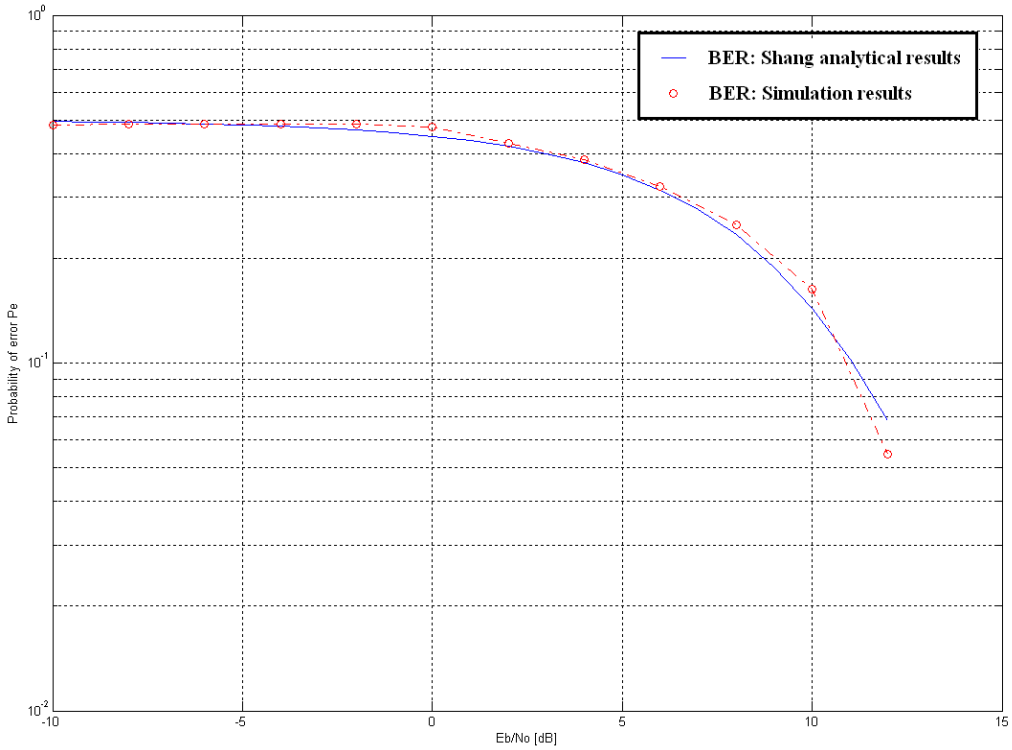

Figure 87: Comparing between the simulation results and the analytical work of Shang

3. Fourier series of a square signal

The Fourier series of the square wave (See Figure 88) is given in Equation 0-1.

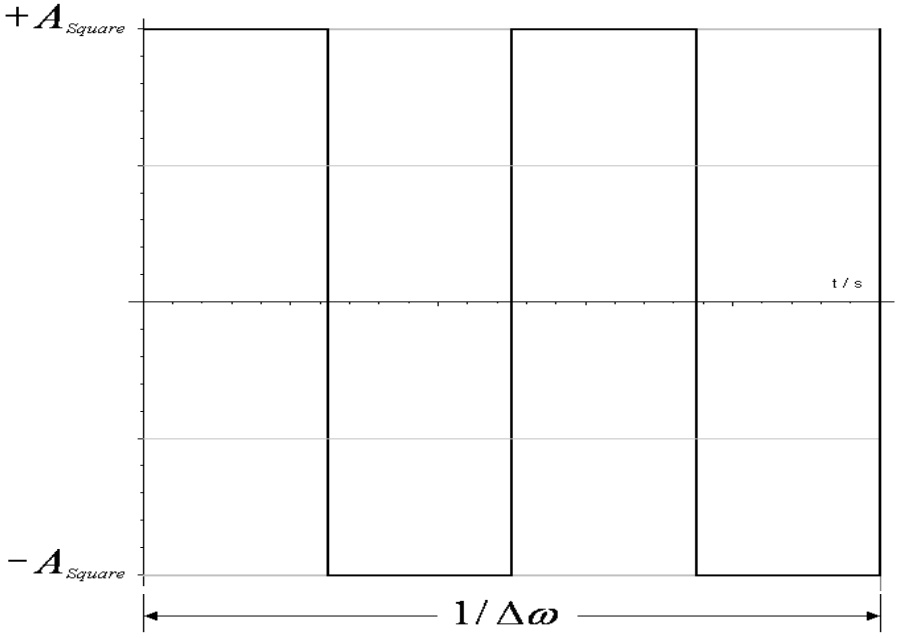

Figure 88: Square signal

$$X_{\Delta\omega}(t)=\begin{cases}\sum_{n=1}^{\infty}\frac{4A_{Square}}{n\pi}\times\cos\left(n\,\Delta\omega\,t-n\frac{\pi}{2}\right) & \text{When n = odd number}\\ 0 \quad \text{When n = odd number}\end{cases}$$

Equation 0-1

4. Bulk effect derivation of the Square component

$$I_{out} = \left[\beta V_{GT} V_{RF1} - \frac{\beta}{2} V_{RF1}^2\right] - \left[\beta V_{GT}(-V_{RF2}) - \frac{\beta}{2} V_{RF2}^2 + \beta V_{RF2}^2\right]$$

$$= \left[\beta (V_G - V_{Tho}) V_{RF1} - \frac{\beta}{2} V_{RF1}^2\right] - \left[\beta (V_G - V_{Th})(-V_{RF2}) + \frac{\beta}{2} V_{RF2}^2\right]$$

$$= \beta (V_G - V_{Tho}) V_{RF1} + \beta (V_G - V_{Th})(V_{RF2}) - \beta V_{RF2}^2$$

But: $V_{RF2} = -V_{RF1}$

$$I_{out} = \beta (V_G - V_{Tho}) V_{RF1} - \beta (V_G - V_{Th}) V_{RF1} - \beta V_{RF1}^2$$

$$= -\beta V_{Tho} V_{RF1} + \beta V_{Th} V_{RF1} - \beta V_{RF1}^2$$

$$= -\beta V_{Tho} V_{RF1} + \beta V_{Th} V_{RF1} - \beta V_{RF1}^2$$

Therefore:

$$I_{out} = -\beta V_{Tho} V_{RF1} + \beta \left(V_{Tho} + \gamma \left(\sqrt{|2\Phi_F + V_{SB2}|} - \sqrt{|2\Phi_F|}\right)\right) V_{RF1} - \beta V_{RF1}^2$$

Where $\Phi_F = \frac{kT}{q} \ln\left(\frac{N_{sub}}{n_i}\right)$ [V] N_{sub} : Dopping concentration of the substrate

γ : body effect coefficient [$\sqrt{\text{V}}$]

But: $V_{S2} = V_{RF2}$

$$I_{out} = -\beta V_{Tho} V_{RF1} + \beta \left(V_{Tho} + \gamma \left(\sqrt{|2\Phi_F + V_{RF2}|} - \sqrt{|2\Phi_F|}\right)\right) V_{RF1} - \beta V_{RF1}^2$$

$$= \beta\gamma \left(\sqrt{|2\Phi_F - V_{RF1}|} - \sqrt{|2\Phi_F|}\right) V_{RF1} - \beta V_{RF1}^2$$

$$= \beta\gamma \sqrt{|2\Phi_F - V_{RF1}|} V_{RF1} - \beta\gamma \sqrt{|2\Phi_F|}\, V_{RF1} - \beta V_{RF1}^2$$

As you know that the Taylor expansion of a square root at x = 0 is:

$$\sqrt{1+x} = 1 + \frac{1}{2}x - \frac{1}{8}x^2 + \ldots\ldots$$

But: $2\Phi_F > V_{RF1}$

Therefore:

$$I_{out} = \beta\gamma \sqrt{2\Phi_F - V_{RF1}} V_{RF1} - \beta\gamma \sqrt{2\Phi_F}\, V_{RF1} - \beta V_{RF1}^2$$

$$= \beta\gamma \sqrt{2\Phi_F} \sqrt{1 + \left(-\frac{V_{RF1}}{2\Phi_F}\right)} V_{RF1} - \beta\gamma \sqrt{2\Phi_F}\, V_{RF1} - \beta V_{RF1}^2$$

$$= \beta\gamma \sqrt{2\Phi_F} \left(1 + \frac{1}{2}\left(-\frac{V_{RF1}}{2\Phi_F}\right) - \frac{1}{8}\left(-\frac{V_{RF1}}{2\Phi_F}\right)^2\right) V_{RF1} - \beta\gamma \sqrt{2\Phi_F}\, V_{RF1} - \beta V_{RF1}^2$$

$$= \beta\gamma \sqrt{2\Phi_F} V_{RF1} - \frac{1}{2}\beta\gamma \frac{1}{\sqrt{2\Phi_F}} V_{RF1}^2 - \frac{1}{8}\beta\gamma \frac{1}{\sqrt{(2\Phi_F)^3}} V_{RF1}^3 - \beta\gamma \sqrt{2\Phi_F}\, V_{RF1} - \beta V_{RF1}^2$$

$$= \underbrace{-\beta\left(1 + \frac{1}{2}\frac{\gamma}{\sqrt{2\Phi_F}}\right) V_{RF1}^2}_{\text{Square current}} \underbrace{- \frac{1}{8}\beta\gamma \frac{1}{\sqrt{(2\Phi_F)^3}} V_{RF1}^3}_{\text{Bulf effect current distortion}}$$

5. Taylor expansion of I_{out}

In the equation of the output current, there are two square roots:

$$I_{out} = \frac{-2-2\beta R_S V_{GT} + \sqrt{1-2\beta R_S V_{RF1} + 2\beta R_S V_{GT} + (\beta R_S V_{GT})^2} + \sqrt{1+2\beta R_S V_{RF1} + 2\beta R_S V_{GT} + (\beta R_S V_{GT})^2}}{\beta R_S^2}$$

As you know that the Taylor expansion of a square root at x = 0 is:

$$\sqrt{1+x} = 1 + \frac{1}{2}x - \frac{1}{8}x^2 + ...$$

Therefore:

$$\sqrt{1-2\beta R_S V_{RF1} + 2\beta R_S V_{GT} + (\beta R_S V_{GT})^2} = \sqrt{\underbrace{1+2\beta R_S V_{GT} + (\beta R_S V_{GT})^2}_{\text{Constant}}}\sqrt{1 + \frac{-2\beta R_S V_{RF1}}{1+2\beta R_S V_{GT} + (\beta R_S V_{GT})^2}}$$

$$= \sqrt{1+2\beta R_S V_{GT} + (\beta R_S V_{GT})^2}\left[1 + \frac{1}{2}\left(\frac{-2\beta R_S V_{RF1}}{1+2\beta R_S V_{GT} + (\beta R_S V_{GT})^2}\right) - \frac{1}{8}\left(\frac{-2\beta R_S V_{RF1}}{1+2\beta R_S V_{GT} + (\beta R_S V_{GT})^2}\right)^2\right]$$

$$= \sqrt{1+2\beta R_S V_{GT} + (\beta R_S V_{GT})^2}\left[1 - \frac{1}{2}\left(\frac{2\beta R_S V_{RF1}}{1+2\beta R_S V_{GT} + (\beta R_S V_{GT})^2}\right) - \frac{1}{8}\left(\frac{2\beta R_S V_{RF1}}{1+2\beta R_S V_{GT} + (\beta R_S V_{GT})^2}\right)^2\right]$$

And:

$$\sqrt{1+2\beta R_S V_{RF1} + 2\beta R_S V_{GT} + (\beta R_S V_{GT})^2} = \sqrt{\underbrace{1+2\beta R_S V_{GT} + (\beta R_S V_{GT})^2}_{\text{Constant}}}\sqrt{1 + \frac{2\beta R_S V_{RF1}}{1+2\beta R_S V_{GT} + (\beta R_S V_{GT})^2}}$$

$$= \sqrt{1+2\beta R_S V_{GT} + (\beta R_S V_{GT})^2}\left[1 + \frac{1}{2}\left(\frac{2\beta R_S V_{RF1}}{1+2\beta R_S V_{GT} + (\beta R_S V_{GT})^2}\right) - \frac{1}{8}\left(\frac{2\beta R_S V_{RF1}}{1+2\beta R_S V_{GT} + (\beta R_S V_{GT})^2}\right)^2\right]$$

$$= \sqrt{1+2\beta R_S V_{GT} + (\beta R_S V_{GT})^2}\left[1 + \frac{1}{2}\left(\frac{2\beta R_S V_{RF1}}{1+2\beta R_S V_{GT} + (\beta R_S V_{GT})^2}\right) - \frac{1}{8}\left(\frac{2\beta R_S V_{RF1}}{1+2\beta R_S V_{GT} + (\beta R_S V_{GT})^2}\right)^2\right]$$

Then:

$$\sqrt{1-2\beta R_S V_{RF1} + 2\beta R_S V_{GT} + (\beta R_S V_{GT})^2} + \sqrt{1+2\beta R_S V_{RF1} + 2\beta R_S V_{GT} + (\beta R_S V_{GT})^2} = \sqrt{1+2\beta R_S V_{GT} + (\beta R_S V_{GT})^2}\left[2 - \frac{1}{4}\left(\frac{2\beta R_S V_{RF1}}{1+2\beta R_S V_{GT} + (\beta R_S V_{GT})^2}\right)^2\right]$$

Filling this result in I_{out} results:

$$I_{out} = \frac{-2-2\beta R_S V_{GT} + \sqrt{1+2\beta R_S V_{GT} + (\beta R_S V_{GT})^2}\left[2 - \frac{1}{4}\left(\frac{2\beta R_S V_{RF1}}{1+2\beta R_S V_{GT} + (\beta R_S V_{GT})^2}\right)^2\right]}{\beta R_S^2}$$

$$= \frac{-2-2\beta R_S V_{GT} + 2\sqrt{1+2\beta R_S V_{GT} + (\beta R_S V_{GT})^2}}{\beta R_S^2} - \frac{\beta}{\left(1+2\beta R_S V_{GT} + (\beta R_S V_{GT})^2\right)^{\frac{3}{2}}} V_{RF1}^2$$

$$= \underbrace{\frac{-2-2\beta R_S V_{GT} + 2\sqrt{(1+\beta R_S V_{GT})^2}}{\beta R_S^2}}_{=0} - \frac{\beta}{\left((1+\beta R_S V_{GT})^2\right)^{\frac{3}{2}}} V_{RF1}^2$$

$$= -\frac{\beta}{(1+\beta R_S V_{GT})^3} V_{RF1}^2$$

6. NF derivation for the Squarer Block

$$NF_{QS-IV} = \frac{V_{RF1}^2}{\overline{V_{R_S}^2}} \frac{\left[2\left(\frac{\overline{V_{R_S}^2} + \overline{V_{R_{on}}^2}}{(R_S + R_{on})^2} \right) R_{IV}^2 + \overline{V_{R_{IV}}^2} + \overline{V_{n-Op}^2} \left(\frac{2R_{IV}}{R_S + R_{on}} \right)^2 \right]}{(I_{out} R_{IV})^2}$$

$$= 2\frac{V_{RF1}^2}{\overline{V_{R_S}^2}} \frac{1}{(I_{out} R_{IV})^2} \left(\frac{\overline{V_{R_S}^2} + \overline{V_{R_{on}}^2}}{(R_S + R_{on})^2} \right) R_{IV}^2 + \frac{V_{RF1}^2}{\overline{V_{R_S}^2}} \frac{1}{(I_{out} R_{IV})^2} \overline{V_{R_{IV}}^2} + \frac{V_{RF1}^2}{\overline{V_{R_S}^2}} \frac{1}{(I_{out} R_{IV})^2} \overline{V_{n-Op}^2} \left(\frac{2R_{IV}}{R_S + R_{on}} \right)^2$$

$$= 2\left(\frac{V_{RF1}}{I_{out}} \right)^2 \frac{1}{R_S (R_S + R_{on})} + \frac{1}{\left(\frac{I_{out} R_{IV}}{V_{RF1}} \right)^2} \frac{R_{IV}}{R_S} + 4\frac{1}{\left(\frac{I_{out} R_{IV}}{V_{RF1}} \right)^2} \frac{\overline{V_{n-Op}^2}}{\overline{V_{R_S}^2}} \left(\frac{R_{IV}}{R_S + R_{on}} \right)^2$$

From here, we can go in two ways with NF derivation. The firs one is to highlight the effect of $Av_{SQ\text{-}IV}$ and NF_{SQ} on the total NF of the whole Square block:

$$NF_{QS-IV} = 2\left(\frac{V_{RF1}}{I_{out}} \right)^2 \frac{1}{R_S (R_S + R_{on})} + \frac{1}{\left(\frac{I_{out} R_{IV}}{V_{RF1}} \right)^2} \frac{R_{IV}}{R_S} + 4\frac{1}{\left(\frac{I_{out} R_{IV}}{V_{RF1}} \right)^2} \frac{\overline{V_{n-Op}^2}}{\overline{V_{R_S}^2}} \left(\frac{R_{IV}}{R_S + R_{on}} \right)^2$$

$$= 2\left(\frac{V_{RF1}}{I_{out}} \right)^2 \frac{1}{R_S (R_S + R_{on})} + \frac{1}{\left(\frac{I_{out} R_{IV}}{\frac{V_{RF}}{2}} \right)^2} \frac{R_{IV}}{R_S} + 4\frac{1}{\left(\frac{I_{out} R_{IV}}{\frac{V_{RF}}{2}} \right)^2} \frac{\overline{V_{n-Op}^2}}{\overline{V_{R_S}^2}} \left(\frac{R_{IV}}{R_S + R_{on}} \right)^2$$

$$2\left(\frac{V_{RF1}}{I_{out}} \right)^2 \frac{1}{R_S (R_S + R_{on})} + \frac{1}{\left(\frac{I_{out} R_{IV}}{\frac{1}{2} V_{in} \frac{R_S + R_{on}}{R_{on}}} \right)^2} \frac{R_{IV}}{R_S} + 4\frac{1}{\left(\frac{I_{out} R_{IV}}{\frac{1}{2} V_{in} \frac{R_S + R_{on}}{R_{on}}} \right)^2} \frac{\overline{V_{n-Op}^2}}{\overline{V_{R_S}^2}} \left(\frac{R_{IV}}{R_S + R_{on}} \right)^2$$

But R_{on} is equal to $2R_S$

$$= 2\left(\frac{V_{RF1}}{I_{out}} \right)^2 \frac{1}{R_S (R_S + R_{on})} + \frac{1}{\left(2\frac{I_{out} R_{IV}}{V_{in}} \frac{2}{3} \right)^2} \frac{R_{IV}}{R_S} + \frac{1}{\left(2\frac{I_{out} R_{IV}}{V_{in}} \right)^2} \frac{\overline{V_{n-Op}^2}}{\overline{V_{R_S}^2}} \left(\frac{R_{IV}}{R_S} \right)^2$$

$$= NF_{QS} + \frac{9}{16} \frac{\frac{R_{IV}}{R_S}}{Av_{QS-IV}^2} + \frac{1}{4} \frac{\frac{\overline{V_{n-Op}^2}}{\overline{V_{R_S}^2}} \left(\frac{R_{IV}}{R_S} \right)^2}{Av_{QS-IV}^2}$$

The second one is to highlight the effect of fundamental parameters, namely $\beta, R_S, R_{IV}, V_{GT}, V_{RF1}$ and $\overline{V_{n-Op}^2}$ on the total NF of the whole Square block:

$$NF_{QS-IV} = 2\left(\frac{V_{RF1}}{I_{out}}\right)^2 \frac{1}{R_S\left(R_S + R_{on}\right)} + \frac{1}{\left(\frac{I_{out}R_{IV}}{V_{RF1}}\right)^2}\frac{R_{IV}}{R_S} + 4\frac{1}{\left(\frac{I_{out}R_{IV}}{V_{RF1}}\right)^2}\frac{\overline{V_{n-Op}^2}}{\overline{V_{R_S}^2}}\left(\frac{R_{IV}}{R_S + R_{on}}\right)^2$$

But R_{on} is equal to $2R_S$

$$= \frac{2}{3}\left(\frac{V_{RF1}}{I_{out}}\right)^2 \frac{1}{R_S^2} + \left(\frac{V_{RF1}}{I_{out}}\right)^2 \frac{1}{R_S R_{IV}} + \frac{4}{9}\left(\frac{V_{RF1}}{I_{out}}\right)^2 \frac{\overline{V_{n-Op}^2}}{\overline{V_{R_S}^2}}\frac{1}{R_S^2}$$

$$= \frac{2}{3}\left(\frac{\left(1+\beta R_S V_{GT}\right)^3}{\beta}\frac{1}{V_{RF1}}\right)^2 \frac{1}{R_S^2} + \left(\frac{\left(1+\beta R_S V_{GT}\right)^3}{\beta}\frac{1}{V_{RF1}}\right)^2 \frac{1}{R_S R_{IV}} + \frac{4}{9}\left(\frac{\left(1+\beta R_S V_{GT}\right)^3}{\beta}\frac{1}{V_{RF1}}\right)^2 \frac{\overline{V_{n-Op}^2}}{\overline{V_{R_S}^2}}\frac{1}{R_S^2}$$

$$= \frac{2}{3}\frac{\left(1+\beta R_S V_{GT}\right)^6}{\beta^2}\frac{1}{R_S^2}\left(\frac{1}{V_{RF1}^2}\right) + \frac{\left(1+\beta R_S V_{GT}\right)^6}{\beta^2}\frac{1}{R_S R_{IV}}\left(\frac{1}{V_{RF1}^2}\right) + \frac{4}{9}\frac{\left(1+\beta R_S V_{GT}\right)^6}{\beta^2}\left(\frac{1}{V_{RF1}^2}\right)\frac{\overline{V_{n-Op}^2}}{\overline{V_{R_S}^2}}\frac{1}{R_S^2}$$

$$= \frac{\left(1+\beta R_S V_{GT}\right)^6}{\beta^2}\left(\frac{1}{V_{RF1}^2}\right)\left[\frac{2}{3}\frac{1}{R_S^2} + \frac{1}{R_S R_{IV}} + \frac{4}{9}\frac{\overline{V_{n-Op}^2}}{\overline{V_{R_S}^2}}\frac{1}{R_S^2}\right]$$

7. Voltage gain derivation for the Squarer Block

$$Av_{SQ-IV} = \frac{I_{out} R_{IV}}{V_{in}} = \frac{\beta}{(1+\beta R_S V_{GT})^3} V_{RF1}^2 \frac{R_{IV}}{V_{in}} = \frac{1}{\left(V_{RF} \frac{R_{on}}{R_{on}+R_S}\right)} \frac{1}{\left(1+\frac{R_S}{R_{on}}\right)^3} \beta R_{IV} V_{RF1}^2$$

$$= \frac{1}{\left(2V_{RF1}\frac{2}{3}\right)} \frac{1}{\left(1+\frac{1}{2}\right)^3} \beta R_{IV} V_{RF1}^2 = \frac{3}{4}\frac{8}{27} \beta R_{IV} V_{RF1} = \frac{2}{9} \beta R_{IV} V_{RF1}$$

8. Sensitivity equation vs. Friis NF equation

In this Appendix, the sensitivity and the Friis equations will be explored to show the relation between the sensitivity of an RF receiver and its block specifications. This way of understanding has been applied in our level diagram in Chapter 4.

The NF of the Front End is:

$$NF_{FE} = \frac{SNRin}{SNRout} = \frac{P_{sig} / P_{Rantenna}}{SNRout} \qquad \textbf{Equation 0-2}$$

Where P_{sig} denotes the input signal power measured at R_{FEin} and $P_{Rantenna}$ is the source resistance noise power measured on R_{FEin} , both per unit bandwidth. It follows that:

$$P_{sig} = P_{Rantenna}.NF_{FE}.SNRout$$

The overall signal power is distributed across the channel bandwidth, B, the two side of the equation above must be integrated over the bandwidth to obtain the total mean square power. Thus:

$$P_{sig,tot} = P_{Rantenna}.NF_{FE}.SNRout.B$$

This equation equation predicts the sensitivity as the minimum input signal that yields value for the output SNR. Changing the notation slightly and expressing the quantities in dB or dBm, we have:

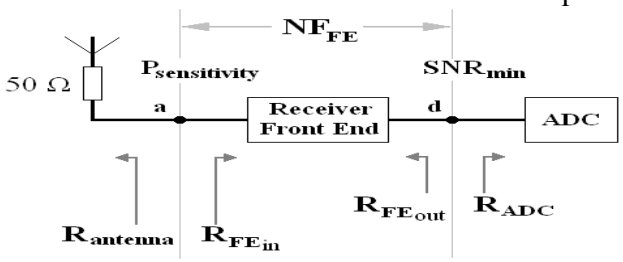

Figure 89: Receiver diagram (Top view)

$$P_{in,\min}\big|_{dBm} = P_{Rantenna}\big|_{dBm/Hz} + NF_{FE}\big|_{dBm} + SNR_{\min}\big|_{dBm} + 10\log(B) \qquad \textbf{Equation 0-3}$$

Wehe $P_{in,\min}$ is the minimum input level that achieves $SNR_{\min}$ and does not depend on the gain of the system. Thus, NF_{FE} of Equation 0-3 has a reference at point d (see Figure 89). Now, let's assume that the Frond End consists of three blocks as shown in Figure 90.

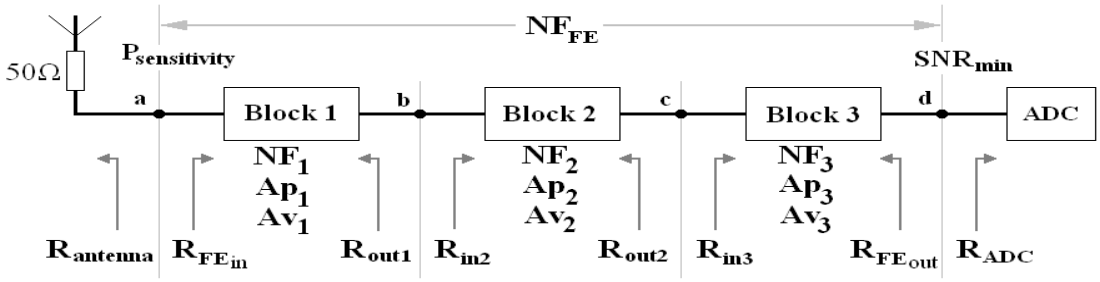

Figure 90: Receiver blocks diagram

Taking point d as a reference means that $NF_d = 0$. Therefore [8]:

$$NF_c = NF_3 + \frac{NF_d - 1}{Ap_3} = NF_3 \qquad \textbf{Equation 0-4}$$

Where Ap_3 is the available power gain and is equal to [8]:

$$Ap = \left(\frac{R_{in3}}{R_{in3} + R_{out2}} \right) Av_3^2 \frac{R_{out2}}{R_{FEout}} \qquad \textbf{Equation 0-5}$$

Where Av_3 is the unloaded voltage gain of the 3rd block.

Let's return back to NF chain:

$$NF_b = NF_2 + \frac{NF_c - 1}{Ap_2} \qquad \textbf{Equation 0-6}$$

$$= NF_2 + \frac{NF_3 - 1}{Ap_2} \qquad \textbf{Equation 0-7}$$

And:

$$NF_a = NF_1 + \frac{NF_b - 1}{Ap_1} \qquad \textbf{Equation 0-8}$$

$$= NF_1 + \frac{\left(NF_2 + \frac{NF_3 - 1}{Ap_2} \right)_b - 1}{Ap_1}$$

$$= NF_1 + \frac{NF_2}{Ap_1} + \frac{NF_3 - 1}{Ap_1 Ap_2} \qquad \textbf{Equation 0-9}$$

Equation 0-9 is simply the Friis equation of the Frond End NF, NF_{FE} and combining it with Equation 0-3 gives almost[12] the needed picture about our the Front End. We

[12] To complete the picture it is necessary to include IIP_3 calculation. In our system, the NF is the only serious concern.

9. Second iteration level diagram with LNA

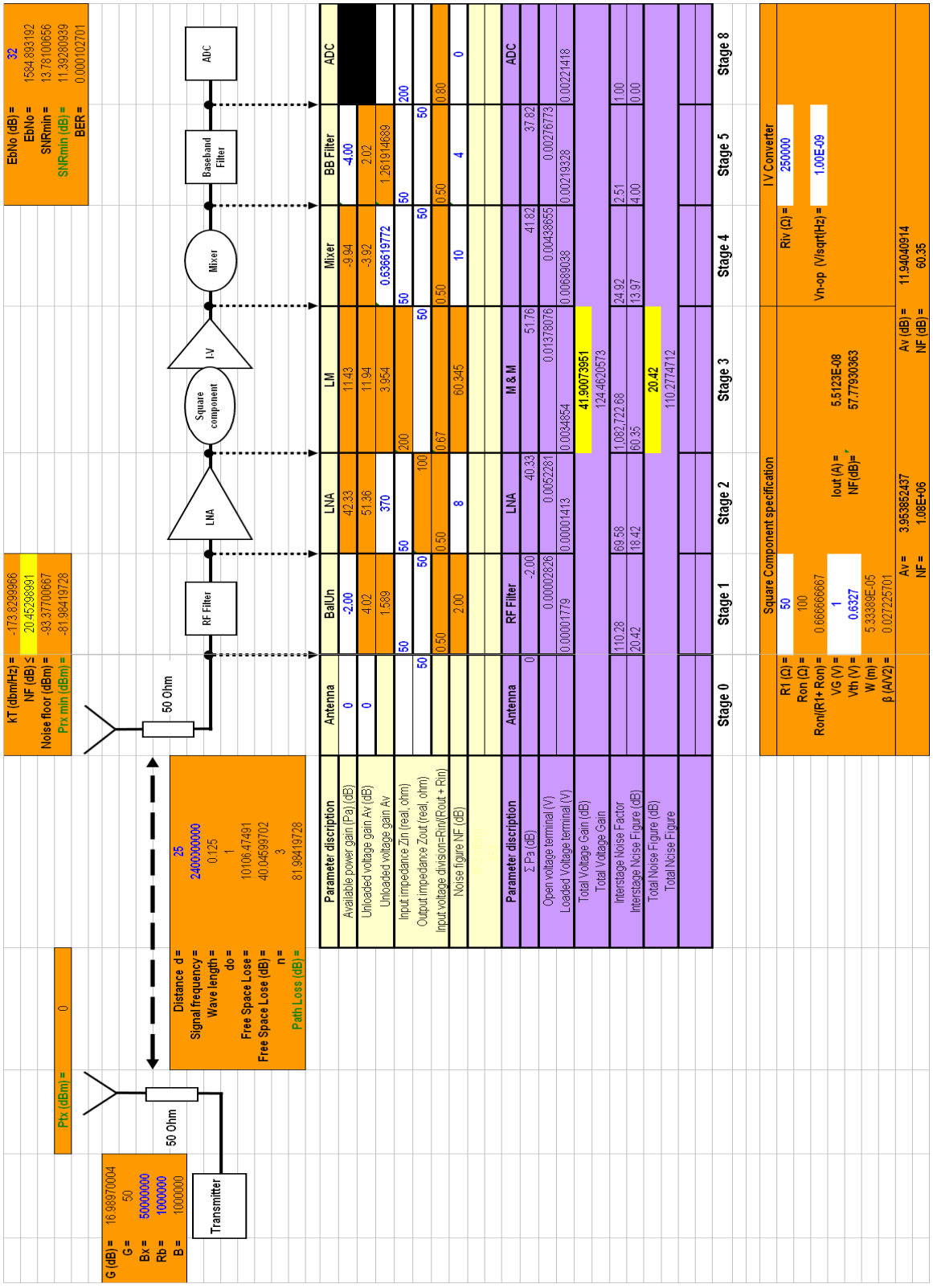

10. Distance (d) vs. current consumption derivation

The noise figure of the Squarer block is:

$$NF_{SQ-IV} = \frac{81}{4}\left(\frac{V_{GT}}{V_{RF1}}\right)^2\left[\frac{3}{2}+\frac{R_{n-OpAmp}}{R_S}\right] = 81\left(\frac{V_{GT}}{V_{RF}}\right)^2\left[\frac{3}{2}+\frac{R_{n-OpAmp}}{R_S}\right]$$

$$= 81\left(\frac{V_{GT}}{V_{RF}}\right)^2\left[\frac{3}{2}+\frac{3}{2}\frac{2}{3}\frac{R_{n-OpAmp}}{R_S}\right] = 81\left(\frac{V_{GT}}{V_{RF}}\right)^2\frac{3}{2}\left[1+\frac{2}{3}\frac{R_{n-OpAmp}}{R_S}\right]$$

But V_{RF} is:

$$V_{RF} = V_R Av_{LNA} = V_R\left(gm_{LNA}R_{LNA}\right) = V_R\left(\frac{2I_{LNA}}{V_{GT\_OpAmp}}R_{LNA}\right)$$

$$= V_R\left(\frac{2R_{LNA}}{V_{GT\_OpAmp}}\right)I_{LNA} = \left(\frac{1000}{3}\right)V_R I_{LNA}$$

Where we assume that $V_{GT\_OpAmp} = 300mV$ and $R_{LNA} = 50\Omega$

And $R_{n-OpAmp}$ is:

$$R_{n-OpAmp} = \frac{V_{GT\_OpAmp}}{2I_{OpAmp}} = \frac{300\times10^{-3}}{2}\frac{1}{I_{OpAmp}} = 150\times10^{-3}\frac{1}{I_{OpAmp}}$$

Substituting V_{RF} and $R_{n-OpAmp}$ in the equation of NF_{SQ-IV} gives:

$$NF_{SQ-IV} = 81\left(\frac{V_{GT}}{V_{RF}}\right)^2\frac{3}{2}\left[1+\frac{2}{3}\frac{R_{n-OpAmp}}{R_S}\right]$$

$$= 81\frac{V_{GT}^2}{\left(\left(\frac{1000}{3}\right)V_R I_{LNA}\right)^2}\frac{3}{2}\left[1+\frac{2}{3}\frac{\left(150\times10^{-3}\frac{1}{I_{OpAmp}}\right)}{R_S}\right]$$

$$= \frac{81\times3}{\left(\frac{1000}{3}\right)^2\times2}\frac{V_{GT}^2}{\left(V_R I_{LNA}\right)^2}\left[1+\frac{2}{3}150\times10^{-3}\frac{1}{50I_{OpAmp}}\right] = \frac{3^7}{1000^2\times2}\frac{V_{GT}^2}{\left(V_R I_{LNA}\right)^2}\left[1+\frac{2\times10^{-3}}{I_{OpAmp}}\right]$$

But as you know that:

$$P_R = P_T - PL(d)$$

$$10\log\left(\frac{V_R^2}{50\times0.001}\right) = 10\log\left(\frac{V_T^2}{50\times0.001}\right) - 10\log\left(\left(\frac{4\pi}{\lambda}\right)^2 d^n\right)$$

$$V_R^2 = \frac{V_T^2}{\left(\frac{4\pi}{\lambda}\right)^2 d^n} = V_T^2\left(\frac{\lambda}{4\pi}\right)^2\frac{1}{d^n}$$

$$V_R = V_T\left(\frac{\lambda}{4\pi}\right)\frac{1}{\sqrt{d^n}}$$

And the noise figure of the Front End is:

$$NF_{FE}=\frac{\frac{V_T^2}{50\times 0.001}}{\left(\frac{4\pi}{\lambda}\right)^2 d^n}=\frac{\frac{V_T^2}{50\times 0.001}}{\left(\frac{4\pi}{\lambda}\right)^2 d^n\times kTB\times SNR_{\min}}=\left(\frac{\lambda}{4\pi}\right)^2\frac{1}{50\times 0.001\times kTB\times SNR_{\min}}\frac{V_T^2}{d^n}$$

The Friis equation for two blocks, namely LNA and the Squarer block is:

$$NF_{FE}(d)=NF_{LNA}(I_{LNA})+\frac{NF_{SQ-IV}(I_{OpAmp},I_{LNA})-1}{Ap_{LNA}(I_{LNA})}\approx\frac{NF_{SQ-IV}(I_{OpAmp},I_{LNA})-1}{Ap_{LNA}(I_{LNA})}$$

$$NF_{FE}(d)\approx\frac{NF_{SQ-IV}(I_{OpAmp},I_{LNA})-1}{Ap_{LNA}(I_{LNA})}$$

Now let's substitute the equation of NF_{FE}, V_R, NF_{SQ-IV} and Av_{LNA} in the Friis equation:

$$\left(\frac{\lambda}{4\pi}\right)^2\frac{1}{50\times 0.001\times kTB\times SNR_{\min}}\frac{V_T^2}{d^n}=4\frac{\frac{3^7}{1000^2\times 2}\frac{V_{GT}^2}{(V_R I_{LNA})^2}\left[1+\frac{2\times 10^{-3}}{I_{OpAmp}}\right]-1}{\left(\left(\frac{1000}{3}\right)I_{LNA}\right)^2}$$

$$=\frac{\frac{4\times 3^7}{1000^2\times 2}\frac{V_{GT}^2}{V_R^2 I_{LNA}^2}\left[1+\frac{2\times 10^{-3}}{I_{OpAmp}}\right]}{\left(\frac{1000}{3}\right)^2 I_{LNA}^2}$$

$$=\frac{2\times 3^9}{1000^4}\frac{V_{GT}^2}{V_R^2}\frac{1}{I_{LNA}^4}\left[1+\frac{2\times 10^{-3}}{I_{OpAmp}}\right]$$

$$=\frac{2\times 3^9}{1000^4}\frac{V_{GT}^2}{\left(V_T^2\left(\frac{\lambda}{4\pi}\right)^2\frac{1}{d^n}\right)}\frac{1}{I_{LNA}^4}\left[1+\frac{2\times 10^{-3}}{I_{OpAmp}}\right]$$

$$=\frac{2\times 3^9}{1000^4}\left(\frac{4\pi}{\lambda}\right)^2 d^n\frac{V_{GT}^2}{V_T^2}\frac{1}{I_{LNA}^4}\left[1+\frac{2\times 10^{-3}}{I_{OpAmp}}\right]$$

$$\left(\frac{\lambda}{4\pi}\right)^4\frac{1000^4}{50\times 0.001\times 2\times 3^9\times kTB\times SNR_{\min}}\frac{V_T^4}{V_{GT}^2}\frac{1}{d^{2n}}=\frac{\left[1+\frac{2\times 10^{-3}}{I_{OpAmp}}\right]}{I_{LNA}^4}$$

$$\frac{d^{2n}}{\left(\frac{\lambda}{4\pi}\right)^4\frac{1000^4}{50\times 0.001\times 2\times 3^9\times kTB\times SNR_{\min}}\frac{V_T^4}{V_{GT}^2}}=\frac{I_{LNA}^4}{\left[1+\frac{2\times 10^{-3}}{I_{OpAmp}}\right]}$$

$$d^{2n} = \left(\frac{\lambda}{4\pi}\right)^4 \frac{1000^4}{50\times 0.001\times 2\times 3^9\times kTB\times SNR_{\min}} \frac{V_T^4}{V_{GT}^2} \frac{I_{LNA}^4}{\left[1+\frac{2\times 10^{-3}}{I_{OpAmp}}\right]}$$

Then :

$$d = \left(\left(\frac{\lambda}{4\pi}\right)^4 \frac{1000^4}{50\times 0.001\times 2\times 3^9\times kTB\times SNR_{\min}} \frac{V_T^4}{V_{GT}^2} \frac{I_{LNA}^4}{\left[1+\frac{2\times 10^{-3}}{I_{OpAmp}}\right]} \right)^{\frac{1}{2n}}$$

$$= \left(\left(\frac{\lambda}{4\pi}\right)^4 \frac{50\times 1000^5}{2\times 3^9\times kTB\times SNR_{\min}} \frac{P_T^2}{V_{GT}^2} \frac{I_{LNA}^4}{\left[1+\frac{2\times 10^{-3}}{I_{OpAmp}}\right]} \right)^{\frac{1}{2n}}$$

Thus :

$$d = \left(51\times 10^6 \frac{\lambda^4}{kTB\times SNR_{\min}} \frac{P_T^2}{V_{GT}^2} \frac{I_{LNA}^4}{\left[1+\frac{2\times 10^{-3}}{I_{OpAmp}}\right]} \right)^{\frac{1}{2n}}$$